W/C ratio estimation of concrete

Through optical microscopy, electron microscopy and thermogravimetric analysis

J. F. Garzón Amórtegui

Technische Universiteit Delft

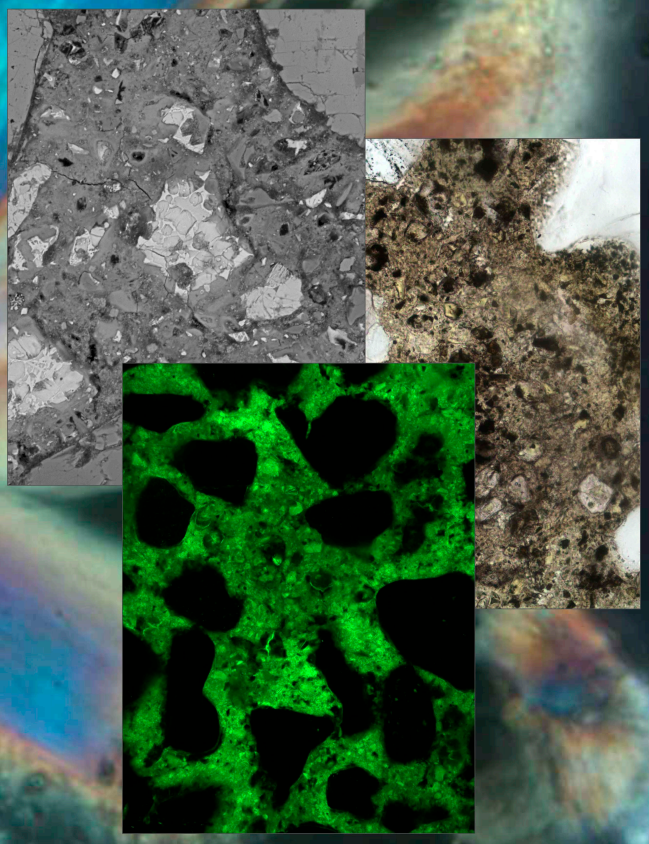

TU Delft Delft University of Technology

Challenge the future

W/C ratio estimation of concrete

Through optical microscopy, electron microscopy and thermogravimetric analysis

by

J. F. Garzón Amórtegui

in partial fulfillment of the requirements for the degree of

Master of Science
in Civil Engineering, track Structural Engineering.

at the Delft University of Technology,
to be defended publicly on Septemeber 2018 .

Supervisor:	Dr. Oğuzhan Çopuroğlu,	TU Delft
Thesis committee:	Prof. Dr. Erik Schlangen,	TU Delft
	Dr. Wolfgang Gard,	TU Delft

An electronic version of this thesis is available at http://repository.tudelft.nl/.

TU Delft Delft University of Technology

Abstract

In the past, concrete mix design was mostly focused on achieving a desired compressive strength which was usually done by adjusting the water to cement ratio (W/C) of the mix, nevertheless, this philosophy has brought durability issues to the structures especially to the ones that are exposed to aggressive environments. Because of this, one of the new challenges of concrete technology is to do a more durable material which can also be achieved by adjusting the W/C in the mix design.

It can be seen that the W/C is a very powerful parameter that influences the strength and durability of concrete. Based on the requirements, in the mix design the W/C is defined, nevertheless, once the concrete hardens, it is difficult to check if the W/C of the structure is the same as the one from the design. Due to this difficulty, the techniques that have been proposed measure usually indirect parameters that are later correlated with the W/C. So far, there are only two techniques that have been accepted as standards, namely the Nordtest Build NT 361-1999 and the BS 1881-124.

Based on this, it was decided to explore currently available techniques and propose alternative ones that can provide relatively accurate results for the W/C estimation of concrete. Literature established that there are two ways to assess the W/C estimation, using direct measurements in which the water and the cement are quantified and through indirect measurement in which a parameter is compared to the W/C. The most common parameter is the porosity, although mineralogical features such as calcium hydroxide (CH) content have been used too.

The techniques that were used in this document are circular polarization microscopy (CPL) and thermogravimetric analysis (TGA) to quantify the CH content, the UV light microscopy to quantify the capillary porosity and scanning electron microscopy (SEM) + Powers and Brownyard approach to quantify the water and cement contents. The goal of the project was to see if CH quantification through CPL technique can be considered as an alternative W/C estimation technique compared to the existing ones. The idea was to use these techniques in order to estimate the W/C of concrete samples that were part of a Round Robin test organized by the Applied Petrography Group (APG). For the CPL and UV-light microscopy applications, standards from TU Delft were used to estimate the W/C of the unknowns.

Depending on the methodology, a specific sample preparation was done. Thin sections, polished sections and powderized samples were prepared using a protocol established in chapter 3. Afterwards, for the microscopy techniques different procedures were followed for the acquisition of the micrographs. Another protocol was described for the ignition of the powderized samples. Later on, depending on the methodology, a specific approach was used to quantify the capillary porosity, calcium hydroxide, chemically bound water and cement.

The results from the standards had a good correlation with UV light and the CPL measurement results. Likewise, the W/C of the APG samples was obtained using both techniques independently an then in combination. On the other hand, the results obtained from the SEM + Powers and Brownyard were not very successful due to a problem with the quantification of the water and cement. Four approaches were done to segment the micrographs, but none of them gave accurate result. At the end, results from each of the approaches were chosen for the analysis. Finally, for the TGA, due to presence of the aggregates, the CH content itself couldn't be quantified, instead a ratio between the mass loss of the CH content and the chemically bound water was computed.

Overall, the results from the techniques were in the same trend, for instance the sample with the higher W/C always had the highest porosity and calcium hydroxide content. Later, it was decided to choose which technique gave the best results. For this, three guidelines were defined, representativeness, reproducibility and reliability. A score was given for every technique and later the average was obtained.

The technique with the highest average value was considered as the best one. As a single technique, the CPL methodology obtained the highest value for different reasons; it had less constrains than the UV light, the parameters that affect it can be compensated by the type of segmentation that is used, in comparison with the SEM micrographs it analyses a higher amount of mass and in comparison with the TGA the person can choose which area can be analyzed and which ones should be avoid. Moreover, the combination of the UV + CPL was the technique with the best results because of its high reliability. By using both techniques at the same time, each of them compensated for the other so the final W/C estimation is closer to the real APG ratios than if they are used separately.

Finally, it can be said that there is a relationship between the capillary porosity and calcium hydroxide content with the W/C regardless of the technique that is used. The guidelines allowed to see the pros and cons of each methodology. Also, thanks to image analysis, the CH content micrographs can also be used to estimate the reactivity of the mineral admixtures among other aspects. The TGA can be very helpful to double check the results obtained from the microscopy techniques, especially since this one analyses the largest amount of area. The SEM + Powers and Brownyard is a very good technique with a solid background although it is difficult to reproduce and only analysis a small mass of concrete.

Acknowledgements

First, I would like to thank my thesis supervisor Dr. Oğuzhan Çopuroğlu for his help and guidance through this project. I am thankful with him for giving me the opportunity to work as a teaching assistant for the Materials and Environment section and for the talks we had and the advices he gave me about the professional and personal aspects of life. Likewise, I want to thank Prof. Dr. Erik Schlangen and Dr. Wolfgang Gard for the their comments and feedback that allowed me to improve my research.

I first came to The Netherlands to obtain a master degree, but here I have gain so much more, I have met new people who became very good friends. I want to thank Sanchez, Luisa, Manuela, Luis, Maria, Teni, Vassia, Mathijs, Stefan, Valery, Sakshi, Marco, Alvaro, Arturo, Gabi and Gina among others for being part of this experience. Thank you for studying, suffering, enjoying, drinking, sharing and travelling with me. Thanks to the people from the Microlab, specially Claudia, Emanuele and Stefan. It was a pleasure to work with all of you. I also want to thank my friends back home for the support in the difficult times, Alejandra, Brandon, Felipe and Diego.

Finally I want to thank my family. A mis papas, as a son and as a civil engineer I have deep admiration for you, thank you for teaching me the love for structural engineering. To my brother, Luis, thank you for your calls to ask about me and for your unconditional support. This document is a culmination of a journey that I couldn't have done without the three of you. Los amo.

Contents

List of Tables

List of Figures

1

Introduction

Concrete is the most used construction material in the world. In general terms it contributes to around 50% of a country national wealth, in the case of The Netherlands it is €1.9 trillion. The main reason why concrete is so popular that its raw materials can be found almost worldwide, allowing the development of different mix designs that can offer particular properties based on the needs of every situation. In the past, concrete was considered as an eternal material that would never face any problems during the structure service life span. In those days, mix design of concrete was focused on achieving a desired workability in the fresh state and a compressive strength in the hardened state which is achieved usually by adjusting the water to cement ratio (W/C) of the mixes.

Many structures whose mix design only took fresh and hardened state properties of the concrete into account are now showing durability problems which require an important investment for their maintenance and have a big environmental impact. For instance, The Netherlands spends, approximately, on the maintenance of its infrastructure €1 billion per year. These expenses are mandatory for every country, since they need to have an adequate infrastructure for a proper functionality, therefore the need of developing a durable construction material has been a priority in the last decades for the concrete technology industry. Likewise, since cement production contributes to approximately 6- 8% of the CO_2 emissions of the world, a durable material can reduce the global production of concrete which will directly contribute positively to the environment.

A durable concrete can be defined as a material whose mechanical properties will prevail during the entire service life span of the structure. Nevertheless, concrete is a porous material meaning that aggressive external agents such as chlorides, carbon dioxide or sulfates can penetrate it and compromise its durability. In order to avoid this, the material must have a specific W/C ratio in its mix design that will reduce the porosity and a permeability of the cement matrix slowing down these processes. EN-206 [1] has established exposure classes with maximum values for the W/C ratio based on the exposure conditions that the structure will have, these values are usually lower in comparison with the

W/C required to achieve the design strength of that particular structure.

Having said that, it can be seen that the W/C is fundamentally important parameter in a mix design of concrete, it not only defines fresh and hardened state properties but also its durability[2]. In practice, it is a reliable indicator to assess the quality assurance of concrete production and to estimate the durability of a structure [3], especially if a forensic analysis is required when the material doesn't perform as expected.

Several techniques have been proposed to obtain the W/C ratio of an existing concrete structure, most of them relied on correlations between the W/C and the concrete capillary porosity. Other techniques propose the actual quantification of water and cement by different methodologies (See section 2.4). Although there can be found different techniques in the literature, only two of them have been standardized, Nordtest Build NT 361-1999[4] and BS 1881-124[5]. The former proposes an approach based on a correlation between capillary porosity and W/C and the latter based on the quantification of water and cement. Nevertheless, both techniques have their own limitations. Concerning the NT 361-1999 some authors claim to obtain a accuracy within +/- 0.01 [6, 7], although other researches disagree [8, 9] and said that the accuracy is of 0.10, which is the same as for the BS 1881-124.

Since only two methodologies have been accepted as standards, it is of interest to propose new approaches and analyse their viability and precision in comparison with the current standard. In this case with the NT 361. Likewise, since the NT 361 is the most commonly used method, it can be worthy to analyse the different aspects of the technique and how they can affect the final results, either positively or negatively.

1.1. Objectives

- Main objective

  In this study the main objective is to estimate and compare the W/C of different CEM I concrete samples cast and cured in lab conditions with known and unknown mix designs using four different techniques; circular polarization microscopy (CPL), UV light microscopy, thermogravimetric analysis (TGA) and scanning electron microscopy (SEM). The results will be analyze in order to define the precision, advantages and disadvantages of each technique.

- Secondary objectives

  The secondary objectives of this study can be summarized as follows:

  - The circular polarization microscopy technique is a feasible method to analyze the calcium hydroxide clusters in the concrete. It is of interest to check if there is any correlation between variation in quantity and distribution of the Portlandite clusters and the W/C ratio of concrete.
  - The feasibility of the Nordtest Build NT 361-1999 will be evaluated. The influence of the amount of the fluopigment in the low viscosity epoxy, the thickness of the thin sections and

the use of reflected and transmitted light for the light intensity measure will also be study.

- The TGA technique will be used to quantify the amount of calcium hydroxide in the concrete and then analyze if it can be used to estimate the W/C of the concrete samples. Also, it will be compare with the amount of calcium hydroxide obtained with CPL.
- The scanning electron microscopy (SEM) + Powers and Brownyard model method proposed by Wong *et al.* [10] will be replicated in order to compare its results with the other techniques.

1.2. Research question

Is the Portlandite content quantification through CPL a more reliable and reproducible technique for the W/C estimation in CEM I concrete in comparison with the UV light, SEM + Power and Brownyard model and Thermogravimetric analysis?

1.3. Project plan

The samples used for the present work are divided into two sets. The first samples correspond to thin sections from Delft University of Technology and the second to the concrete samples from a Round Robin test performed by the Applied Petrograhpy Group (APG). The aim of the Round Robin test was to estimate the W/C of unknown concrete samples using the UV light approach or any other methodology, and then compare the values obtained between the different laboratories. Likewise, the project was divided into three parts, sample preparation, micrograph acquisition and ignition of powderized samples, and data analysis.

Initially, depending on the different techniques, i.e. UV light and CPL, TGA and SEM, the concrete samples were prepared as thin sections, powderized and polished sections, respectively. In the second part, micrographs of the thin and polished sections were acquired by the optical and electronic microscope respectively. For the TGA, the samples were ignited and the change of mass during the process was determined. In the final stage, the micrographs and the data from the TGA were processed and analyzed. Conclusions and recommendations were made. Figure 1.1 shows the the origin of the samples and the techniques that were applied and figure 1.2 gives a schematic view of the project plan.

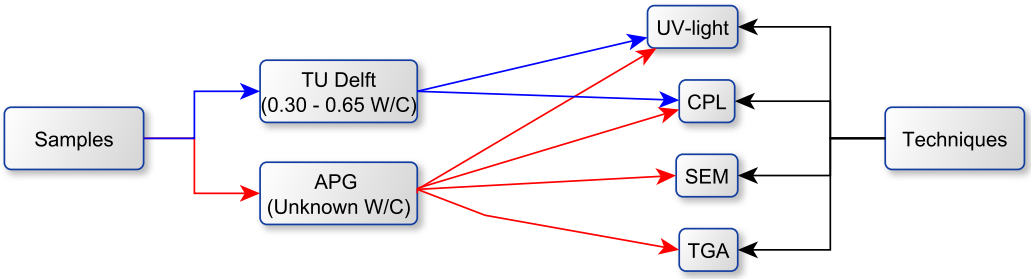

Figure 1.1: Samples and techniques

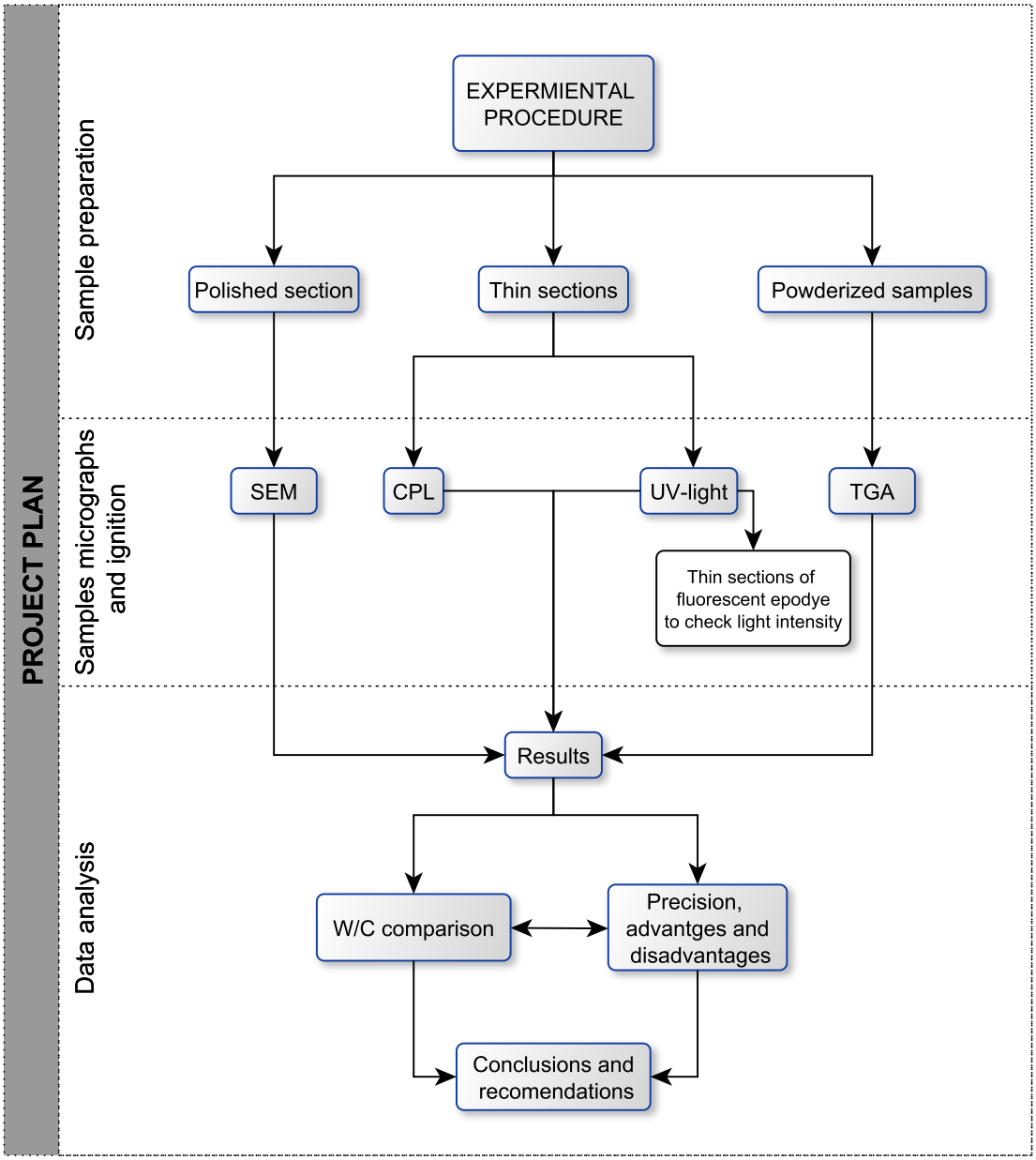

Figure 1.2: Schematic view project plan

2

Literature Survey

2.1. Defining water to cement ratio (W/C)

Water to cement ratio is defined as the mass of water and cement available that are in the mixture of a cement paste, mortar or concrete at the moment of casting. The parameter is considered to be one of the most relevant in concrete technology since it has a major influence on the mechanical properties and durability of the material.

It is important to distinguish the amount of water and cement that are used for the W/C ratio. For the former one, the water to be used is the free water in the mix, meaning that is the one available for hydration at the moment of mixing [8]. It can be influenced by the moisture of the aggregates which can change the result of the W/C up to 0.05 in comparison with the original value, either by adding or removing water from the mix. The water lost due to bleeding can change the W/C up to 0.1 especially in mixes with high W/C [11].

Modern cements are usually produced by blending Portland cement with mineral admixtures (SCM), therefore it has been claimed that the correct term for the W/C of this type of cements should not be "water to cement ratio" but "water to binder or cementitious material ratio". Nevertheless, since most of the cements include SCM, the term "water to cement ratio" is commonly used, although it is important to keep in mind that the SCM must be taken into account when computing or discussing about this value [9].

2.2. Hydration process

The hydrated cement is composed of solid hydration products and gel pores. The former includes the non-evaporable or chemically bound water, which can be estimated as 23% of the dry mass of the cement, although it is important to keep in mind that it depends on the type of binder to be used. Its volume is defined as the sum of volumes of anhydrous cement and water less 0.254 of the volume of

non-evaporable water [2]. It can be expressed as:

$$V_{HP} = \left[V_C - 0.23 \times M_C \times (1 - 0.254)\right] \times \alpha \tag{2.1}$$

Where:

- V_{HP} = Volume of hydration products
- V_C = Volume of cement
- M_C = Mass of cement
- α = Degree of hydration

Likewise, it can be assumed that for an ordinary Portland cement paste the gel porosity was reported as 28% [2], then one can solve from the following equation the gel water:

$$\frac{V_{gw}}{V_{HP} + V_{gw}} = 0.28 \tag{2.2}$$

Where

- V_{gw} = Volume of gel water

Once the non-evaporable and gel water are known, the remaining water in the mix (if there is) will turn into capillary water. Furthermore, if there is still a difference of volume between the original volume of water and cement, and the hydrated cement and capillary water, the difference will be equal to the empty capillary pores also known as capillary dry. Both type of capillary will contribute to the final capillary porosity of the cement paste [2]. The expressions for the capillaries are:

$$V_{cw} = V_W - V_{NonW} - V_{gw} \tag{2.3}$$

$$V_{cd} = V_C + V_W - V_{HP} - V_{gw} - V_{cw} - V_C \times (1 - \alpha) \tag{2.4}$$

Where

- V_{cw} = Volume of capillary water
- V_{NonW} = Volume of non-evaporable water
- V_W = Volume of water
- V_{cd} = Volume of capillary dry

From the equations, it can be seen that for a constant cement mass, a higher content of water will imply a higher W/C ratio and therefore higher capillary. However if the amount of water is lower than the required for full hydration, the cement paste will never be able to reach its fully degree of hydration, and some unreacted cement grains will stay in the matrix. Likewise, the capillary pores are a function of the degree of hydration, so young concrete will always have a higher capillary in comparison with an old one with the same characteristics. Figure 2.1 shows the phase distribution of cement paste based on the W/C and the degree of hydration.

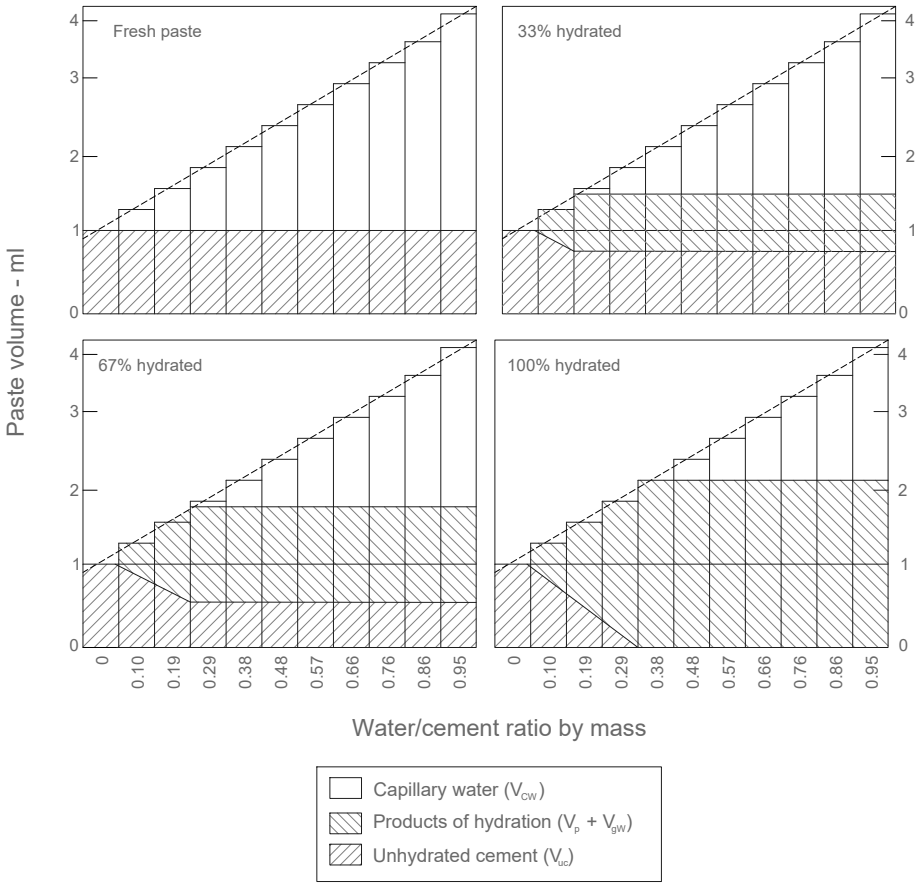

Figure 2.1: Relation between W/C, degree of hydration and cement paste phase [9, 12]

Finally, it is important to realize from equations 2.1 to 2.4 that the gel pores are independent of the W/C or degree of hydration, which means that the gel is formed at all the stages of the hydration and it depends mostly on the type of cement [8].

2.3. W/C and concrete properties

Although the hydration processes of cement are complex, the pore structures are directly related to the strength of the cement paste and the concrete. For instance, the typical strength of hardened cement is up 1000 times lower than the theoretically strength due to the Griffiths' theory of fracture mechanics [9, 13]. Micro-defects and discontinuities in the material cause stress concentrations at the tip of those areas. Cement paste has several discontinuities due to the volume of the pores (gel pores and capillary pores), which increases the stresses in the material reducing its ultimate strength.

The micropores are considered as the main flaw that affects the strength, therefore, as seen in section 2.2, a lower content of water and/or a higher degree of hydration will result in less pores (discontinuities), increasing the strength of the material. Likewise, a cement matrix will less capillaries is not only stronger, but it has a lower porosity and permeability, guarantying better durability properties since external agents cannot penetrate the cement matrix that easy. Figure 2.2 shows the relationship

between the water content and the different properties of concrete.

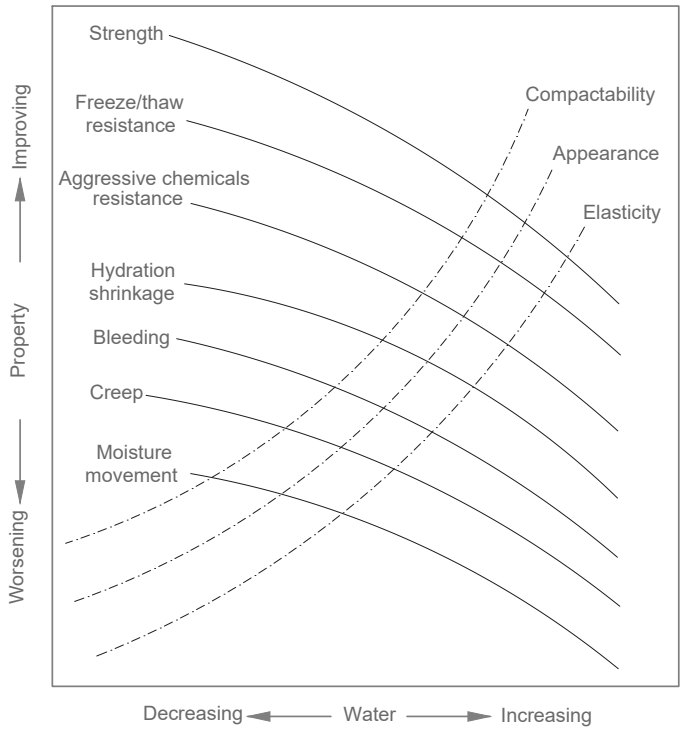

Figure 2.2: Relation between W/C, degree of hydration and cement paste phase [2, 12]

2.4. Parameters correlated with the W/C

Once the concrete has hardened, it is very difficult to go back to the original amount of cement and water in the mix design, since these components have a significant influence in the physical and mineralogical characteristic of the resultant concrete[9], most of the research has been focused on studying different parameters of the material that can be correlated with the W/C in a reliable and reproducible way. Nevertheless, this approach usually gives an indicative of the W/C since external factors can affect the measurement of the features. Current research also focuses on how to control and diminish the external factors in order to have more precise results.

There are mainly two parameters that have shown good correlation with the W/C, the capillary pores and the mineraological features. Measuring the porosity is the most common way to assess the W/C since it can be measured using different techniques, such as UV light and optical microscopy, scanning electron microscopy (SEM), Microwave and acoustic-ultrasonic wave, and chloride ion penetration and resistivity. UV light microscopy is the most common technique and its protocol has been standardized in the Nordtest Build NT 361 [4].

The mineralogical features to take into account are the Calcium Hydroxide (CH) content, the paste microhardness and the degree of hydration, being the former the most interesting of them. As it is shown in cement hydration equations 2.15 to 2.18 there is a relationship between the amount of Port-

landite and the original water and cement phases content, which is also affected by the degree of hydration of the cement paste. High W/C mixes will tend to have a higher degree of hydration and larger capillary pores. This scenario is favorable for the growth of the CH crystals. A higher degree of hydration implies a higher content of hydration products including the CH content. Likewise, in cement paste with high W/C, crystals can grow larger and tend to form cluster, while in cement paste with low W/C they will grow less and be uniformly distributed [9, 14].

$$C_3S + 5.3H = C_{1.7}SH_4 + 1.3CH \tag{2.5}$$

$$C_2S + 4.3H = C_{1.7}SH_4 + 0.3CH \tag{2.6}$$

$$C_3A + 3C\overline{S}H_2 + 26H = C_6A\overline{S}_3H_{32} \tag{2.7}$$

$$C_4AF + 3C\overline{S}H_2 + 30H = C_6(A,F)\overline{S}_3H_{32} + (A,F)H_3 + CH \tag{2.8}$$

The content of CH and the degree of hydration are obtained mainly by thermogravimetric analysis and differential scanning calorimetry (TGA-DSC). Also, optical and scanning electron microscopy are used for the CH content. For the former, Çopuroğlu [15] proposed a new way of quantifying the Portlandite by introducing the circular polarization microscopy (CPL) which promises to be an alternative technique for the estimation of W/C using thin sections.

It is important to clarify that even though one can say that a higher W/C indicates a high degree of hydration, this correlation will oversimplify the problem, since parameters as curing and cement composition have an important influence on it, so this feature on its own will only give a rough estimation of the W/C [9]. Through microindentation, the microhardness of the cement paste has been correlated with the W/C with promising results [16], unfortunately the literature about it is very limited.

Other methodologies have a direct approach in which the goal is to quantify the actual amount of cement and water in the hardened concrete. The BS 1881-124 standard [5], proposes a physico-chemical procedure, in which the cement content is obtained through a chemical analysis and the amount of water through a physical one. This method has several limitations which will be discussed later. Wong and Buenfeld [3] proposed a methodology that estimates the W/C by quantifying the phases of cement paste using SEM and then by using the model of Powers and Brownyard the initial content of cement and water is obtained.

Figure 2.3 shows the different techniques used to measure the W/C, both indirectly through the different parameters and directly by quantifying the actual values of water and cement. Each of them have their own advantages, disadvantages and limitations, which will be discussed in the coming paragraphs.

2.5. Indirect Measurements of the W/C

2.5.1. Porosity

1. Transmitted UV light microscopy

   The UV light microscopy method for thin sections is one of the most common techniques to estimate the W/C either for research purposes or in the field. The protocol has been standardized in

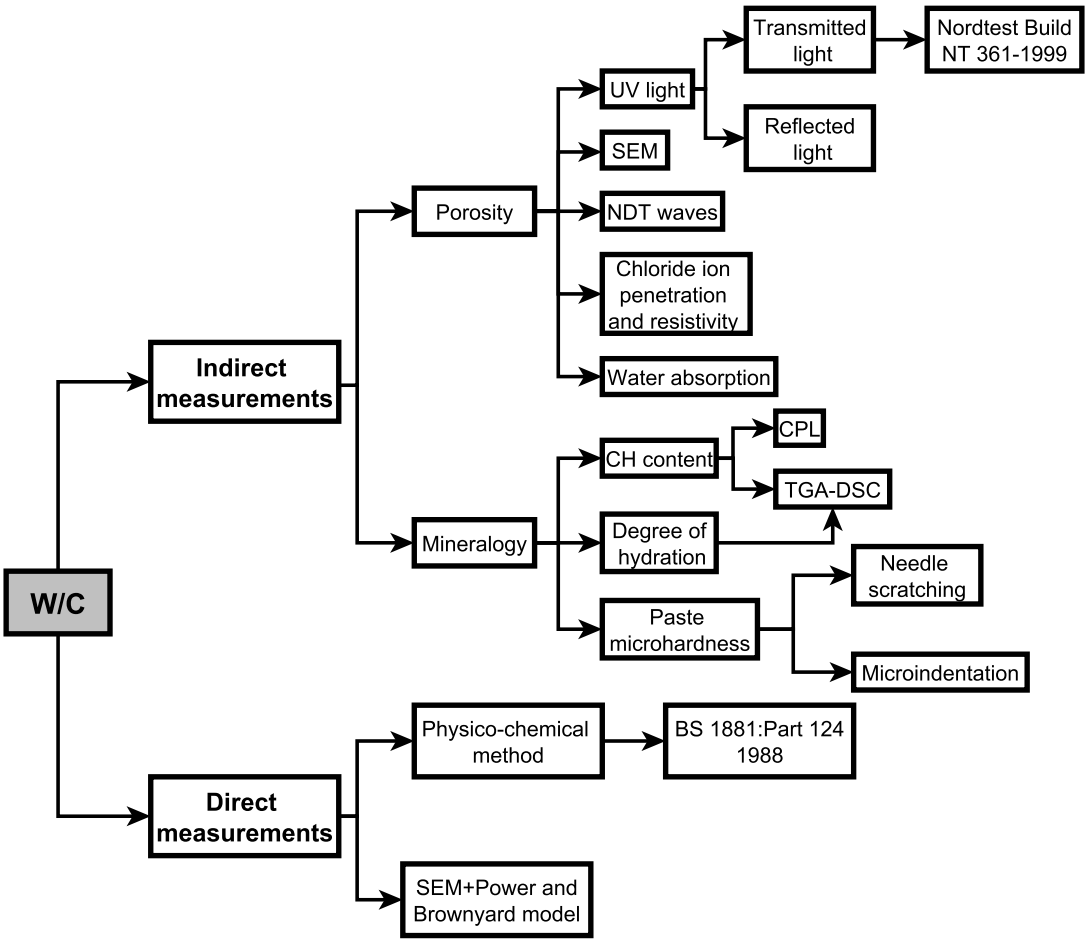

Figure 2.3: Available techniques to measure W/C

the Nordtest Build NT 361 [4] and several literature can be found about, allowing to have a good insight about the pros, cons and limitations of it.

The method is based on a very simple but reliable principle, after the concrete sample has been prepared (See section 3.2.1), the thin section is placed in a petrographic microscope that can provide UV illumination and the fluorescence intensity is measured. The fluorescence intensity of the sample is directly proportional to the amount of low viscosity epoxy resin that went inside during the samples preparation, which is a function of the amount of pores in the cement paste that also depends on the W/C ratio as it is seen in figure 2.4.

The method relies on comparing the fluorescence intensity of the unknown sample with the one of standard samples with different W/C, and then the W/C of the unknown samples can be estimated. It's worth mention that the standard sample have to be made of concrete cast in lab conditions, in which external parameters that can affect the hydration or the microstructure are controlled.

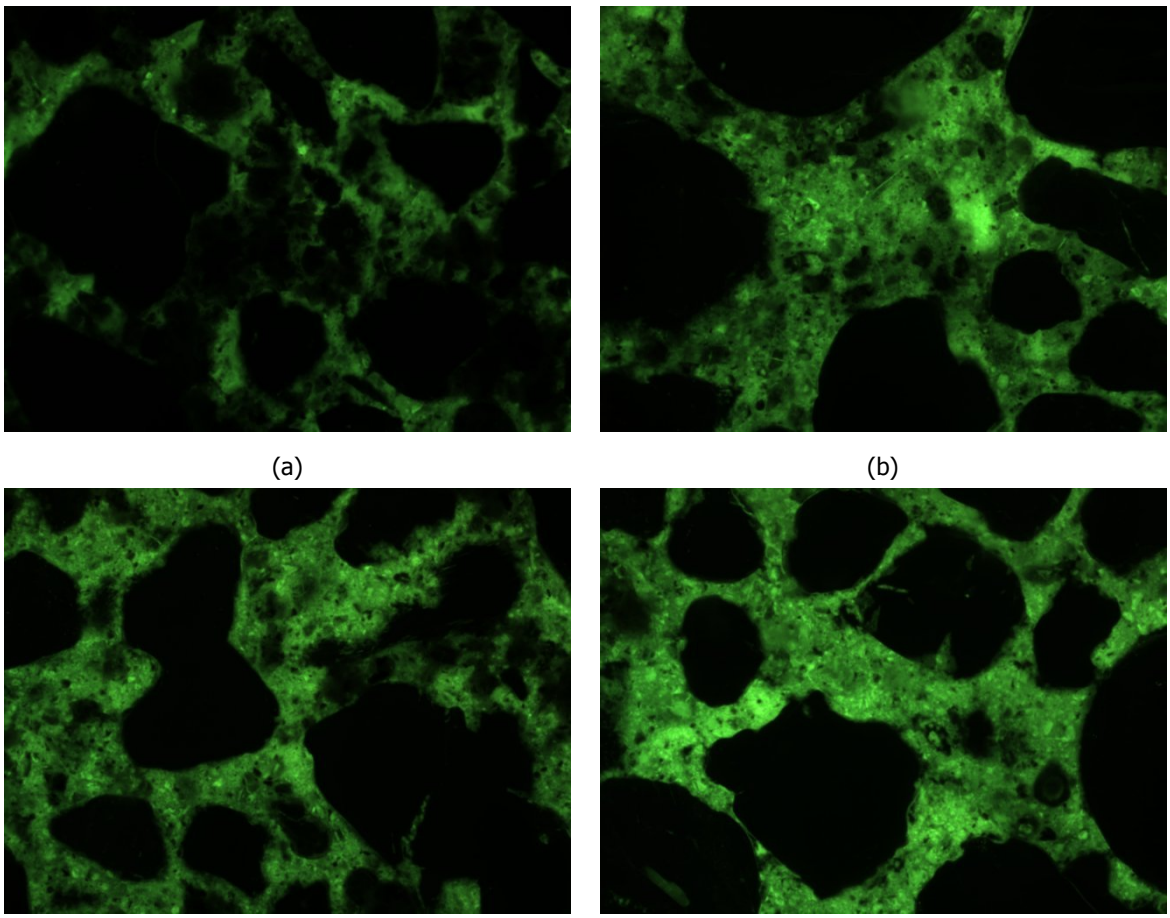

Figure 2.4: UV light intensity vs W/C. (a) W/C = 0.40. (b) W/C = 0.45. (c) W/C = 0.50. (d) W/C = 0.60.

It is important to realize that since the method is based on comparison, the concretes that are going to be use must be similar in terms of cement type, degree of hydration and in some cases aggregate type otherwise the measurements are most likely to be affected [6, 17, 18]. The first two parameters, affect the amount of pores in the sample, as it is known, for two exact concretes, a young one will have more pores than a mature therefore a comparison between them will not be reliable. Because of it, this technique is usually applied in mature concrete where it can be assumed that the hydration of the cement has stopped and there is a good correlation between the capillary porosity and the W/C [6].

When a cement with mineral admixtures is used, the microstructure of the paste changes. For instance, in comparison with only OPC, the blended cements microstructure takes more time to develop but at the end it has less pores than the OPC. Likewise, the microstructure of the concrete cannot be carbonated or affected by any other external factor that changes the porosity of the cement paste.

In the case of slag, Einarsson and Copuroglu [19] measured the W/C at 28 days for concrete with CEM I and CEM III/B. The R^2 for the latter was lower that the CEM I probably due to the

phenomenon of greening. The same procedure was repeated after a year [20], but the greening from the samples was controlled by putting the samples in a dry and oxygen rich environment. The correlation for the CEM III/B samples increase considerably, while the CEM I samples remained almost constant. Also Sibbick *et al.* [21] established that the translucidity of blended cements are higher than the OPC, so the intensity of fluorencese that is measured in the thin sections, even if they have the same thickness, will always be higher. These two examples show the importance of using standards with the same cement type and degree of hydration as the ones of the unknown samples.

Another issue with this technique is the sample preparation, Jakobsen and Brown [7] claimed that this is the most critical part of the method, since the final quality of the product is directly affected by the experience of the technician in charge and the equipment available. Common mistakes in the sample preparation are the wrong amount of epodye, a bad impregnation, a scratch in the sample due to the grinding or a variation in the thickness [6].

Although, most of the literature emphasizes in using the right amount of epodye in the low-viscosity epoxy and the right thickness of the sample, there is not much literature about its actual influence in the final measurement of the intensity of fluorescence. For the sample thickness, Poole and Sims [9], St. John [22] has done a study and stablished that 3 µm thickness changes the light intensity by 10 %. Likewise, figure 2.5 shows the influence of the final value of the W/C and the thickness of the samples for a Round Robin test. The results show that, despite the variation of the data, thicker samples tend to have higher W/C values, confirming the importance of the right thickness of the thin section [7]. On the other hand, de Rooij *et al.* [23] developed a protocol using image analysis software which he claims it can compensate for the thickness or the light intensity of the light bulb by calibrating the histogram of the images.

The fluorescence intensity can also be affected by the microscope and/or camera settings,

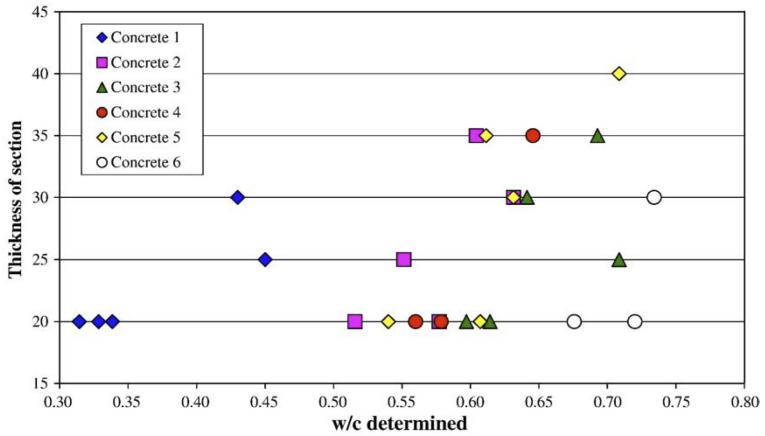

Figure 2.5: Correlation between the determined w/c ratio and the thickness of the thin section. Thickness is in µm[7].

a change in the light intensity of the bulb or a different aperture of the lenses at the moment

of capturing the photomicrograph can affect the final results. The unknown samples must be analysed with the same setting as the standard samples. If the settings of the standard samples are unknown, it is strongly recommended to recalibrate with new settings so the fluorescence intensity of all the samples (known and unknown) is measured under the same conditions.

When performing the measurements, one must be aware that the light intensity of the microscope faded during time affecting mostly the measurement of the last samples to be analysed. One of the samples drop the W/C value from 0.33 to 0.20 showing that one must be aware of the light intensity of the microscope [17]. Nevertheless, with current LED light bulbs, this phenomenon shouldn't take place since this type of light is stable in time.

Likewise, it is important to keep in mind that the thin sections must be kept in a dark place as the intensity of the fluorescent dye decreases in time and during exposure to light [6]. Sibbick *et al.* [18], Sibbick and LaFleur [24] showed the difference between samples of same W/C make in different years, 2002, 2006 and 2011 for different type of cements. The difference was larger for the blended cement samples since they have a different rate for degree of hydration.

Once the samples are ready, the petrographer should do several checks to guarantee its quality before performing any analysis [7]. Also, since the principle is based on the light intensity measurement, any source of light that doesn't come from the cement paste cannot be taken into account, for instance pores from the aggregates, cracks and areas with high content of air voids will affect the measurement [6]. The petrographer must be aware of it. In the past this was a difficult and time consuming task, but thanks to the improvements and availability of image analysis software it has been easier and faster to do, improving the precision of the method [19, 25].

Researchers in[7, 18, 21, 23–25], among others, agree on the fact that the UV light microscopy methodology is reliable even for cases in which the cement has mineral admixtures or the thin sections have different ages, showing that the method indeed is reliable and can give a good insight of the estimation of the W/C. However, one must be aware that most of the literature uses samples casted and cured under lab conditions, therefore as Elsen *et al.* [25] said in his conclusion, the results can't be transferred in a simple way to field concretes which is in most of the cases the ultimate goal.

In terms of precision, Jakobsen *et al.* [6] claims that their manual method can give a W/C value, by a trained operator, of 0.02 in a matter of seconds. Also, by using their semi-automatic method the precision can be up to 0.01 when the samples are stored under normal conditions. For field concrete, he showed two examples for the determination of the W/C, one for the Copenhagen Airport in 1994, in which they claimed to obtain the W/C with a precision of 0.006 and the other in concrete railroad ties with a precision of 0.026. Also, the authors discuss about a Round Robin test that is performed every year in Denmark, and showed that the W/C is estimated with a precision lower than 0.03 in most of the cases. The 3 cases show that the method is precise and can be reproduced in different situations.

Likewise, Jakobsen and Brown [7] discuss about Round Robin test in which the thin sections were made by technicians with different skills and then they were analysed by petrographer with also different skills. The result showed that the W/C of samples from the field could be obtained with a precision of 0.03, showing once more the usefulness of the method.

Although the results in [6, 7] show that the method can actually be reliable and reproducible, Neville [8] used basic statistics to proof that the accuracy stated in the former paper was unfounded. Neville [8], Poole and Sims [9] agree on the fact that both papers don't support sufficiently their results. Instead, they concluded that the best precision that the method could get is 0.05 but in most of the cases it is 0.1, which is already obtained by the BS 1881:Part 124-1988. This is a very valuable remark, although it is important to realize that the results can be highly spread since concrete is a very heterogeneous material, meaning that in order to have an accurate value several samples must be analysed.

2. Reflected UV light microscopy

As it was mentioned, the preparation of thin sections can be challenging and a bad sample can affect the final results. Mayfield [26] decide to try a new approach in which he used polish sections that are less difficult to prepare in comparison of the thin sections. Using the adequate equipment, he measured the emitted radiation from the samples using a photo-diode integral amplifier.

The methodology was executed on cement paste, mortar and concrete. For the cement paste, the correlation obtained was good. The results for the mortar were affected by the dark areas of the sample due to the small sand grains and the unhydrated cement, so an adjustment was done to correct the dark areas, and the calibration curves included the sand/cement ratio. The concrete had a similar problem as the mortar, although fewer samples were analysed in order to have a final reliable conclusion. He concluded that this technique had a good feasibility and corrections due to voltage and fine aggregate/cement ratio were necessary in order to obtained more precise results. Unfortunately no further research has been done using his technique.

In paper [26], the author doesn't discuss about the limitations of his work, but since it is based on the same principle as the UV light transmitted, one can say that its limitations are similar to the ones found on the latter technique. The samples must have a similar cement type, degree of hydration, amount of epodye in the low viscosity epoxy and non-affected microstructure. In terms of the microscope the settings must be the same for all the samples. Also in order to estimate the W/C of unknown samples, standards are required. On the other hand, the samples don't have the problem of achieving a specific thickness and the use of mineral admixtures will not affect the translucidity as Jakobsen and Brown [7] stablished for thin sections.

3. Scanning electron microscope - SEM

Sahu *et al.* [27] proposed a technique based on BSE, in which he measured the porosity of concrete polished sections that had been previously vacuum impregnated with epoxy. The method

relies on the difference between the average backscattering coefficients of the compounds of the material. Using image analysis, the author proposed a thresholding from 0 to 55 on a 256 scale (0 to 255) to segment the pores from the rest of the other phases.

In the same way as the optical microscopy methodologies, any zones of the paste that were affected by carbonation or any other phenomenon were discard. Voids from aggregates or entrained and entrapped air must be discarded too. The method showed a very good correlation, $R^2 = 0.99$, and it was compared with the Nordtest NT 361 and the correlation between them was $R^2 = 0.89$.

In general terms, it can be said that this method has the same pros and cons as the one proposed by Mayfield [26] , with the extra advantage that the concentration of epodye in the epoxy will not affect the final result. Nevertheless, a big disadvantage of this methodology is that it requires SEM which is not always available in many consultancy companies or even universities or research centers.

4. Water absorption

Liu and Khan [28] proposed different techniques to estimate the W/C, one of them relies on the absorption of a drop of water in the concrete surface that has been previously lapped in order to measure the resistance to Needle Scratching. Although the authors found a good correlation between the time that the drop of water disappears and the W/C, they emphasize that the technique should be used in companion with other methodologies and not as stand-alone technique.

The authors established that the type of aggregates can affect the measurement. One can also add that the amount of aggregates can also influence the measurement. Taking into account that must of the porosity of the concrete comes from the cement paste, an increase in the aggregates content will decrease the overall amount of pores in the concrete, therefore a concrete with a low W/C could have a similar time than one with high W/C but high aggregate content. Furthermore, the test must be done in an environment where the relative humidity and the temperature are controlled. For instance if the former has a higher value, it can saturated the sample and increase the time of the water absorption, which will lead to a wrong estimation of the W/C.

5. Non-destructive test: Microwave and acoustic-ultrasonic waves

The use of non-destructive test (NDT) and semi-destructive test for concrete is commonly used, especially in order to estimate the strength of the material. Although some of the techniques have a limited used since their results are not correlated properly with the actual strength of the concrete.

Zoughi *et al.* [29] proposes the use of microwave to obtain the W/C of cement paste and then correlated it with the strength of the material which was their ultimate goal. The samples used for the experiments had different W/C and then they were tested at different ages. The results

showed that the microwave measurements change with the hydration of the samples. The research also showed that a swept microwave frequency technique or a change in the reflection coefficient is related to the W/C, therefore these wave parameters could be correlated with the W/C and then with the strength of the concrete. A similar approach was done by Philippidis and Aggelis [30] using acoustic-ultrasonic waves. They determine the W/C of the samples by formulating a cross-correlation technique and the coherence function of different waveforms. The research also concludes that the measurement of the waves is influenced by the compressive strength, age and water content of the samples.

6. Chloride ion penetration and concrete resistivity

In a similar way as the epoxy or the water absorption, a relation between porosity and chloride ion penetration and resistivity relies on the fact that a mix design with high W/C will have several pores and a higher permeability, allowing chloride ions to pass easily through it and reducing the resistivity of the material.

MacDonald and Northwood [31] proposed a methodology to measure the W/C and the chloride ion diffusion by resistivity measurements of concrete. They obtained a good correlation between the resistivity and the W/C, but this was not stated as a conclusion in their report. Likewise, they established that further investigation regarding the ITZ and the transport phenomena had to be done.

The ASTM C1202[32] had established that the chloride rapid diffusion coefficient test could give a rough estimation of the W/C, although this oversimplified the problem, since the classification didn't take into account parameters such as type of cement or degree of hydration. In the newer version, ASTM has removed this correlation from the standard.

Overall, one can find in literature that there is a strong relationship between the W/C and the Chloride diffusion penetration or the resistivity, nevertheless, there is not a reliable correlation between the former and the two others. For instance, the external humidity, water content and temperature of the sample are some of the parameter that can affect the transportation measurements [33] which can lead to a wrong correlation with the W/C.

2.5.2. Mineralogical

1. Calcium Hydroxide (CH) content

In general terms, few authors have discuss about the relation between the CH and the W/C. Sibbick *et al.* [18] comments about the Portlandite and says that it has some issues that doesn't make it easier to use. For instance, the CH can be consumed in the presence of mineral admixtures and the crystals can be masked by the presence of calcite fines.

Larsen [34] proposed a methodology to quantify the CH crystals on cement paste and gave an example on how it can be used to investigate the leaching by CH in an existing structure. The

procedure is based on linear point counting, and it emphasizes that the sample must be rotated 45° in order to unveil the extinct parts of the crystals. The paper concludes that this method can be a reliable way to quantify the CH although it doesn't discuss about the need of rotating the sample and how it can affect the final results.

The issue of revealing the extinct phases of the Portlandite has been tackled by Çopuroğlu [15] who proposed the used of CPL in order to unveil the entire clusters. One of the big advantages of the technique is that the equipment required for the Nordtest NT 361 and the thin sections themselves can be used for it. For the CPL, two quarter-wave filters are required, which can be easily adapted to a petrographic microscope.

On [15] the technique was applied only to cement paste and the quantification of CH was done using optical microscopy and SEM. Both techniques showed similar results. Since the methodology has only been used in CEM I cement paste, it is of interest to analyse how the results can vary when it is applied to concrete. As mentioned earlier, already the distribution of CH is different depending on the W/C of the samples, now by having the heterogeneity of the concrete, it can be expected that some crystals will probably form in the ITZ, since it is easier for them to grow in this area due to the fact that the voids tend to be larger in comparison with the rest of the matrix.

The methodology shares some of the disadvantages and limitations of the UV light method. The samples must have the same cement type and degree of hydration and any zones of the paste that has been affected by carbonation or any other phenomenon that affects the CH content must be neglected. Likewise, the estimation of the W/C is done by comparison, therefore a set of concrete standards, similar to the one of the unknown sample, is required. As an advantage, the presence of cracks or any other feature (that could be an extra source of light in the UV light method) doesn't affect the measurements.

In terms of the thin sections preparation, as it can be seen in figure 2.6, the thickness influences the quantification of the amount of the CH crystals, therefore the samples must be around 30 - 34 µm . The content of the epodye in the low viscosity-epoxy and its ageing effect are irrelevant since the technique doesn't require any fluorescence. Still, its use is advisable since the same thin section can be used to perform the current methodology and the Nortest NT 361, so one technique can be used to control de other one.

On the other hand, the mineralogical properties of concrete, in particular the cement paste, can also be measured by the TGA-DSC technique. By burning a powderized sample, one can measure the chemically bounded water, the different compounds of cement paste such as gypsum, CH and CSH, the degree of hydration and the degree of carbonation among other parameters [35]. For this particular case, the amount of CH is of interest, since it can be correlated with the W/C of the concrete.

For this case, the sample preparation of this technique is simpler in comparison with the mi-

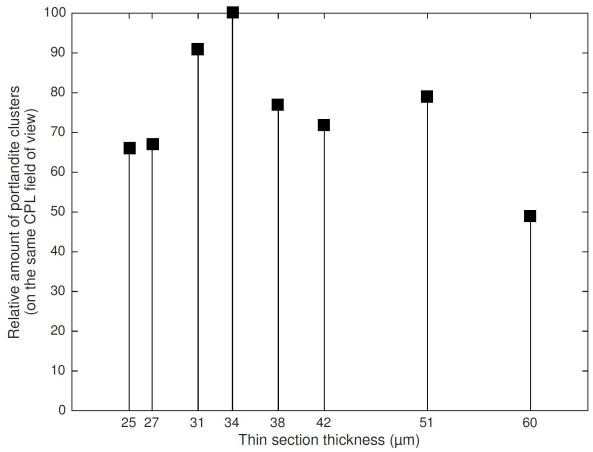

Figure 2.6: Effect of thin section thickness on the portlandite content estimation[15]

croscopy techniques, the sample, either concrete or cement, ”only” has to be powderized and dried until constant weight. Then it is ignited up to 1000° C. The advantages of measuring only the CH is that it dissociates at a 460 °C (for calculation the mass loss between 400°C and 500°C is commonly used [35]), therefore in theory other dissociations such as the $CaCO_3$ from the calcareous aggregates will not affect the measurements, although if the sample is carbonated, the CH content will be underestimated with respect to the real one. In case of having concrete or mortar, one must know the amount of cement paste in the sample which can be challenging in some cases. By knowing the amount of cement paste in the sample, one can know the cement/aggregate ratio and normalize the cement content in order to correlate the Portlandite quantity with the W/C of the sample.

2. Degree of hydration

The degree of hydration is defined as the amount of cement that has fully reacted with water relative to the total amount of cement in the mix. It has a direct relation to the chemically bound water that is in the cement paste [36], therefore by knowing this value one can obtained the degree of hydration of a given sample. The chemically bound water is measured using the TGA-DSC technique. Its value is equal to the weight difference of the sample after drying to 105°C and after ignition to 1000°C.

Once this value is obtained, the degree of hydration can be found by dividing the chemically bound water by the W_n/C ratio of the same or very similar cement. The W_n/C is the ratio assumed for a fully hydrated sample and it varies between 0.18 and 0.26 [36]. Nevertheless, the difference between the weights can also be due to other compounds such as CO_2 either from carbonation or calcareous aggregates or from water inside the aggregates.

As mentioned before, using only the degree of hydration to correlate with the W/C will oversimplify the problem [9]. Instead, this parameter is mostly used as a tool to monitor the hydration of the concrete and how that can be related to the development of the mechanical properties of the material.

3. Paste microhardness

   The paste microhardness has been addressed in two different ways. Liu and Khan [28] used lapped concrete samples and established three categories for the W/C estimation of the specimens. Within each category, the W/C could be estimated with a precision of 0.05. The method is qualitative since in order to establish the category in which the samples could be placed, they used adjectives such as "hard", "smooth", "easy to break", "soft" or "dense" that are not define in the document. Also, it is mentioned that the specimens with lower W/C looked darker in comparison with the ones with higher values, but again without quantifying the intensity or color of the concrete. Finally the authors concluded that a harder paste is related with a low W/C but no graph or correlation value was given.

   Erlin and Campbell [16] proposes a more detailed analysis, using ASTM 384[37] and ASTM E 18[38] they estimate the microhardness of cement paste and correlated with its W/C. The techniques chosen, Knoop and Rockweel, had the advantage over other indentation techniques that they could fit easily between the aggregates of the concrete. In order to do the test, the surface of the samples had to be flat and lapped or polished so the indentation could be measured by means of optical microscopy and then the microhardness could be obtained. The results of the experiments showed a non-linear relation between the W/C and the microhardness in both cases. The Rockwell results could allow for better estimation of the W/C since its graph is more linear and has a greater slope. Furthermore, the paper emphasizes that several research need to be done in order to check the influence of parameters such as degree of hydration, carbonation and indentation size among others.

2.6. Direct Measurements of the W/C

2.6.1. Physico-chemical method

The physico-chemical method establishes the W/C ratio by measuring the amount of cement and water in the sample, the former one is obtain by a chemical measurement and the latter one by a physical one.

For the cement content, the BS1881-124[5] method employs the determination of soluble silica and calcium oxide content to estimate this value in the concrete. The content of the two compounds in concrete is compared with determined or assume values in the cement, then the approximate cement or binder contents in the concrete are calculated [9]. The uncertainty of the methodology relies on the analysis and validity of the content of the soluble silica and calcium oxide used in the calculations. Moreover, most of the modern concrete mixes are out of the scope of the methodology, since it can only be used for Portland cement and in "favorable circumstances" slag. Also, the method can only be used in concrete that doesn't include aggregates with acid-soluble calcium.

The water content is divided in two parts, the water used for hydration and the excess water. The former one is obtained from a pre-dried sample by ignition. The remaining part is measured from the volume of the capillary pores, which is determine by vacuum saturation of a dried sample with a liquid of known density. The problem with the latter water, is that any void, crack or extra pore that is inside

the sample will affect the final estimation of the measurement.

For both of the components, there are different aspects that can affect the measurements, therefore it is expected that the final result for the W/C has a precision of 0.1 [8]. Likewise, the TR 32 precision trial for physico-chemical method decide to advise that the method "did not appear to be sufficiently accurate to provide useful data to the end user".

2.6.2. Scaning electron microscopy (SEM) + Powers and Brownyard model methodology

Wong and Buenfeld [3] proposed a new methodology based on the use of FE-SEM to quantify the phases of the hardened cement paste and then with the use of Powers and Brownyard's model, the original content of free water and cement are estimated. The methodology also allows to measure the degree of hydration of the sample at any point in time and it has the advantage that doesn't require standards to obtain the W/C. So far, the method has been applied on cement paste, mortar, concrete and cement paste with additions of slag [11, 39].

The methodology establishes that at first there is a given volume of water and cement, and then after they are mixed the hardened cement paste is composed of 4 phases independently of the point in time. The phases are the remaining unreacted cement, the hydration products including the gel pores, the capillary pores and the air voids or deliberate entrained air. The latter ones can be neglected since their volume don't change in time. Furthermore, the method assumes that the chemical (Autogenous) shrinkage can be neglected since it is small. Figure 2.7 and equation 2.9 shows the phase diagrams of each stage and the equilibrium between them respectively:

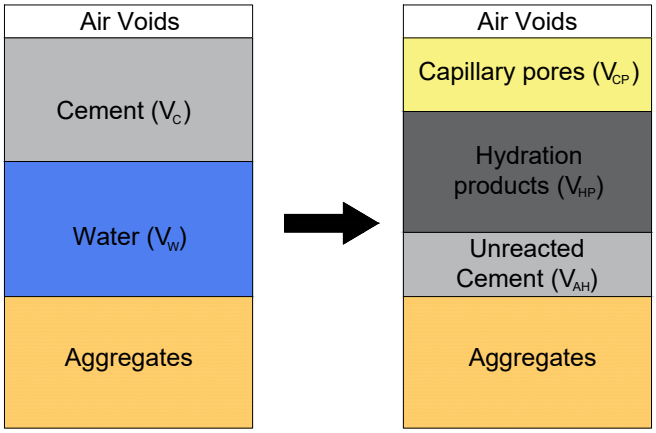

Figure 2.7: Schematic representation of the phase diagrams volumes at the initial time of set(a) and at time t after intial set (b). [11]

$$V_C + V_W = V_{AH} + V_{HP} + V_{CP} = 1 \tag{2.9}$$

Where:

- V_C = Volume of cement

- V_W = Volume of water
- V_{AH} = Volume of anreacted cement
- V_{HP} = Volume of hydration products
- V_{CP} = Volume of capillary pores

Likewise, the volumetric ratio of hydration products to the reacted cement δ_v relates the volume of the hydration products in comparison with the original cement content. This value is often assumed as 2.0 and is a function of the cement chemical composition. A precise value of the δ_v can be obtained by using the Powers and Brownyard's model. By knowing it, the original content of cement can be written as [3]:

$$V_C = V_{AH} + \frac{V_{HP}}{\delta_v} \tag{2.10}$$

Then from equations 2.9 and 2.10, the original volume of water can be express as:

$$V_W = V_{HP} \times \left(1 - \frac{1}{\delta_v}\right) + V_{CP} \tag{2.11}$$

Since the original content of cement and water have been found, the W/C is expressed as:

$$\frac{w}{c} = \frac{V_W}{V_C \times \rho_c} = \frac{V_{HP}\left(\delta_v - 1\right) + \delta_v V_{CP}}{\left(\delta_v V_{AH} + V_{HP}\right)\rho_c} \tag{2.12}$$

Finally the degree of hydration of the cement paste can be express as:

$$m = \frac{V_C - V_{AH}}{V_C} = \frac{V_{HP}}{\delta_v V_{AH} + V_{HP}} \tag{2.13}$$

To obtain the phases of the hardened cement paste, the samples are first vacuum impregnated with epoxy and then polished with diamond up to 1/4-µm. Then, the samples are taken to the FE-SEM and the BSE images are obtained. Since the pixel value of the BSE images is based on the average backscattering coefficients of the compounds of the material, Wong, defined different thresholding to segment the images into the three desire phases.

For the unreacted cement, the authors choose the minimum grey value between the peaks of the hydration products and the unreacted cement. For the capillary pores, the "overflow" method was applied [10]. The inflection point of the cumulative bright mess histogram is taken as the upper threshold value. This is obtained from the intersection of two best-fit lines in the cumulative brightness histogram. The hydration products are obtained by subtracting the other two phases from the images. It is important to say that the method consider the hydration products as whole, so for instance it doesn't take into account the difference in pixel value of the CSH or CH. It is important to mention that during the segmentation process elements that shouldn't no be considered must be excluded from the quantification, for instance entrapped air and cracks. An example of the segmentation is shown in figure 2.9:

The results obtained by Wong were promising, since the author obtained accurate results for the W/C and the degree of hydration of the samples, even when the samples had different ages (3-90 days). Likewise, the method is quantitative so it doesn't require standards in comparison with the

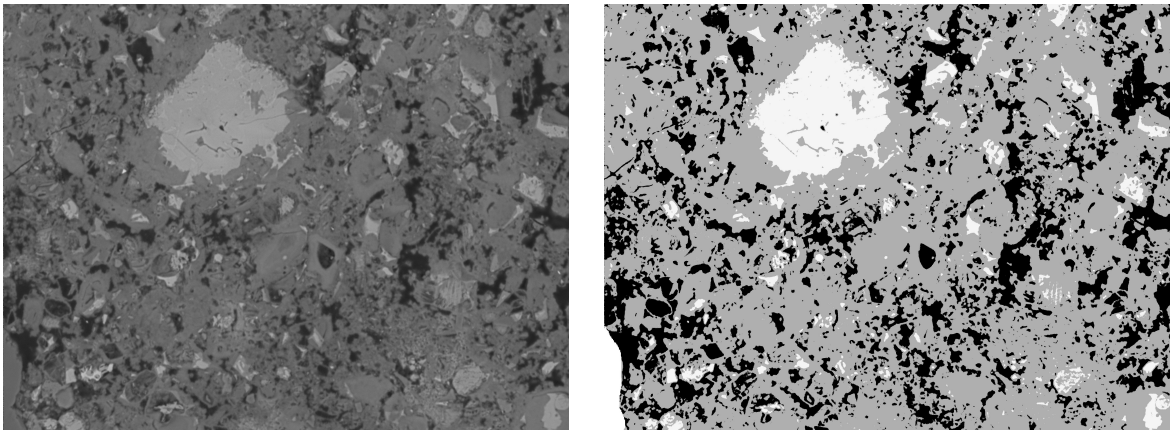

(a) (b)

Figure 2.8: Segmentation APG Sample D

optical methods, although like the previous methodologies, the microstructure of the concrete cannot be affected by carbonation or any other phenomenon that changes the original microstructure of the cement paste.
In [11], the same principle was applied in mortars and concrete with different ages and cure under different conditions. For this case, since the volume of aggregates doesn't change in time (like the entrained and entrapped air) they can be neglected from the phase diagrams, so the equations from [3] can be used as well. After the BSE images were taken, the aggregate phases were removed from the images. First, white boundaries were traced around them, then using binary images the aggregates were segmented and remove from the original images. Likewise, since mortar and concrete microstructures are more heterogeneous in comparison with cement paste, the method required a higher amount of images to process in order to obtain reliable results.

An important remark for this technique is the quantification of the change in water content due to the aggregates moisture and/or bleeding during the hardening period. For the former, the difference in the W/C could change up to 0.1 and in the latter up to 0.05(especially in mixes with high W/C). Although it is important to keep in mind that if these conditions are not taken into account, it wouldn't mean that the results obtained are wrong since the methods measures the available (free) water that reacts with the cement, although the results will not be as expected.

The methodology from [3] was also extended to cement paste added with slag, nevertheless some changes were introduced due to the complexity of the case [39]. Figure 2.9 and equation 2.14 shows the phase diagrams of each stage and the equilibrium between them respectively:

$$V_C + V_S + V_W + V_A = V_{AH} + V_{US} + V_{HP} + V_{CP} + V_A = 1 \tag{2.14}$$

Where:

- V_C = Volume of cement
- V_S = Volume of slag

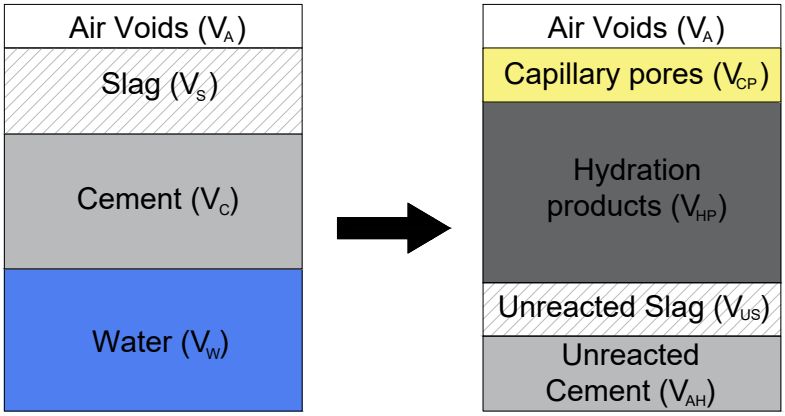

Figure 2.9: Schematic representation of the phase diagrams volumes at the initial time of set(a) and at time t after intial set (b). [39]

- V_W = Volume of water
- V_A = Volume of air voids
- V_{AH} = Volume of unreacted cement
- V_{US} = Volume of unreacted slag
- V_{HP} = Volume of hydration products
- V_{CP} = Volume of capillary pores

From equation 2.14, the original content of cement can be written as:

$$V_C = 1 - (V_S + V_W + V_A) \tag{2.15}$$

The volume of water is obtained by quantifying the evaporable and non-evaporable water in the samples. By knowing this value and the density of the slag and the cement, the water to binder ratio and slag to binder ratio can be written as:

$$\frac{w}{b} = \frac{V_W \times \rho_W}{V_S \times \rho_S + V_C \times \rho_C} = \frac{V_W \times \rho_W}{V_S \times \rho_S + [1 - (V_S + V_W + V_A] \times \rho_C} \tag{2.16}$$

$$\frac{s}{b} = \frac{V_S \times \rho_S}{V_S \times \rho_S + V_C \times \rho_C} = \frac{V_S \times \rho_S}{V_S \times \rho_S + [1 - (V_S + V_W + V_A] \times \rho_C} \tag{2.17}$$

Moreover, the degree of hydration of the slag and the cement can be written as:

$$m_S = \frac{V_{RS}}{V_S} \tag{2.18}$$

$$m_C = 1 - \frac{V_{AH}}{V_C} = 1 - \frac{V_{AH}}{1 - V_S + V_W + V_A} \tag{2.19}$$

The volume of unreacted slag and cement, reacted slag, air voids and limestone filler are obtained by point counting analysis. Furthermore since this methodology could introduce some error, EDS was used when required. Once these values are obtained, they are plugged in equations 2.15 and 2.19 in order to obtain the original volume of cement, the water to binder ratio and slag to binder ratio, and the degree of hydration of the slag and the cement.

2.7. Techniques of interest

A summary of the available techniques can be found in table 2.7. Once the revision and comparison of the techniques was done, it was decided that the methodologies to be used in this research are going to be the optical microscopy, both the transmitted UV light and circular polarization microscopy, the scanning electron microscopy + Powers and Brownyard's model and the TGA-DSC.

The microscopy methods were chosen because with them apart from estimating the W/C the microstructure of the concrete can be observed and analysed, which can be useful especially in forensic analysis. For instance for the W/C estimation, if part of the section is carbonated or with several voids, one can exclude that zone from the analysis. In contrast, the NDT wave methods, the paste microhardness and water absorption cannot tell about these aspects, then one can be analyzing a concrete that can be affected in the inside.

Although the TGA-DSC method doesn't take into account the microstructure of the concrete, it is rather easy in comparison with the other approaches, therefore if it proofs to give a good correlation it can be very helpful. Another advantage is that in the same experiment the degree of hydration of the concrete can be measured and the results can also tell if the concrete is carbonated and in some cases the degree of carbonation can be estimated.

Finally, the BS1881-124 method was excluded since several author agree on the fact that it has a low precision, especially because it depends on two different methodologies to quantify the cement and water, which increases the bias in the measurements.

	Type of measurement	Parameters measured	Sample preparation difficulty	Standards required?	Main external factors affecting the measurements	Can the external factors be noticed?	Is the technique useful to estimate W/C?
Transmitted UV light	Indirect	Porosity	Hard	Yes	Cracks and voids Carbonation	Yes	Yes
Reflected UV light	Indirect	Porosity	Medium	Yes	Cracks and voids Carbonation	Yes	Yes
CH content - CPL	Indirect	Portlandite	Hard	Yes	Carbonation	Yes	Yes
Scaning electron microscopy	Indirect	Porosity	Medium	Yes	Cracks and voids Carbonation	Yes	Yes
CH content - TGA-DSC	Indirect	Portlandite	Easy	Yes	Carbonation	Yes, after the test	Yes
NDT waves	Indirect	Porosity	Medium	Yes	Cracks and voids Carbonation	No	Yes
Chloride penetration and concrete reisitivity	Indirect	Porosity	Medium	Yes	Cracks and voids Carbonation	No	No, although there is a relation with the W/C
Water absorption	Indirect	Porosity	Medium	Yes	Cracks and voids Carbonation	No	It should be used as a complementary test
Degree of hydration	Indirect	Chemically bound water	Easy	Yes	Carbonation	Yes, after the test	Better for controlling cement hydration
Paste microhardness	Indirect	Strenght	Medium	Yes	Cracks and voids Carbonation	No	Yes
Physico-chemical method	Direct	Water and cement	Hard	No	Cracks and voids Carbonation	No	Yes
SEM+Power and Brownyard model	Direct	Water and cement	Medium	No	Cracks and voids Carbonation	Yes	Yes

Table 2.1: Summary available techniques for W/C estimation

3

Samples and Experimental procedure

3.1. Samples

The samples from the Applied Petrography Group (APG) consisted of 5 slabs, each of them with an unknown W/C. The dimensions of each sample were 70x70x20mm. Moreover, the following information about the mix designs was given:

- Coarse aggregate:4/10 mm sized Tunstead Limestone
- Fine aggregate: 0/4 mm sized Alrewas Quartz Sand
- Portland cement: Tunstead CEM I Minimum cement content 450 kg/m3
- The mix proportions saturated surface dry kg/m3,Coarse aggregate 897kg/m3
- The mix proportions saturated surface dry kg/m3,Fine aggregate 897kg/m3
- For the total aggregate content, 50% correspond to the coarse and 50% to the fine aggregate

About the mixes design, the APG established that "*these calibration standards are simplified versions of typical modern concrete and contain no chemical additions or mineral admixtures.*" On the other hand, TU Delft had a batch of ten thin sections that were used as standards, their W/C were 0.30, 0.35, 0.40, 0.42, 0.45, 0.48, 0.50, 0.55, 0.60 and 0.65. The samples were cast using cement CEM I 32.5 R and in Annex A.1.1 their mix design is given.

3.2. Sample preparation

As mentioned in Chapter one, samples were prepared accordingly. Figure 3.1 shows the techniques that were applied in the different concrete sets.

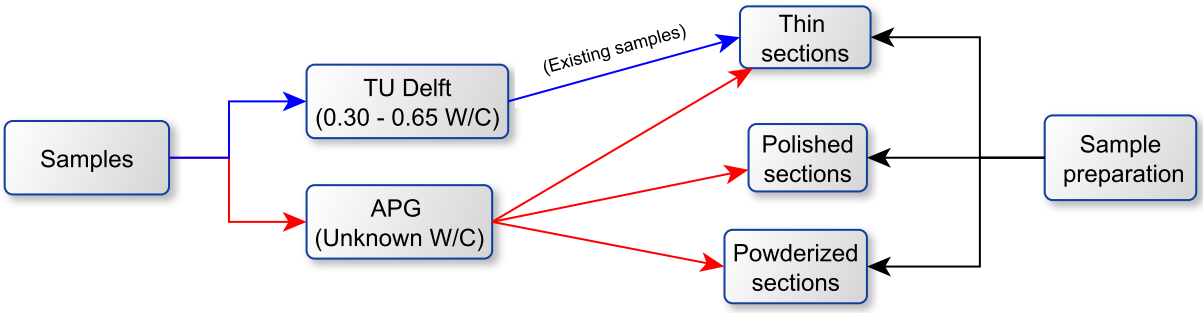

Figure 3.1: Samples and sample preparation

3.2.1. Thin sections

Thin sections are typically manufactured at a thickness of 30 µm since by fixing this value, the interference colors of the materials will remained constant, so their features can be identify without any problem by different people with the use of the optical microscope and the Michel-Levy interference chart. A detailed protocol for preparation of thin section was written by Jakobsen [6]. A similar protocol was followed in achieving the thin sections. For the APG concrete, a total of ten thin sections were prepared, 2 samples per batch.

The thin section making was divided into 2 parts and it was done using an automated machine. For the former part, the samples were glued to the reference glass using a part epoxy glue (plastic padding). Once the glue hardened, the reference glass was placed in the vacuum holder of the machine and the specimens were cut using a diamond blade to a thickness of 10.5 mm. After the cutting, the surface of the samples was not properly flat, therefore, it was grind it until a flat surface was achieved, which was done using a set of three diamond rollers, from coarse to fine.

When the surface of the samples was flat, a impregnation was done with the purpose of having the epoxy into the microstructure for the recognition of the pores and cracks (if present) during the analysis of the specimens. The epoxy used was prepared using 3 different components, the low viscosity epoxy, a fluorescent epodye and the hardener. The use of fluorescent epodye has two functions, first its yellow color helps to identify the voids under plain polarize light (PPL) and it is essential for the UV light analysis since it makes the porous glow allowing the quantification of the fluorescence intensity, which, as mentioned earlier, is correlated with the W/C.

The epodye has a mix proportion of 1 % w/w. Once both components are fully mixed, the new compound is mixed with the hardener with a ratio of 1:3, so for 100 gr of epoxy, 30 gr of hardener was used. For the impregnation process, the samples were placed in an aluminum tray as shown in figure 3.2 (b) and then placed in a vacuum impregnating chamber for 20 minutes. In the first 10 minutes the samples were subjected only to vacuum and in the remaining time (still under vacuum), they were impregnated guaranteeing that all the air voids were gone and that the epoxy got deep enough into the sample.

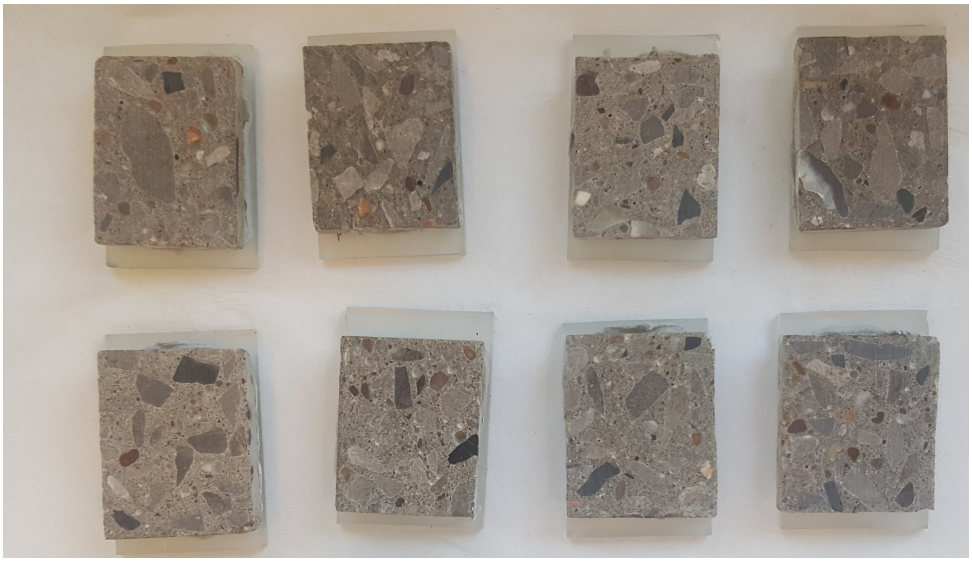

(a)

(b)

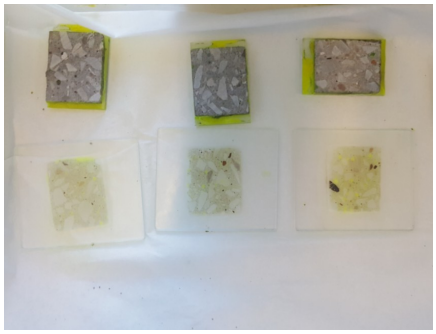

(c)

Figure 3.2: (a) APG thin section preparation. (b) Samples impregnation. (c) Grinding process to reach 30-35 µm

Since the epoxy would also cover the entire surface of the sample, the surface had to be ground again with the finest roller to remove this layer. A full removal of the epoxy was guaranteed if the thickness of the sample was the same as the one before the impregnation. Figure 3.2, shows some steps of the procedure.

For the second part, a working glass with dimensions of 6.5×5.5×0.2 mm was glued to the impregnated flat surface using UV-hardening glue. During this step, the glue had to be evenly distributed on the sample's surface since any irregularity would affect the final result. After the glue had hardened, the specimens were in between the reference glass and the working glass. The working glass was placed in the vacuum holder and the samples were cut with the diamond disc to a thickness of 0.5-0.7 mm. Since the surface would have been uneven as before, the procedure in step 1 was repeated to flatten it.

The grinding process was done until the thickness of the samples was around 30 µm. To ensure that the samples were good, their thickness was measured in different zones. Likewise, by using Michel-

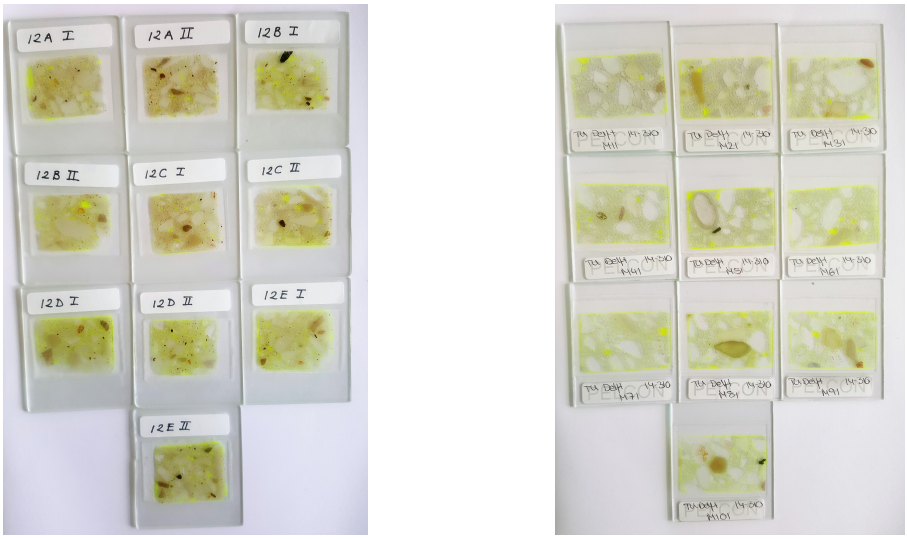

(a) (b)

Figure 3.3: (a) APG thin sections. (b) TU Delft thin sections

Levy interference chart the color of the quartz grain was checked. For a 30 µm sample the quartz grain have a very pale yellow color, therefore if the grains in the sample have this tone one can be sure that the thickness is correct.

After the checks, using the UV-hardening glue, a cover class was glued to the surface of the sample to protect it from abrasion and environmental effects such as carbonation. Examples of the final thin sections are shown in figure 3.3.

3.2.2. Polished sections

Polished sections preparation was also divided into 2 parts, the former consist in grinding and impregnating the sample, and the latter in polishing it. The procedure for the former part is the same as the one for the thin sections, the samples are glued to the reference glass and using the automated machine they are grind and then impregnated with the epoxy under vacuum. For the APG concrete, one polish section was done per sample.

For the latter part, the samples were ground with a SiC sandpaper No. 1200 and water, then they were polished with sandpaper from 6 µm to 1/4 µm with diamond paste and ethanol. For this part, in between every step the samples were subjected to ultrasonic baths for 5 - 10 seconds to remove the impurities that could be accumulated within the pores and/or cracks. Examples of the final polished sections are shown in figure 3.4.

At first, the polishing was done using liquid diamond, nevertheless with this approach remaining of the liquid stayed in the sample, affecting considerably the picture quality. Later on, in order to try to fix this, the same samples were polish with sandaper 4000 and lab-grade ethanol, which improved the quality of the images but not enough. Finally, the samples were polished all over again using the

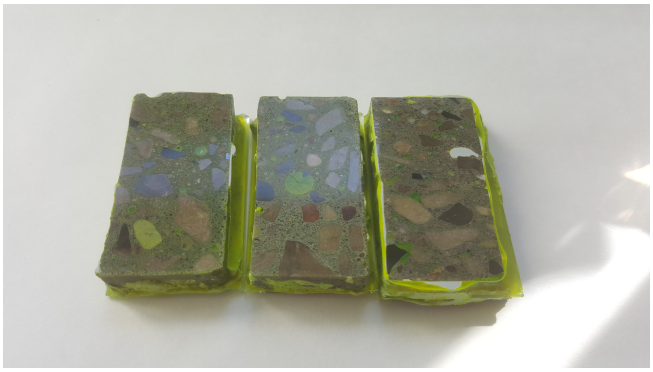

Figure 3.4: APG Polished sections

diamond paste and the results were satisfactory. This small example shows the importance of the specimen preparation, since a single detail can affect the quality of the micrographs and therefore all the calculations that are based on it. Figure 3.5 shows an example of every image based on the type of lubricant used during its sample preparation.

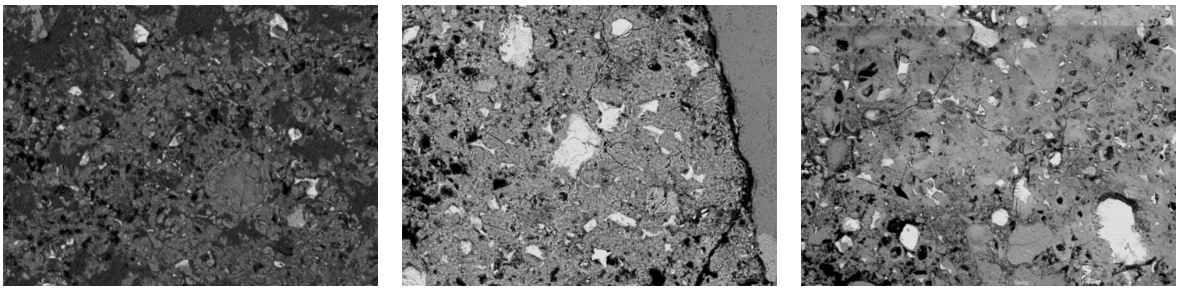

(a) (b) (c)

Figure 3.5: Images results based on the polishing lubricant (a) Diamond liquid. (b) Ethanol. (c) Diamond paste

3.2.3. Powderized samples

Since carbonation cannot be seen before the test is performed, the sampling was done from within the slabs of the concrete. Also, it was checked with phenolftaleine that the zones of interest didn't have a carbonation profile. Later the samples were powderize mechanically using a metallic sphere. During the process, large aggregate particles were removed manually in order to have as much cement paste as possible.

Once the samples were powderized, they were stored until constant weight in a vacuum oven at a temperature of 25-26C, this way the samples could dry out completely and the results will not be altered by internal water content or carbonation. It is worth mentioning that the concrete from the APG was assumed to be mature, therefore since it had a high degree of hydration it was not necessary to do an intermediate step to stop the hydration process. Figure 3.6 shows some steps of the procedure.


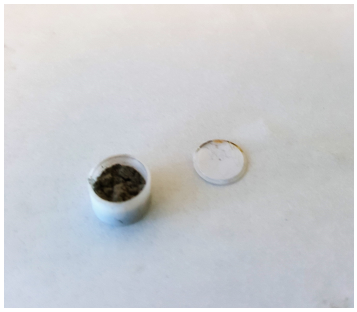
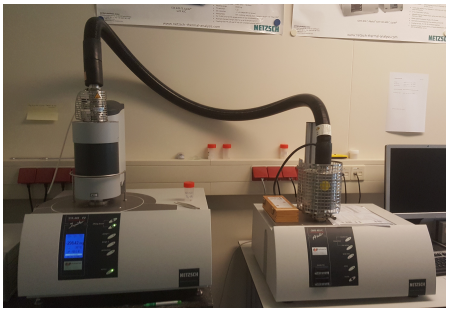

(a) (b) (c)

Figure 3.6: (a) APG Powderize samples. (b) Sample, 30 - 35 mg. (c) TGA settings

3.3. Micrographs acquisition

3.3.1. UV light

1. Thin section revision

   As mentioned in section 2.5.1, once the thin sections were ready, some checks were done in order to guarantee that the samples can be used. For instance, that the areas to be used are not carbonated, don't have entrapped air or large voids, scratches, extra glowing and that the aggregates tones do not resemble the microstructure tones. Figure 3.7 shows some examples of the images that should be avoided. The mistakes that can be seen in these images are: (a) shows an extra glow around the voids that affects the brightness of the cement paste and the aggregates, in (b) the aggregate microstructure resembles the cement paste microstructure, in (c) there is not an actual mistake, although the micrograph is mostly aggregate, therefore only a small area can be analyse and in (d) there is glowing in the aggregates probably due to sample preparation mistakes.

2. Micrographs Settings

   The thin sections were analysed using a Leica DMRXP microscope with a Leica DFC420, an example of the setting is shown in figure 3.8. For each sample, 13 UV light RGB micrographs were taken since with this number of images the cumulative average pixel value of each sample converge. Before starting to capture all the images, several pictures of the upper (0.65) and lower (0.30) W/C were taken in order to adjust the settings of the microscope and the camera.
   The images were acquired with a x10 lens using transmitted and reflected light, depending on this, the microscope parameters were adjusted. Regardless of the light mode, all the light source was always sent to the camera and not to the binoculars of the microscope. For the transmitted light, the aperture diaphragm, field diaphragm, grey (neutral density) filter and illumination intensity control were set and then grey (neutral density) filter was always OFF. For the reflected light the microscope didn't allow significant changes, so it wasn't worth to do any adjustments. On the other hand, the camera settings were defined using its software. In the calibration panel, the parameters to be defined are exposure, gain, saturation and gamma. A summary of the microscope and camera settings are shown in table 3.1 and 3.2.
   The calibration process was done until the "best quality" images were acquired. Unfortunately,

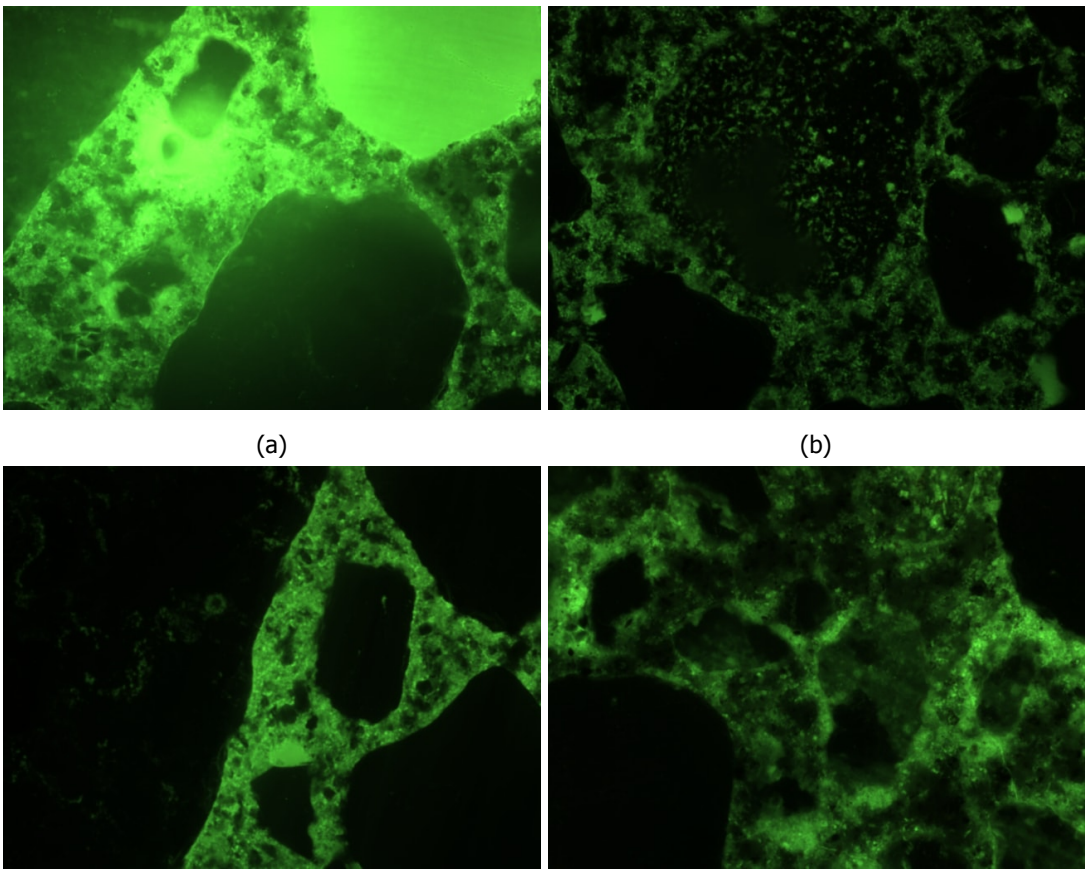

Figure 3.7: Incorrect UV light micrographs.

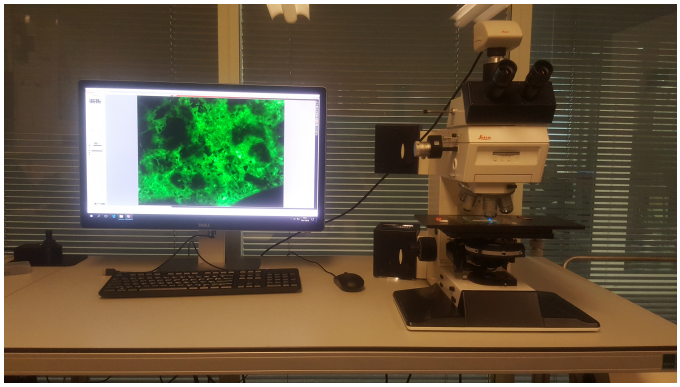

Figure 3.8: Polarized light and fluorescence microscopy (PFM) setup used in the current study.

there is not a proper definition for the term "best quality", so this term was defined based on the criteria of the author. It should be noted that since the micrographs were always captured with the same settings, there was no need to do calibrations to correct the histograms once the images were taken.

Using the advantages of digital imaging, it was decided to use the function of white-balancing and flat-field correction in order to have a better quality image. Before doing the white-balancing

	Aperture diaphragm	**Field diaphragm (mm)**	**Illumination intensity control**
Microscope (Transmitted light)	Aperture that allow to see the entire field of view	45	Max value

Table 3.1: Microscope settings for UV light micrographs acquisition

	Exposure (ms)	**Gain**	**Saturation**	**Gamma**
Camera	303.9	1.0	1.0	1.0

Table 3.2: Camara settings for UV light micrographs acquisition

process, a neutral reference had to be established. This was done by setting the microscope in transmitted light with the same parameters used for the capture of the images, nevertheless, for the camera the exposure was set to a value of 10 ms instead of 303.9 ms.

Once the neutral reference was defined, the white balanced function was used in the different zones of the image, with the idea of having a picture "as white as possible" which was done in an iterative way by selecting different zones of the images but without following a clear procedure. This approach lead to a good quality imaging, but without actually knowing how to get there in case the settings were changed, therefore the procedure was repeated using a standard protocol. The software itself provides a white balancing function for the entire image, which may not be as good as the iterative process but it could be reproduced when needed.

The next step was to apply the flat field correction in order to illuminate the field view uniformly. Since the software included this function, it was very easy to implement in the images. An example of this procedure can be seen in figure 3.9. At the end, for every micrograph there were 4 types of images, 2 using transmitted light, with and without the flat field correction and 2 using reflected light, also with and without flat field correction.

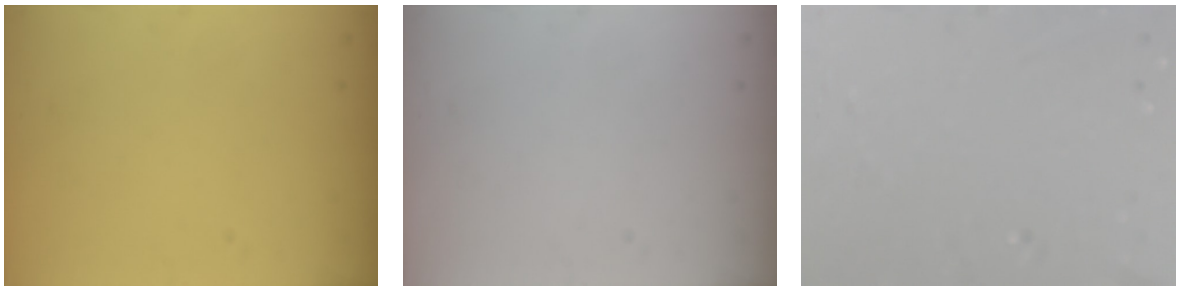

(a) (b) (c)

Figure 3.9: White balancing

3. W/C estimation through average pixel value

As it was mentioned earlier, samples with higher porosity will have a higher fluorescence intensity and this can be linearly correlated with the W/C, therefore it is important to define how this intensity can be quantify. It was decided that the best way to do it is by using the average pixel value of each sample.

The RGB images taken from the standards were split into their red, green and blue components. The red and blue images were discarded and only the green was used because it was the most predominant component in the micrographs. Later, using equation 3.1 the weighted pixel value of every micrograph was obtained and then the 13 results were averaged in order to have one single value per sample. Once every sample had its own average pixel value they were linearly correlated with the W/C.

$$P_{AVG} = \sum_{i=0}^{255} \frac{P(i) \times f(i)}{f(i)} \tag{3.1}$$

Where:

- P_{AVG} = Average pixel value
- i = Gray scales value
- $P(i)$ = Pixel value
- $f(i)$ = Frequency value

As it can be seen from formula 3.1 the pixel value is a function of the gray levels (0 – 255), therefore by finding the right grey values one can obtained the best possible correlation with the W/C, which can be measured using the Coefficient of determination, R^2 . This process was done iteratively using Microsoft Excel and thresholds were used for the upper and lower boundaries. Figure 3.10 (a) shows the averaged histograms of every samples, and figures 3.10 (b) and (c) show the behaviour of the histograms when they are close to 0 and 255 respectively. Based on these figures, it was decided that the threshold for the lower boundary was going to be between 15 and 120, and for the upper boundary between 130 and 245. Moreover, by defining these values one should neglect the influence of the aggregates and the voids which are the grey levels lower than 15 and higher than 245 respectively, meaning that there is no need to create binary images to segment these two phases from the images.

Once the best correlation was found, the line of the equation that fitted the points was also obtained, then using its boundaries and the same procedure, the average pixel value of the unknown samples from APG was obtained and then plugged into this equation in order to obtain the W/C of each sample. Figure 3.11 summarizes the procedure that was followed.

4. Epoxy thin sections

The main idea of the epoxy thin sections was to see how the pixel value changes as a function of the thickness and the content of the fluopigment (also known as epodye) in the low viscosity

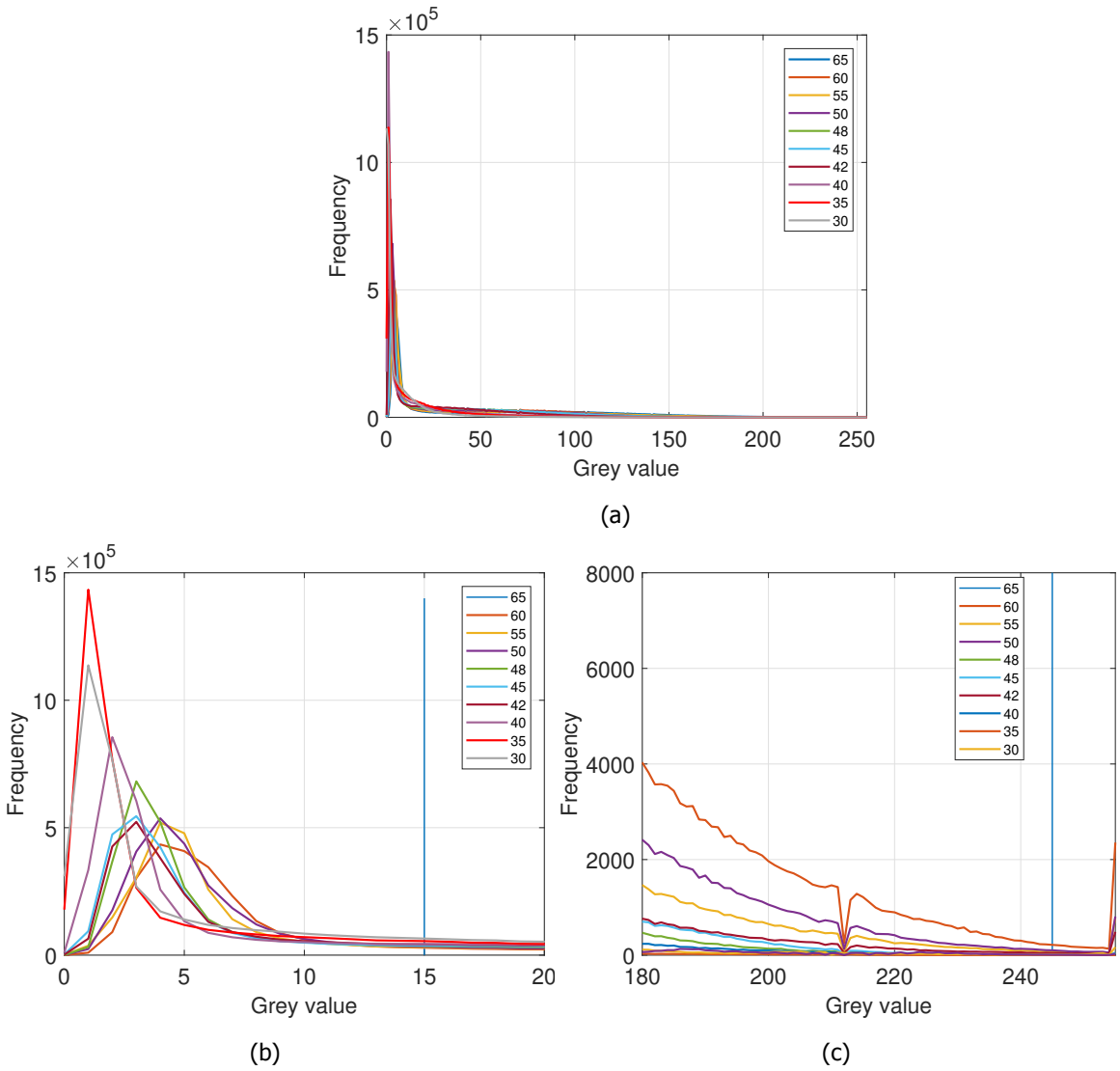

Figure 3.10: Histograms UV light TUD Standards, green channel. Figures (b) and (c) show the behaviour of the histograms close to the 0 and 55 gray scale value respectively.

epoxy. The percentages for the epodye that were chosen are 0.5%, 1%, 2% and 3%, being the second one the value that is normally used. Nevertheless, it was seen that for the last two values, the epodye was not dispersed properly in the epoxy, so in the bottom of the mixtures there was a minor precipitation of the powder, meaning that the actual percentage of the epodye wasn't 2% and 3%, although it was assumed so. 3.12 shows the different steps for the preparation of the epoxy thin section.

In order to do these measurements, the same procedure used for the sample preparation of normal thin sections was followed. When the thickness of the thin section was around 60 µm, 5 pictures were acquired for each epodye concentration using transmitted light with white balanced and flat field correction, then the thin section was ground again, measured and new micrographs were acquired. This process was done until the thin section had a thickness of around

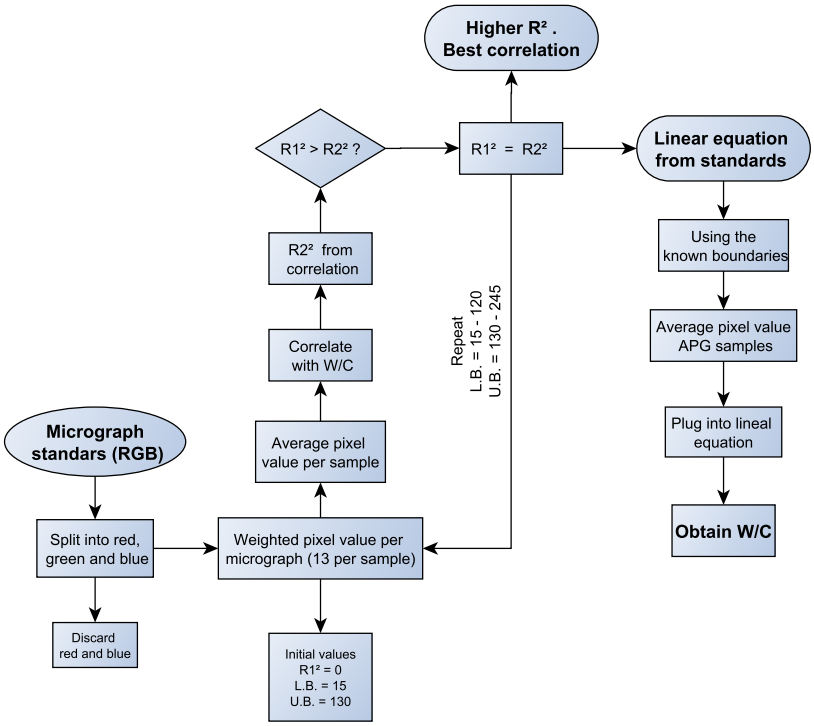

Figure 3.11: Average pixel value estimation through UV light

30 µm. Later, for every thickness, using the same procedure as for the UV light images but with the entire histogram, the average pixel value of each epodye concentration was obtained.

3.3.2. Circular polarization microscopy

1. Thin section revision

In comparison with the UV light images, the microstructure of the concrete for the CPL light mode have less constrains. Basically the only aspect that must be taken into account is to avoid the areas that are carbonated since this process consumes Calcium Hydroxide meaning that the amount quantify of this phase in those areas cannot be compared with the W/C of the mix. On the other hand, large voids or entrapped air will allow the growth of large CH crystal but still those crystals come from the hydration process meaning that in comparison with UV light images, CPL images can include these type of voids.

2. Micrograph Settings

The thin sections were analysed with the same microscope and camera as the UV light micrographs (Leica DMRXP microscope and Leica DFC420 camera). For each sample, 15 zones were captured with the light modes of plain polarized light (PPL), crossed polarize light (XPL) and circular polarization light microscopy (CPL).The images were acquired with a x20 lens. The microscope and camera settings used for the acquisition of the microgphas can be seen in the tables 3.3 and 3.4 respectively. Likewise, in all the cases,the grey filter of the microscope was ON and the light was sent to the binoculars of the microscope and the camera.

(a)

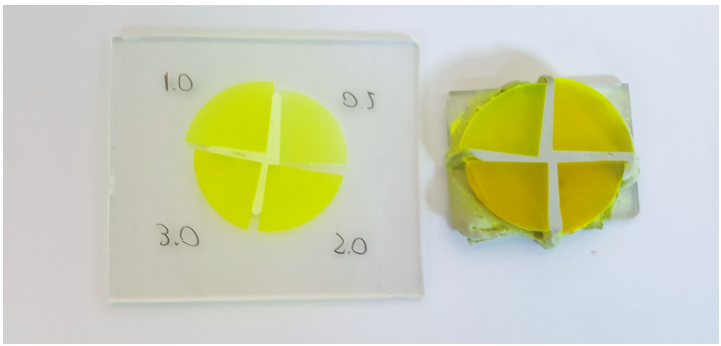

(b)

Figure 3.12: (a) Initial hardened epoxy.(b) Epoxy thin section.

	Aperture diaphragm	**Field diaphragm**	**Illumination intensity control**
Microscope (Transmitted light)	Aperture that allow to see the entire field of view	Max Value	Max value

Table 3.3: Microscope settings for CPL-XPL micrographs acquisition

	Exposure (ms)	**Gain**	**Saturation**	**Gamma**
Standards - PPL	33.8	1.0	1.0	0.90
Standards - CPL	70.5	1.5	1.0	0.85
APG Samples - PPL	27.9	1.3	1.0	0.95
APG Samples - CPL	70.5	1.5	1.0	0.85

Table 3.4: Camara settings for CPL-XPL micrographs acquisition

As for the UV light images, the calibration process was done until the best quality micrographs were obtain and later the white-balancing process and flat field correction procedures were also applied. For this case, the best quality image was defined, on one hand on the criteria of the author but on the other hand on how easily can be to segment the Calcium Hydroxide (CPL and XPL) or the unhydrated particles (PPL) from the images once they were acquired which is

why there are different camera settings for the standards and the APG samples. As it can be seen in figure 3.13, the aggregates are to bright, meaning that some information about them is being lost, nevertheless since they are not relevant for this study it was fine to lose some data in exchange of acquiring a better quality image for the cement paste.

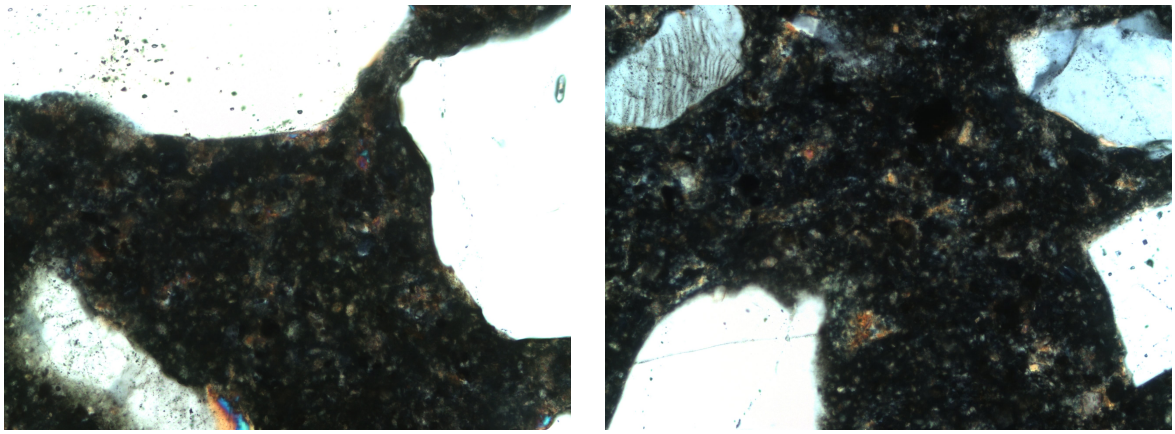

(a) (b)

Figure 3.13: (a) CPL micrograph APG Sample D. (b) CPL micrograph APG Sample E.

3. W/C Estimation

The general idea of this approach was to quantify the amount of CH in the CPL micrographs and correlated with the W/C of the samples using a reproducible and automatic approach. Based on this, there was the need to segment the CH from the cement paste using image analysis. The process was done using a plugin based on machine learning from the software Image J called Weka Trainable Segmentation. The principle of the plugin is that a classifier is trained using selected areas of the images and then its training is used to segment all the micrographs.

Before starting the training, the categories in which the user desires to segment the images had to be created. At first, the idea was to segment only the CPL images since they are the ones that show the calcium hydroxide crystals, nevertheless due to some issues, that will be discussed later, it was decided that the PPL images had to be segmented too. For the PPL micrographs 3 classes were created, paste, unhydrated particles and aggregates and for the CPL also 3 classes were created, paste, aggregates and Calcium Hydroxyde.

To segment the images, the user has to manually classify some pixels into the established categories. With the input data, the classifier learns about the pixels classification and used the training feature to predict the category of the non-classify pixels and segment the entire picture. As a rule of thumb, the more manually classified pixels the better the segmentation, nevertheless this procedure would have been very time consuming, instead, it was wise to classify a few pixels and let the software classify the image. The first results were very accurate, but then the software allowed the user to know which pixels were more difficult to classify, so one could focus on those and get a good classifier and segmentation in less time.

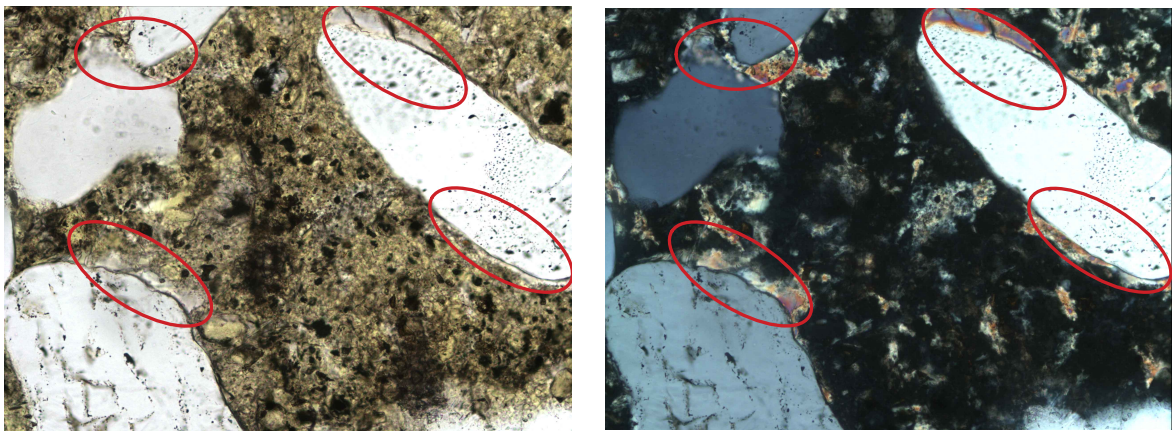

(a) (b)

Figure 3.14: (a) PPL migrograph - W/C = 0.65. (b) CPL migrograph - W/C = 0.65

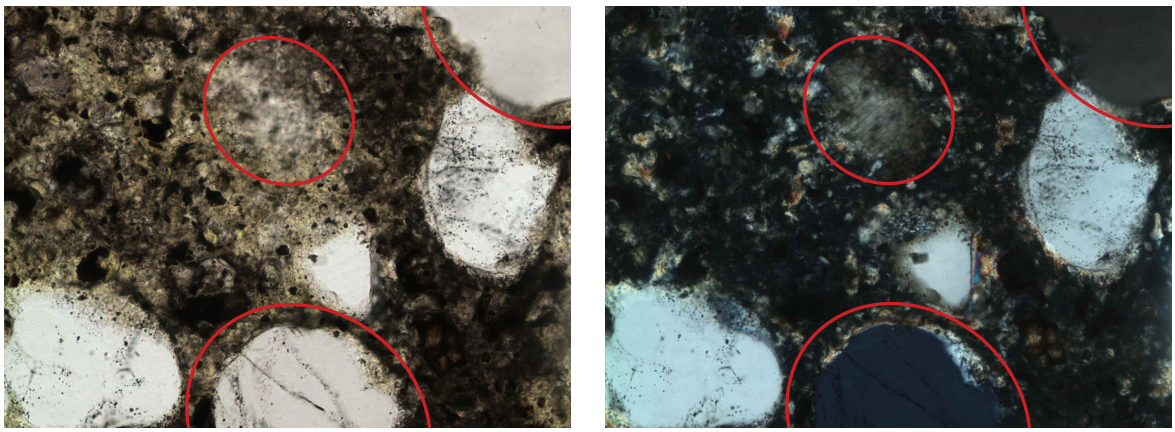

(a) (b)

Figure 3.15: (a) PPL migrograph - W/C = 0.50. (b) CPL migrograph - W/C = 0.50

At first, the aggregates were coloured manually, being this part the only manual step of the procedure. The aggregates were drawn using PPL and CPL images simultaneously by using one to double check the other because in some cases the boundaries of the aggregates couldn't be distinguished properly especially since the CH tends to grow around the former. As it can be seen in figure 3.14, in PPL mode the CH has the same color as the aggregate nevertheless in CPL both can be distinguish very easily. Another reason to colour manually the aggregates was because of the different tones they might have in CPL based on their orientation. As it can be seen in Figure 3.15 the aggregates can be white, blue, grey or black and with several tones in between each of them, meaning that in some cases the aggregates might look like either cement paste or CH.

As mentioned before, at first only the CPL/XPL micrographs were segmented and the results were good for high W/C, nevertheless, as mentioned by Çopuroğlu [15], the interference colours of Calcium Hydroxide might look similar to belite, alite or ettringite especially for low W/C where

the unhydrated phases are relatively abundant. Figure 3.16 shows two micrograph with W/C = 0.30 and 0.60 respectively. It can be seen that for a high W/C, the cement paste looks black and homogeneous while for the other image the matrix looks heterogeneous with different phases that the software confused with CH, therefore when the classifier was applied to these images the segmentation obtained was wrong.

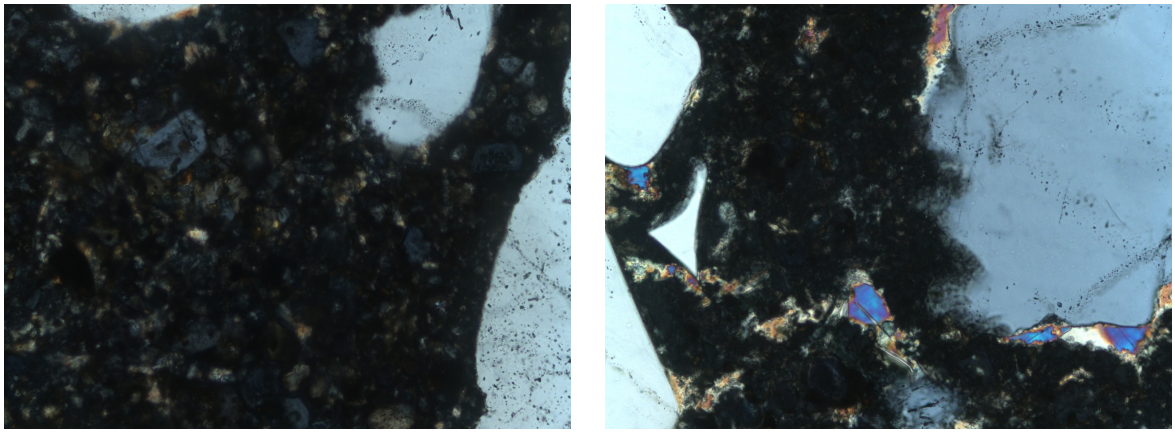

(a) (b)

Figure 3.16: (a) CPL migrograph - W/C = 0.30. (b) CPL migrograph - W/C = 0.60

To overcome this problem, it was noted that in the PPL images the hydrated zones had a lighter tone while the unhydrated particles had darker one, meaning that they could be segmented using the Weka plugin. Afterwards, binary images were created with the unhydrated particles and it was used to mask these zones in the CPL/XPL images. Later, the new CPL/XPL images were segmented, nevertheless, in some cases the classifier confused the CH with the aggregates, so the segmented image was masked by an aggregate binary image. Moreover, the CH phase was turned into a binary image and it was eroded twice and the dilated also twice with the aim of cleaning the small particles that might be noise. Finally to finish the cleaning of the image, the areas of CH that had a value lower than 0.00002 mm^2 were neglected, after this process the CH images were used for the W/C estimation. Figure 3.17 summarises the procedure that was followed. Likewise figure 3.18 shows an example of every image in the different stages.

3.3.3. Scanning electron microscopy

1. Micrographs Settings

The acquisition of the back scattered electron (BSE) micrographs was done using the guidelines from [10][11][3], nevertheless the desired pictures couldn't be obtained with the given settings therefore new ones were adopted in order to fulfill with the desire images. An ESEM Philips XL 30 was used to acquire the images, the polished sections were not coated and the settings used for the microscope can be seen in table 3.5.

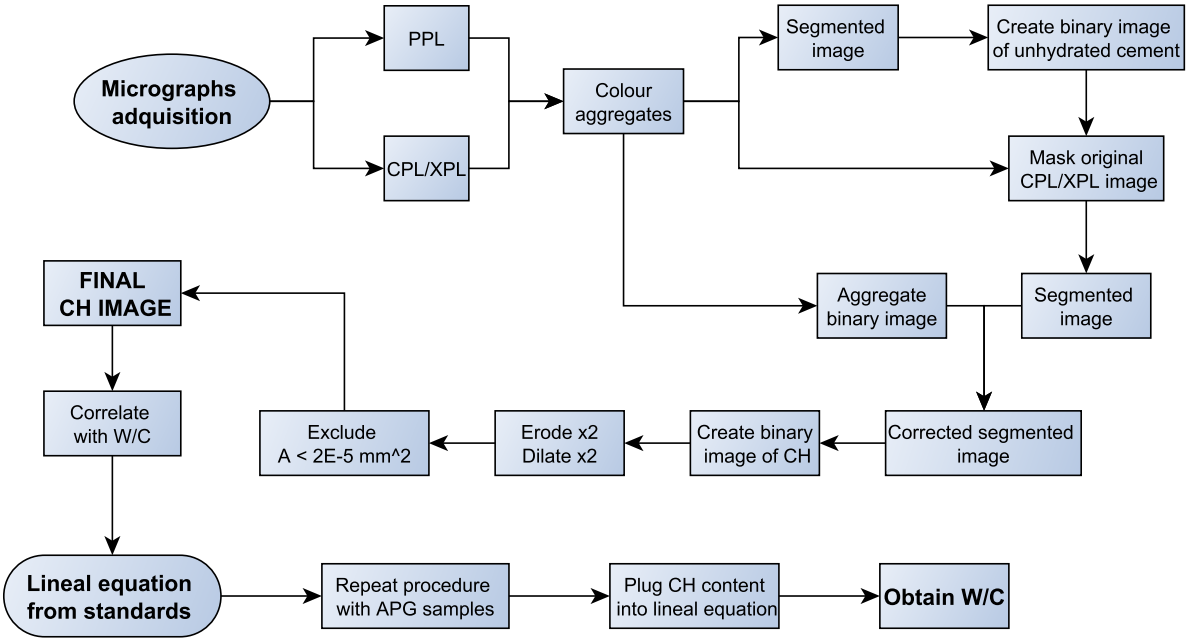

Figure 3.17: W/C estimation through CH quantification

In general terms, it was established that the histogram had to be properly centred and stretched to span the entire dynamic range of the available grey scale, in order to avoid accumulations in the shades of 0 or 255, a way of doing this was to guarantee that the first and last 10 values of the histogram were zero, although this couldn't be achieved in some pictures. The calibration was done for sample A from the APG and then the same settings were used for the acquisition of the other samples. In total 30 images were acquire per sample since with this number, the cumulative average value of the phases converged.

Vacuum	Voltage	Zoom	Brightness	Contrast
Low (0.5 torr)	15 kV	500x	78	44

Table 3.5: SEM micrographs settings

2. W/C Estimation SEM + POWERS

Once the images were acquired, the aggregates and cracks were removed from the images by drawing manually a white boundary (grey value = 255) around them since their inclusion, specially the aggregates, would have affected the measurements. The segmentation procedure for the unhydrated cement grains was done following the guidelines [3]. The procedure was straight forward, the threshold is the minimum value between the hydration product peak and the unhydrated cement grain peak, nevertheless, in some cases this approach had some issues.

For some images the histogram had a minimum value very close to the second peak, then if this value was chosen it would have underestimated the amount of unhydrated cement since

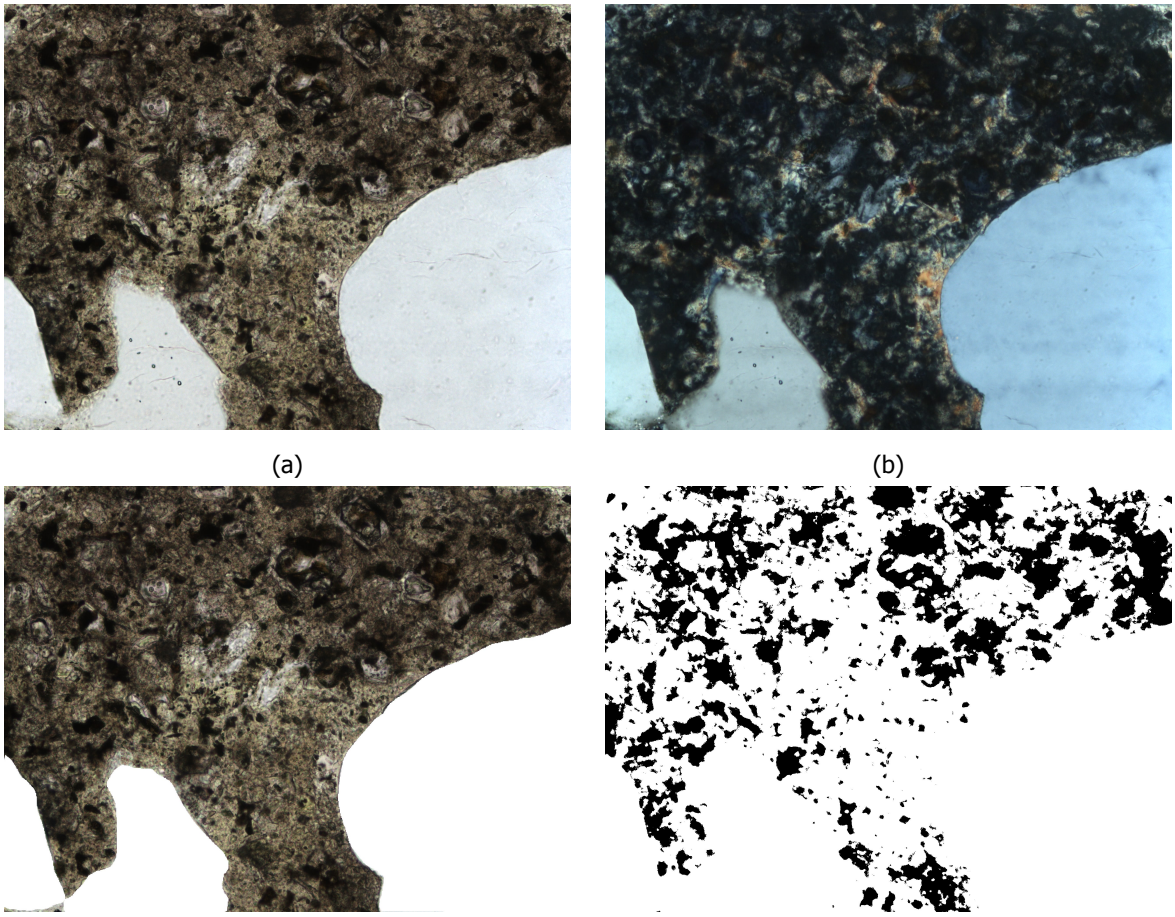

Figure 3.18: Micrographs W/C = 0.48.(a) Original PPL. (b) Original CPL . (c) PPL with colour aggregates. (d)Binary image unhydrated cement particles from PPL.

the second minimum value which laid more to the center and is the one that fit better with the methodology was neglected. Because of this, it was decided to compute two values, the minimum and the minimum mode between both peaks. In most of the cases both values coincide, nevertheless when they didn't, based on the criteria of the author one of them was chosen, this criteria was applied for all the set of micrographs from the same sample. Likewise, the samples with high W/C had a lower content of cement grains meaning that in some cases there was not a second peak therefore the methodology couldn't be applied. For these cases, the threshold from the other micrographs of the same sample were used. Figure 3.19 summarizes the procedure that was followed. This methodology was done using the sofware R and the script can be seen in A.2.1.

On the other hand, the approach for the capillary porosity is not as straight forward as for the unhydrated cement grains, Wong *et al.* [10] establishes that from the cumulative histograms, the threshold for the porosity *"can be estimated from the intersection between the two linear segments (...). The grey value at this intersection can be used as the upper threshold level for porosity."* Although, it is also established that this value can overestimate the amount of pores in

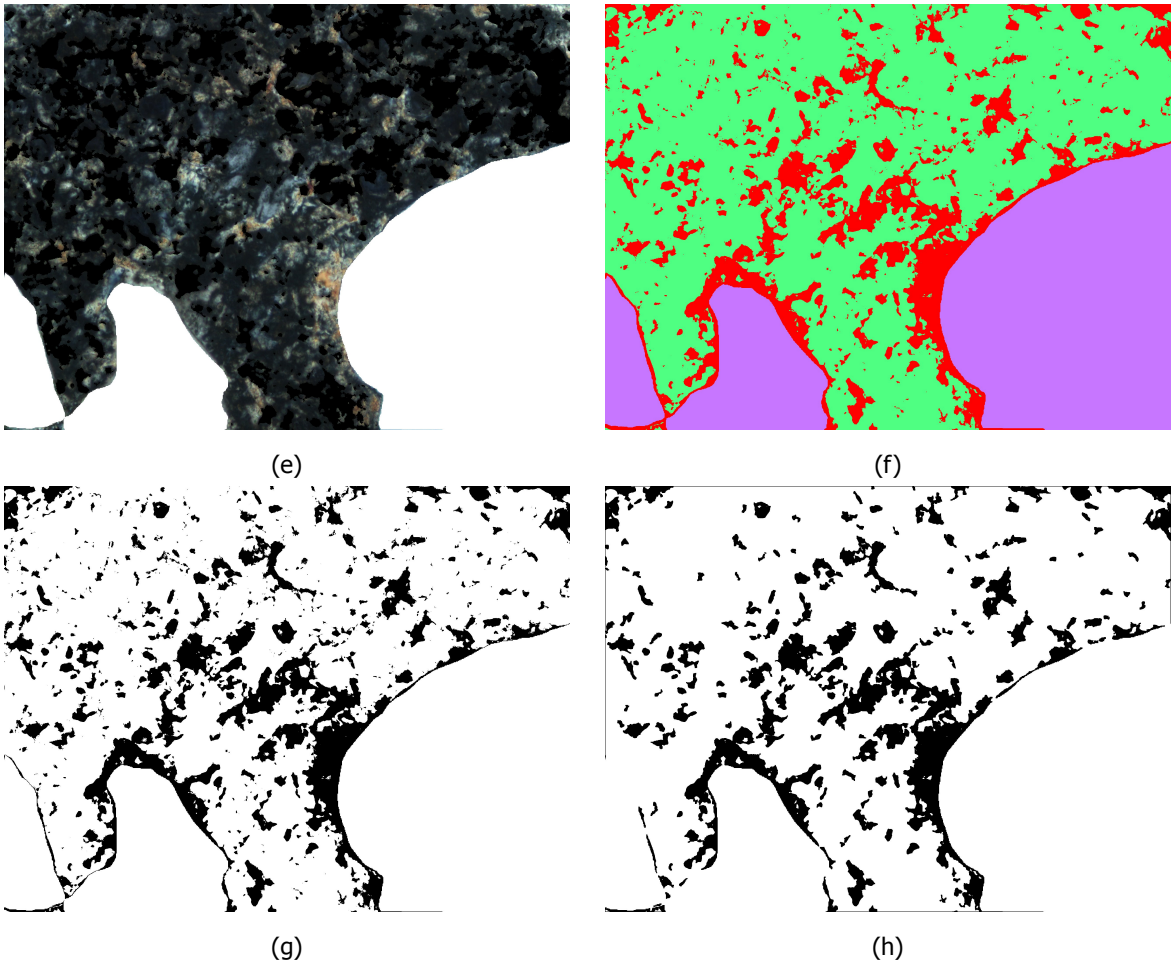

Figure 3.18: Micrographs W/C = 0.48.(e) CPL with colour aggregates plus binary unhydrated cement. (f) Semengented image. (g) CH Binary image of CH. (h) CH final binary image

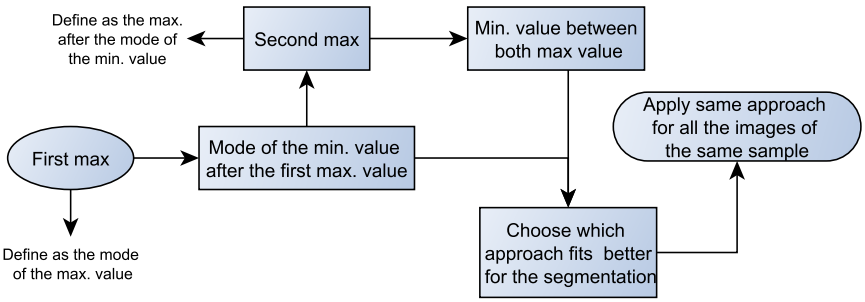

Figure 3.19: Cement grains segmentation process

the sample, therefore it can be multiplied by a value of 0.9. Both approaches were done, nevertheless the results obtained were not satisfactory for all the samples, so another two approaches were proposed.

Since the value of the inflection point times 0.9 was still high, it was decided to use approaches that aim for a value much lower that the current ones. The first approach gave a low value and the second a value in between the original approach (0.9*inflection point) and the former one.

In order to do this, using also the software R some data was created, the cumulative histograms, their first and second derivative and the ratio between the 1st derivative and the cumulative values. It is worth mentioning that the part of this data was also used to obtained the inflection point of the cumulative histograms.

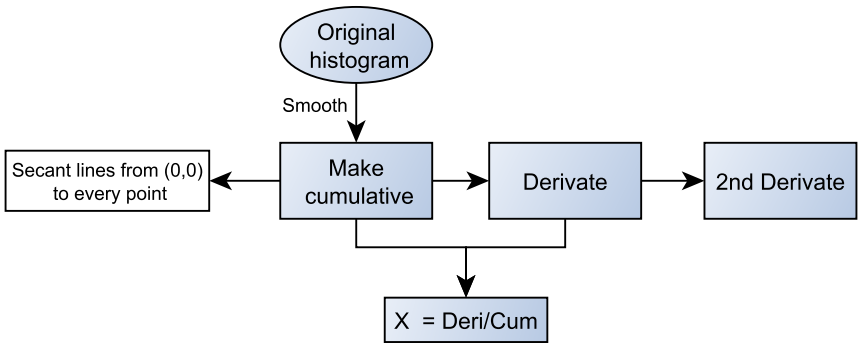

Figure 3.20: Data required for the capillary pores segmentation process

Figure 3.20 and 3.21 show the process to obtained the data and the values for the inflection point. Likewise, the procedure for the first and second approach(the third and fourth in total) can be seen in figure 3.22. The scripts to obtain these values can be seen in Appendixes A.2.2 and A.2.3.

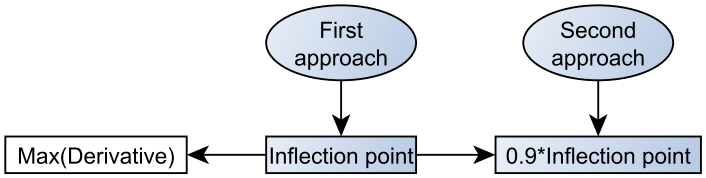

Figure 3.21: Capillary pores segmentation process I and II

3.4. TGA Analysis

The equipment used for the experiments was a Netzsch Jupiter STA 449 F3, between 30-35 mg of the powderized samples was placed in a ceramic crucible and then in the machine to ignite until 1000°C. For the APG concrete 3 test were perform per sample for a total of 15 repetitions.

The TGA results were used to quantify the amount of Portlandite in the sample, although since the samples included an unknown amount of aggregates and the results were given in percentage, they couldn't be compared since their value is a function of the amount of aggregates and cement paste. For instance it cannot be said that a sample with a lower content of Portlandite had a lower W/C because this could also be due to a higher content of aggregates within the powderized sample. Because of this, it was necessary to define a way to compare the Portlandite content in each sample but only using the information provided by the TGA results.

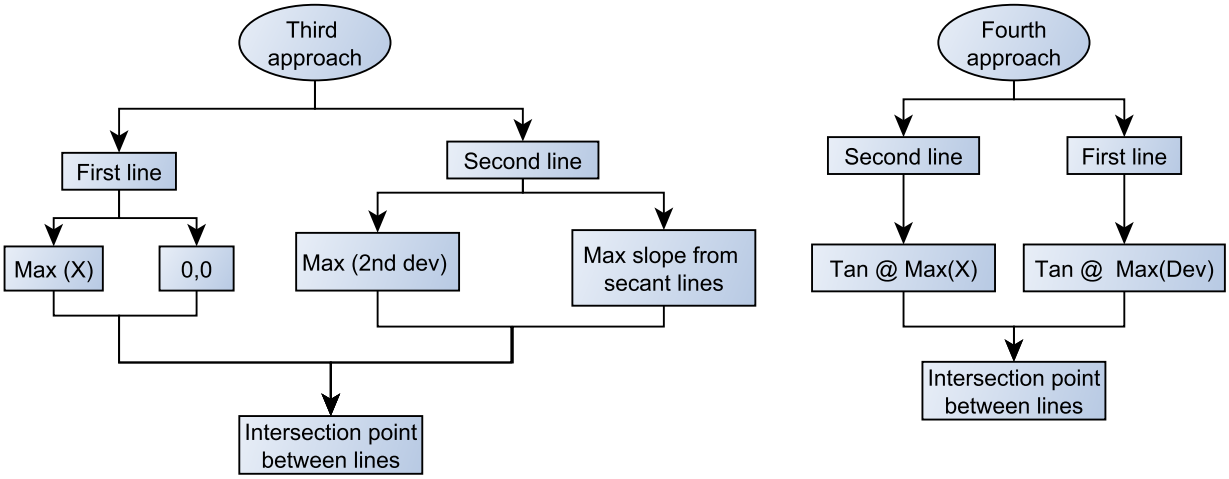

Figure 3.22: Capillary pores segmentation process III and IV

As mentioned in section 2.2, the chemically bound water is part of the hydration products, therefore it was decided that the total amount of water lost from the Portlandite was going to be divided by the total loss of the chemically bound water since the latter is related to the cement paste.

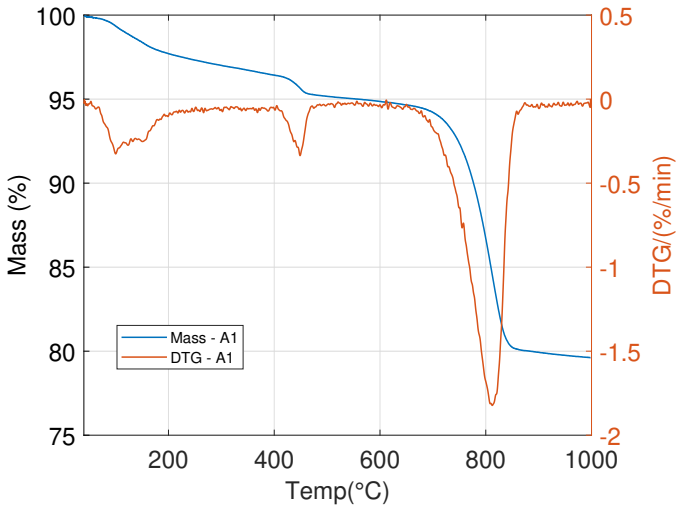

Figure 3.23: Sample A1, TGA-DSC

It's worth mentioning that since the actual amount of cement was not known, it was not possible to quantify the actual amount of Portlantide, so for the calculations it was only used the amount of water that is lost from it. This value was defined as the mass loss between 400°C and 500°C [35]. Likewise, since some calcareous aggregates were present in the sample there is a big loss from the CO_2 around 700°C, meaning that this range was excluded from the calculation of the chemically bound water. The threshold for the CO_2 loss was defined using the DTG graphs since it shows better the changes in the mass loss. As it can be seen figure 3.23, there is an important loss of mass 640°C and 870°C from the

CO_2 of the aggregates.

Finally, the mass loss from the following temperatures were used: first temperature , 400°C, 500°C, 640°C, 870°C and the last temperature. The chemically bound water was defined as the difference between the last and the first temperature, excluding the mass loss from the CO_2.

4

Results of the techniques used

4.1. UV light microscopy

4.1.1. Calibration curves

As mentioned before, the procedure was done twice, the first time without registering the white-balance process of the image and the second with a proper protocol, nevertheless, the results from both methodologies can be used and are defined as batch 1 and batch 2 respectively. Another difference between each batch was the exposure time, for the former it was 494.7 ms and for the former 303.9 ms. Likewise, for each batch there were 4 light modes, reflected light with flat field correction (RF), reflected light without flat field correction (RNF), transmitted light with flat field correction (TF) and transmitted light without flat field correction (TNF). Furthermore, a different set of images(RF3) was acquired by a third person using reflected light with flat field correction but with a different microscope and camera. The procedure established was also applied to these micrographs. Table 4.1 shows the lower and upper boundaries, the coefficient of determination R^2 for the given boundaries and the coefficient of determination R^2 assuming the full range of gray values (15 - 245).

Although the methodology gave the best correlation with the W/C based on the boundaries, it was later decided to see what would happened with it if the entire range of gray scale was used. Since the results obtained with this approach were equally good, it can be said that they are more representative since by taking the entire range, 15 to 245, the entire cement paste is taken into account. It is worth mentioning that this doesn't mean that always the full range will be the best option, since during the iteration process it was seen that boundaries close to the full range gave lower correlations in comparison with the best one, which is a reference for comparison in case one wants to change the boundaries. Finally, it was decided to compare the results from the proposed methodology and with the complete range of gray scale.

Light Mode	R^2	Lower boundary	Upper boundary	R^2 (15 - 245)
RF1	0.97	15	245	0.97
RNF1	0.96	20	199	0.96
TF1	0.95	20	168	0.95
TNF1	0.95	20	163	0.95
RF2	0.95	15	186	0.95
RNF2	0.95	15	183	0.95
TF2	0.95	15	245	0.95
TNF2	0.96	15	243	0.96
RF3	0.96	15	168	0.94

Table 4.1: Calibration curves boundaries and coefficient of determination R^2.

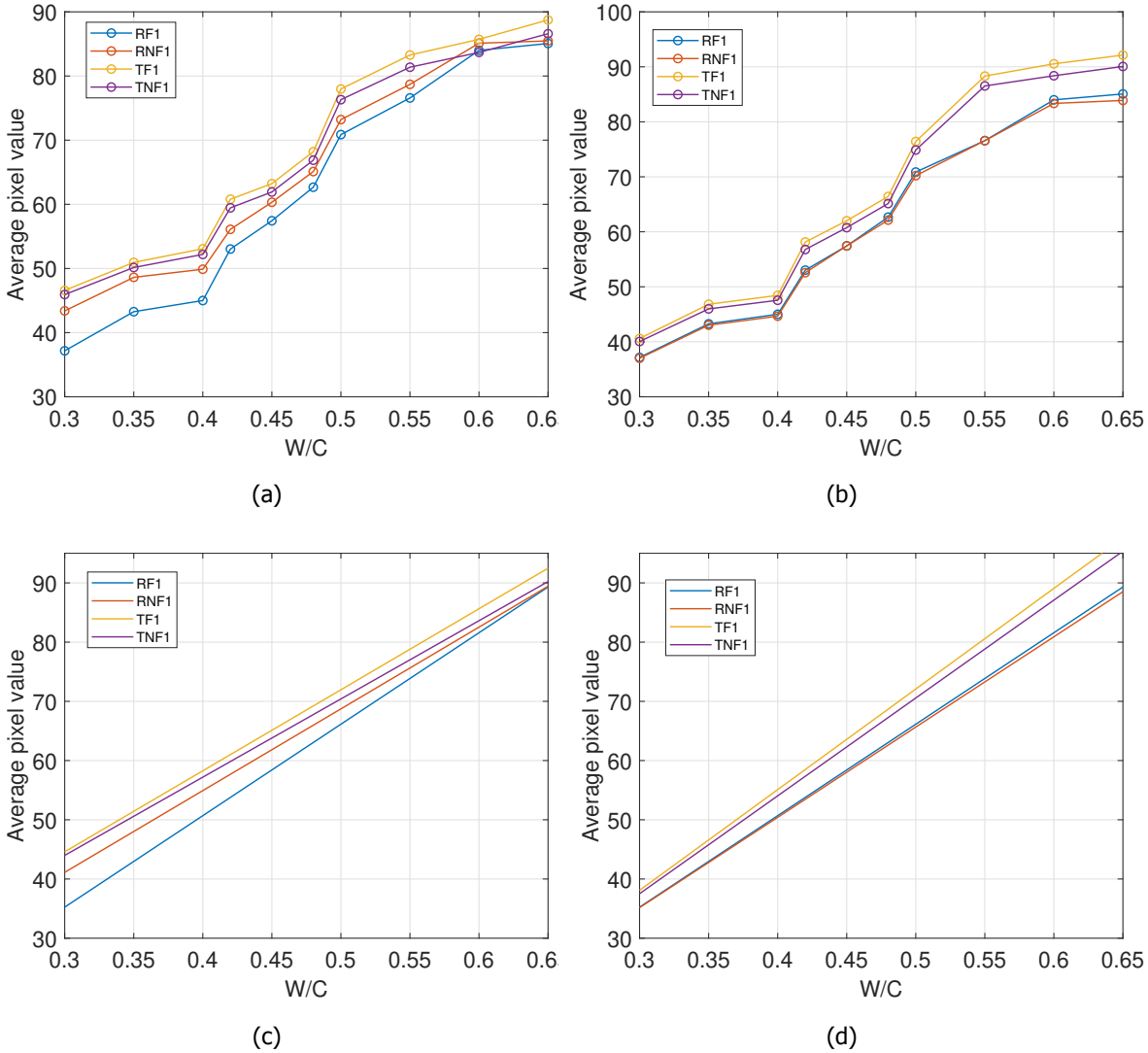

Figure 4.1: Batch No. 1: (a) W/C vs AVG pixel value. (b) W/C vs AVG pixel value - fix boundaries. (c) W/C vs AVG pixel value, linear regression. (d) W/C vs AVG pixel value,linear regression - fix boundaries

Figures 4.1 (a) and (b) show the correlation for batch No. 1 using the boundaries from table 4.1 and the entire range respectively and the different light modes. In general terms it can be seen that regardless of the method or the light mode, all the graphs have a good linear behaviour which is expected from the R^2 shown previously. The transmitted light has a higher intensity meaning that the pixel value used for this type of light will always be higher, for instance, in figure 4.1 (a) it would have been expected that since the TF upper boundaries were lower in comparison with the RF, the pixel values should be also lower, nevertheless the values were higher. For 4.1 (b), it can be seen that the reflected light is more stable at high W/C meaning that it should provide more accurate measurements in this zone. Moreover, figures 4.1 (c) and (d) show the lineal regression for the different batches and light modes. It can be seen that in the case of figures 4.1 (d), the graphs tend to diverge, meaning that the sensitivity of the measurements is higher for higher W/C ratio.

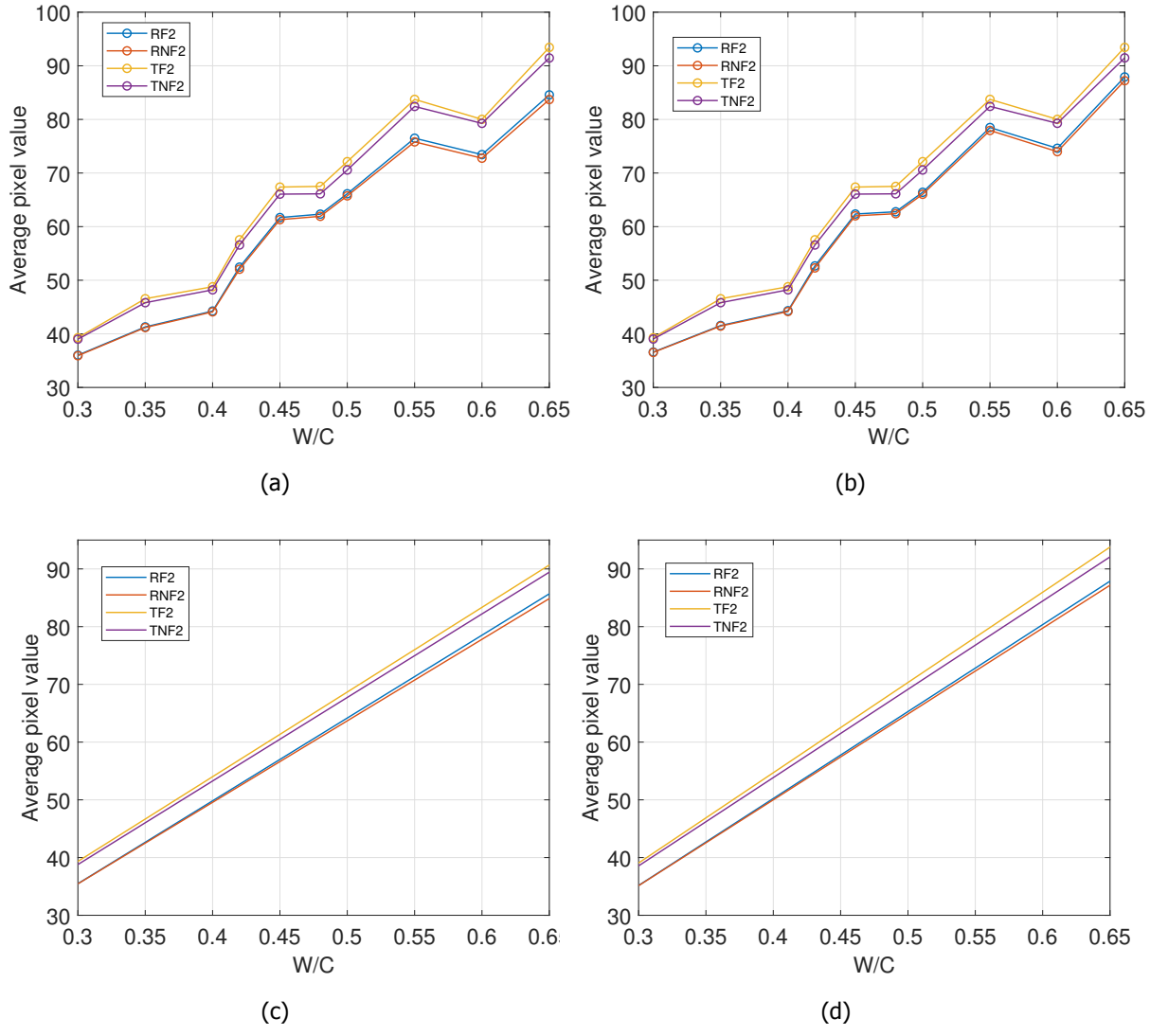

Figure 4.2: Batch No. 2: (a) W/C vs AVG pixel value. (b) W/C vs AVG pixel value - fix boundaries. (c) W/C vs AVG pixel value, linear regression. (d) W/C vs AVG pixel value,linear regression - fix boundaries

Figures 4.2 show the same information as 4.1. For this case, it can be seen that in general terms the behaviour of the graphs is more stable in comparison with the first batch, for instance the graphs from 4.2 (c) and (d) are almost parallel regarding the boundaries to compute the average pixel value. As it is known, the method is sensitive to light settings, therefore a possible reason for this can be that since the exposure of the camera for this case was lower that the one in the first batch, 303 ms vs 497 ms, it would give a better behaviour, although, it can also be seen that the graphs tend to diverge when they reach higher W/C values as in the previous batch.

4.1.2. Light modes comparison

The aim of flat field correction was to compensate for the pixel to pixel variations that take place specially on the edges of the micrographs due to the way the light is captured. It can be seen in figures 4.1 and 4.2 that the behaviour of the RF vs the RNF is almost the same, nevertheless, for the TF and TNF the behaviour had some slight changes. This shows that on its own the reflected light gives better quality images than the transmitted light, since the correction due to the flat field has a lower impact on it.

Figures 4.3 shows the difference between the maximum and minimum average pixel value of the micrographs per sample for each batch and light mode using the entire histogram. At first it can be seen that for all the cases this difference increases for higher W/C since the heterogeneity of the microstructure also increases. Figure 4.3 (b) shows almost a linear relation for this parameter in comparison with 4.3 (a). A similar case was shown in figures 4.1 and 4.2 where the graphs from the second batch had a uniform behaviour and the ones from the first one, especially for the higher W/C had variations in their behaviour.

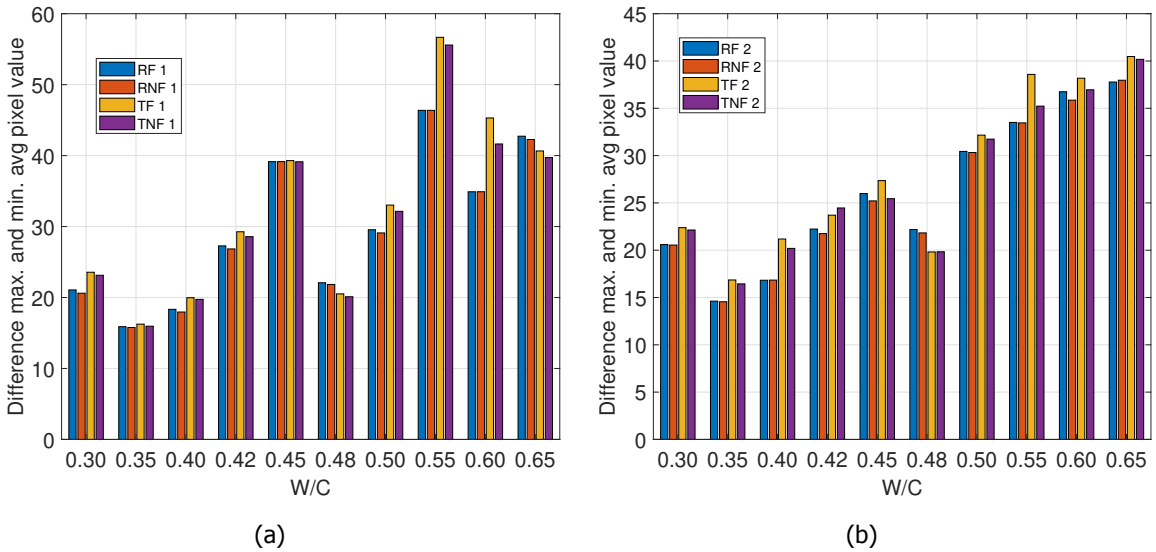

Figure 4.3: Max. and min. values per batch for the different light modes(full histogram). (a) Batch No.1. (b)Batch No. 2

On the other had, at comparing between each light mode, it can be seen that in most of the cases the reflected light images had the lower difference, and in the cases that it was higher than the transmitted light the difference was not that large. This phenomenon shows once again that the use of reflected light and the flat field correction gives more precise results reducing the scatter in the measurements.

4.1.3. Epoxy thin section

In total 5 thicknesses were measured (See Annex B.1.2) and with this information in figure 4.4 a normalize contour plot shows the variation of the average pixel value as a function of the thickness and the fluopigment (epodye) concentration.

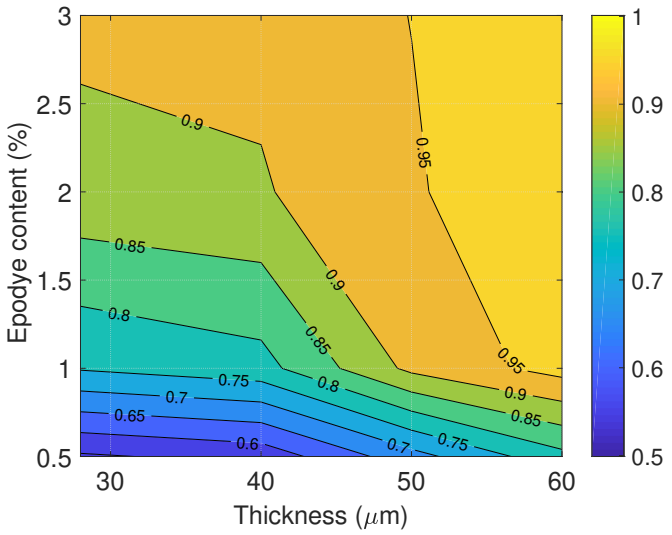

Figure 4.4: Influence of the epodye content and thickness on the average pixel value quantification

At first it can be seen that the influence of these parameters can influence up to 50% the average pixel value. Using as a guideline figure 4.2, a variation of this magnitude can change the W/C from 0.30 up to 0.60, although it's important to mention that this would be an extreme scenario which is not likely to happen. The results obtained here are similar to the one obtained by Jakobsen and Brown [7]shown in figure 2.5, where thicker samples had a higher W/C, for this case, thicker samples have a higher average pixel value that is translate as a higher W/C too.

For a thickness higher than 50 µm, the epodye concentration plays a minor role and the average pixel value is relatively stable, specially for an epodye content higher or equal to 1%. For a thickness between 30 and 40 µm, which is of higher interest, the epodye concentration has a big influence while the thickness has a lower impact, for instance a variation in the epodye of 1% can have a variation up to 20% of the average pixel value.

Another parameter that affect this measurement is the working distance between the sample and the lenses. This aspect is really difficult to control since the distance can change because of the lenses magnification or when trying to focus. Overall, it can be said that these parameters that are usually

taken for granted play an important role in the light measurement of the images which affects directly the estimation of the W/C.

4.1.4. W/C estimation of APG samples

Eight different W/C estimations were made based on the different batches and light modes. It's very important to mention that the micrograph for every unknown sample were acquired with the same light settings as the standards, this way one can be sure that the measurements will not be affected by the changes of the microscope or the camera.

Likewise, the W/C ratios of the unknown samples were also estimated by visual comparison based on the criteria of the author. Since this method is by comparison, it turned out that the brightness of samples B, D and E was not actually the same or similar to the standards, therefore it was decided that they were in the middle of some of them, for instance, for sample B, it was decided that it was between 0.42 and 0.45, therefore the final W/C was 0.43. In the case of sample A, since it was the darkest one, it resembled the 0.30 W/C from the standards and similarly for sample C which was the "second darkest" sample it brightness resembled the one from the 0.35 W/C.

Figures 4.5 (a) and 4.5 (b) show the results for both batches with the different light modes and with the boundaries from table 4.1 and the full gray scale value respectively. As mentioned before, 2 thin sections were analyzed per samples, therefore the W/C value presented in the graphs correspond to their average. Tables with the data can be seen in B.1.1.

As it can be seen in figures 4.5 (a) and4.5 (b), for all the APG samples there are different results, therefore one of them approaches has to be define as "the best one" in order to be the reference for further analysis and comparisons. Based on the results from 4.2.1 and 4.1.2, it was decided that the best results are the ones from the 2 batch using reflected light with flat field correction and the entire range of gray scale. The decision was made based on the fact that first, this methodology can be replicated since all the protocol was controlled, the reflected light with flat field correction has a lower scatter than the other ones, and since by using the grey scale from 15 to 245 the R^2 is equally good as the best one, this result represents better the reality of the microstructure since it takes it all into account.

The UV light method has two main issues, the images that are being acquired and the type of light that is being used. Due to the highly heterogeneity of the concrete microstructure, for each batch different micrographs are acquired meaning that the input data for the proposed methodology is always different causing a change in the computation of the W/C, which ideally should be minimum. Moreover, in the calibration curves it was seen that some light modes or settings gave higher or lower pixel values for the same W/C, in theory this shouldn't matter either because the micrographs from the unknown samples were also acquired with the same settings, therefore the W/C estimation regarding the light mode should be the same.

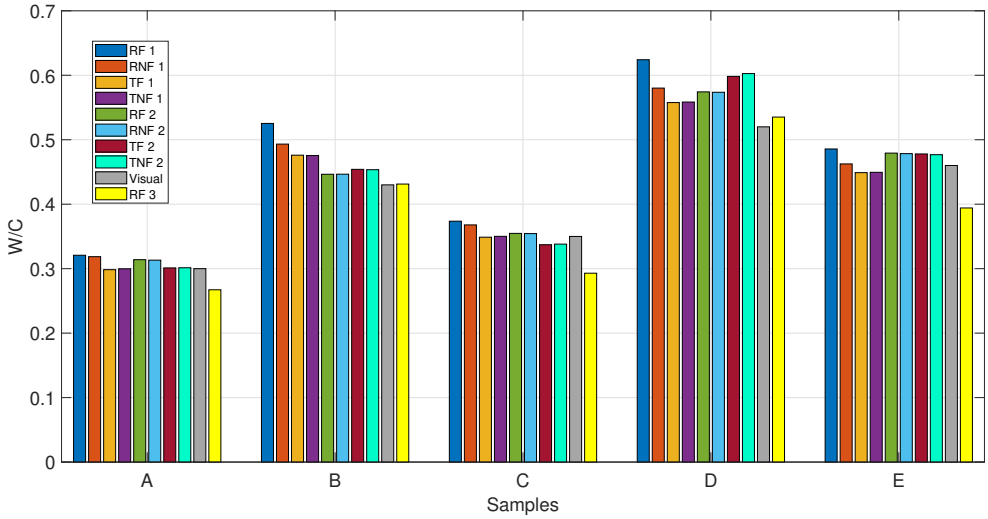

(a)

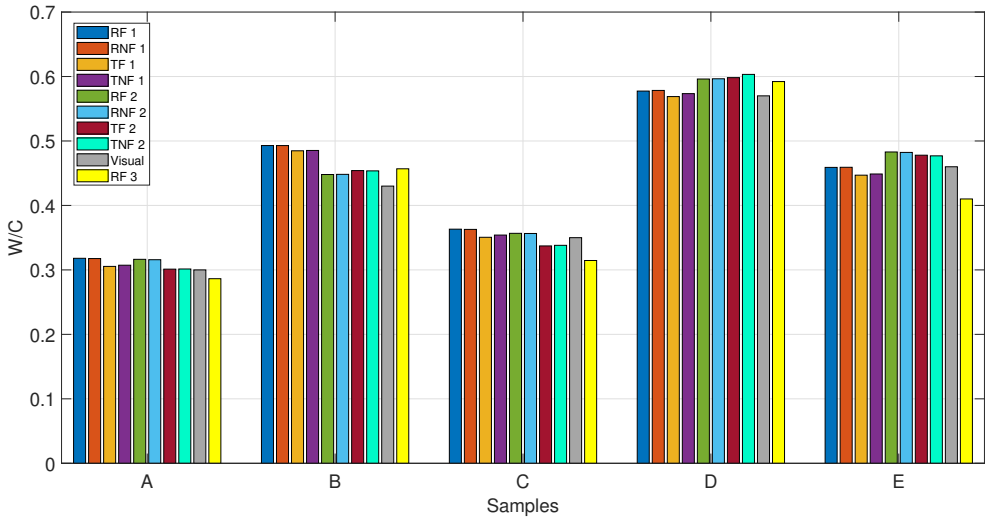

(b)

Figure 4.5: a Results W/C samples APG. (b)Results W/C samples APG with the entire gray scale range

Nevertheless it can be seen that the W/C value of the APG samples changes based on the images acquired, light and camera settings, and the boundaries that are chosen for the correlation. Table 4.2 shows the standard deviation (σ) for the W/C using the entire gray value between each batch, so a variation only based on the light settings, and also due to both batches and the light.

It can be seen that in general terms the light doesn't create a big scatter although it was also seen that that the reflected light has more stability and since this technique has several factors that influence the results, it's advisable to use the reflect light in order to improve the measurements. On the other hand, for batch No. 1 and No. 2, it can be said that the higher the W/C the higher the heterogeneity of the concrete, this can be seen in samples A, C which have the lower W/C estimated and the lower σ, being the most accurate measurements.

Sample	σ Batch No. 1	σ Batch No. 2	σ Batch No. 1 and No. 2	σ Batch No. 1, No. 2 and No. 3
A	0.007	0.009	0.007	0.011
B	0.005	0.003	0.021	0.020
C	0.006	0.011	0.010	0.016
D	0.004	0.003	0.013	0.013
E	0.007	0.003	0.015	0.024

Table 4.2: Standard deviation between light modes and batches

On the other hand, it can be seen that samples B, E and D have a low σ for the light modes, but a higher one when taken into account the first two batches, meaning that the micrographs from one batch to another were significantly different. Similarly, when the three batches were analyzed, still sample A has the lower σ, and sample C has also a low value in comparison with the other samples. Likewise, samples B and E that have a higher W/C also have a higher σ, surprisingly, sample D had a low σ value in comparison with the rest of the samples.

Overall the highest σ was 0.024 for sample E, which is still a good result, considering [7] in which was claimed to have a standard deviation between 0.02 - 0.03 with a method based on visual comparison which in contrast with the proposed methodology cannot be replicated. It's also important to clarify that [7] has a higher amount of data, therefore the results are perhaps more reliable. Nevertheless, this also shows that the proposed methodology is set in the right direction especially since the data to compute the standard deviation is influenced by the use of different microscopes, cameras and persons that acquired the micrographs.

For the visual comparison results, it can be said that for samples A, C and D the results were within the range from the results obtained with the analytical approach, nevertheless, in the visual approach sample E was higher than B which is the opposite from the UV light proposed methodology. The results from this method are not completely reliable, on the one hand, as it was mentioned, the W/C is based on comparisons, therefore for samples A and C, the closer samples were 0.30 and 0.35 W/C but it cannot be said that those are their actual W/C. The same limitation applies to the other samples

Likewise, if there were more standards, the method could be more precise but still it will have a completely qualitative approach, meaning that the results depend on the experience of the person who is doing the test, and this experience cannot be quantified. Although this methodology has some issues, it can be used as a guidance to double check the results obtained by other analytical methods but it's not advisable to use it as a method on its own.

4.2. Circular Polarization Microscopy

4.2.1. Calibration curves

As explained in the previous chapter, a classifier was trained to segment the micrographs, in general terms the idea was to use a single classifier for all the PPL and CPL/XPL images. For every batch, after the segmentation was finished, the author checked if the process was done properly or not. The procedure was considered as successful if the phases were classified in the right categories, if so, then the same classifier was used for the next W/C. For the other case, a new classifier was trained until the right segmentation was obtained, later the procedure was repeated. It's worth mentioning that this methodology takes into account errors since in some cases small areas were not properly classified, although, they have a minor impact in the global result.

For the CPL/XPL micrographs a classifier based on the W/C = 0.65 was used to segmented all the images successfully despite of the different W/C. For the PPL micrographs two classifiers had to be used, one from 0.65 to 0.48 and one from 0.45 to 0.30. The reason for this was that for high W/C there was a big difference between the hydrated and unhydrated zones, being the latter considerably darker than the the former. For the case of low W/C, this difference was lower therefore at the moment of applying the classifier for high W/C in low W/C samples, some parts that were hydrated were assumed as unhydrated, overestimating the latter phase. Figure 4.6 shows an example of the PPL micrographs for W/C = 0.65 and 0.40.

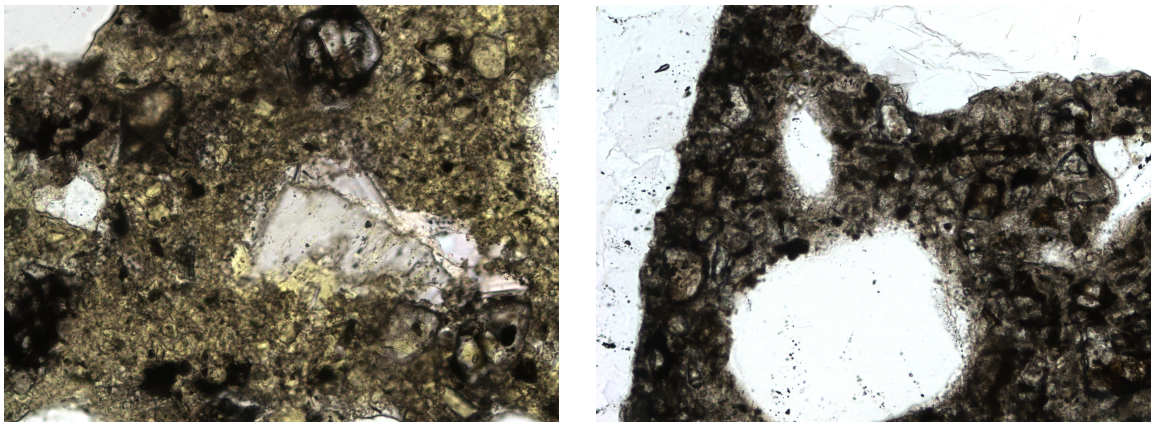

(a) (b)

Figure 4.6: PPL migrographs: (a) W/C = 0.65. (b) W/C = 0.40

Figures 4.7 (a) and (b) show the correlation for the Calcium Hydroxide content from the CPL and XPL micrographs with the W/C. It can be seen that the XPL approach has a slightly higher R^2 in comparsion with CPL. Nevertheless, as it can be seen in figure 4.7 (c), XPL images show between 40% and 60% of the CPL, which shows all the CH crystals, therefore the results obtained with the latter are more reliable even if its correlation is lower.

Moreover, using a similar approach Çopuroğlu [15] quantified the CH content for cement paste with a W/C = 0.60 obtaining similar results as the ones shown in figure 4.7 (c) and 4.8 (b). This is of

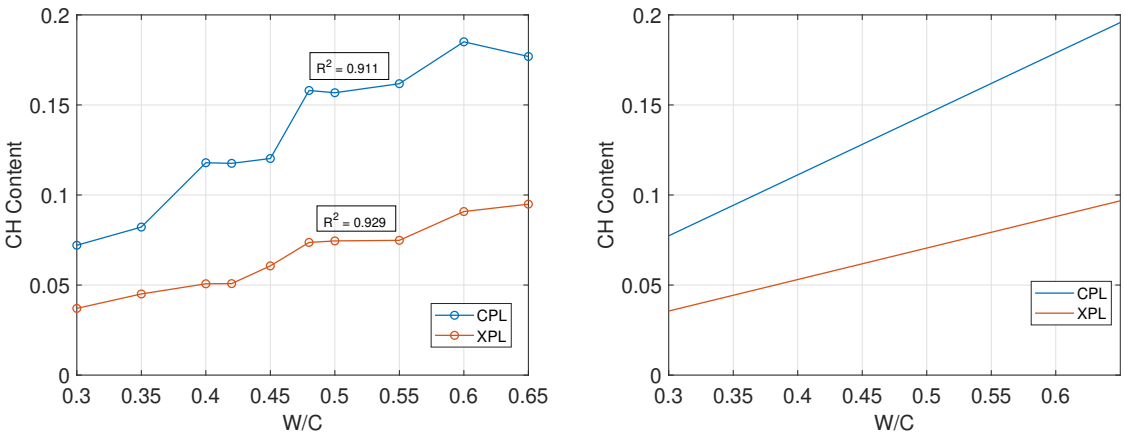

Figure 4.7: (a) W/C vs CH content - CPL/XPL. (b) W/C vs CH content - CPL/XPL, linear regression.

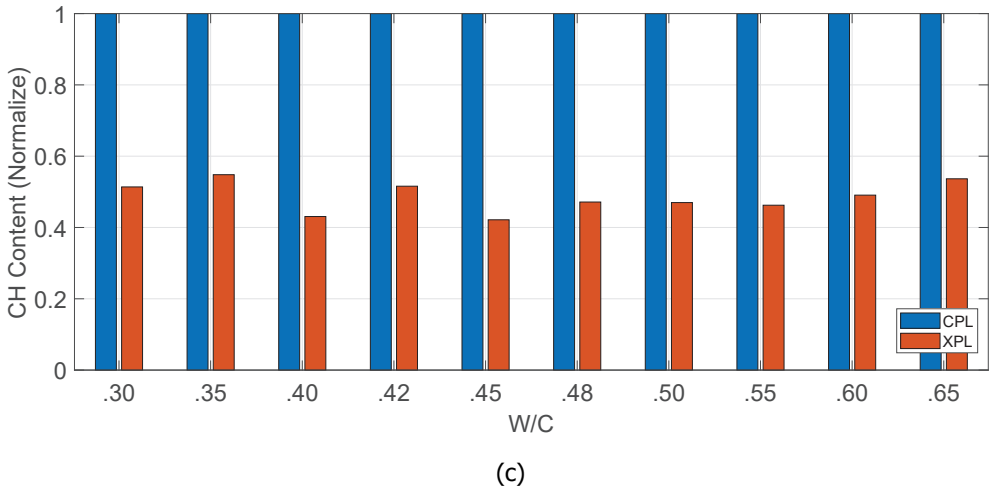

Figure 4.7: (c) Normalize CH content for every W/C

interested because the results obtained in this document confirm the results from the paper and, even more important, it shows that the quantification of CH using XPL or CPL modes is not affected by the variation of the W/C and the aggregate content or type.

4.2.2. W/C estimation APG samples

The CH content of the APG samples was obtained using the same methodology as the standards, although for this case more classifiers were used. Two classifiers, one for PPL and other for CPL, were obtained from sample A2 to segment the PPL and CPL/XPL images of samples A1, A2, C1 and C2. Meanwhile another two classifiers from sample B2 were used to segment samples B1, B2, D1, D2, E1 and E2. This situation, shows that samples A and C can be considered as concrete with low W/C and the other samples as concrete with high W/C. Finally, once the CH content was obtained, its value was plugged in the lineal equations obtained from the standards. Figures 4.8 (a) and (b) show the W/C estimation and the CH content of the APG samples for the CPL and XPL modes respectively. A table

with the values is presented in annex B.2.1.

In comparison with the UV light approach, the W/C obtained for sample A is considerably lower

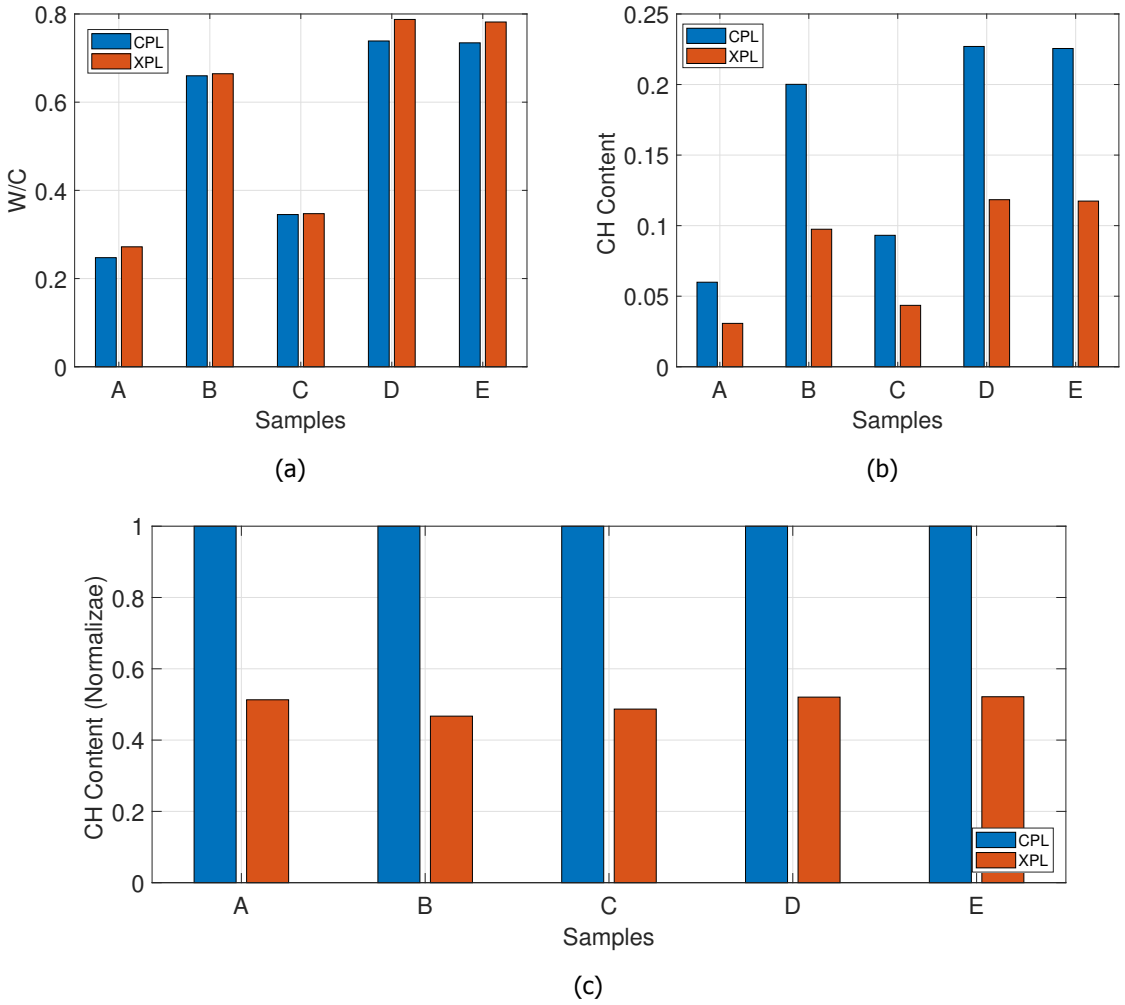

Figure 4.8: (a) W/C obtained APG samples - CPL/XPL (b) CH content APG samples - CPL/XPL. (c) Normalize CH content APG sample - CPL/XPL

and the values from samples B ,D and E are very high and also similar to each other which was unexpected. From the previous technique, the samples were analyzed visually and it was noted that sample D was much brighter than B and E, therefore the fact that the W/C obtained by this methodology gives similar W/C between each of them was unexpected. Moreover, the W/C value obtained by CPL and XPL is similar, although, once again one of the technique has to be consider as "better" in comparison with the other. For this case, as seen in figures 4.8 (b) and (c), the amount of CH content obtained by CPL is higher than the one of XPL, for that reason it was decided that the results from the CPL are more reliable.

Since the results obtained in figure 4.8 (a) were not as expected, it was decided to change the threshold for the minimum size area of the CH cluster and check its influence in the W/C estimation. The cluster size varied from $2.0 \cdot 10^{-5}$ to $2.6 \cdot 10^{-4}$ mm² . For every threshold value a new regression was done.

Area (mm²)	$2.0 \cdot 10^{-5}$	$6.0 \cdot 10^{-5}$	$1.0 \cdot 10^{-4}$	$1.4 \cdot 10^{-4}$	$1.8 \cdot 10^{-4}$	$2.2 \cdot 10^{-4}$	$2.6 \cdot 10^{-4}$
R²	0.91	0.90	0.92	0.92	0.92	0.93	0.93

Table 4.3: Calibration curves boundaries and coefficient of determination R² based on minimum CH cluster size

Table 4.3 shows the value of the R² , figure 4.9 the graphs for the standards and figure 4.10 the W/C estimated for the APG samples based on the cluster size.

It can be seen that when the minimum area of CH clusters are increased, the coefficient of de-

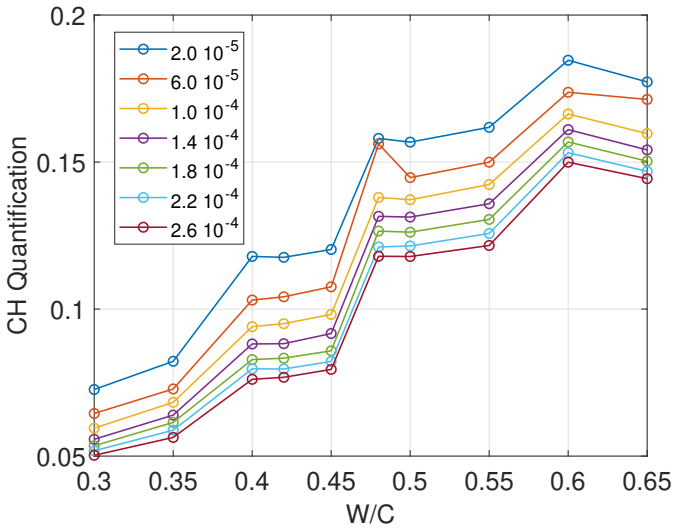

Figure 4.9: W/C as a function of the CH quantification and minimum CH cluster size

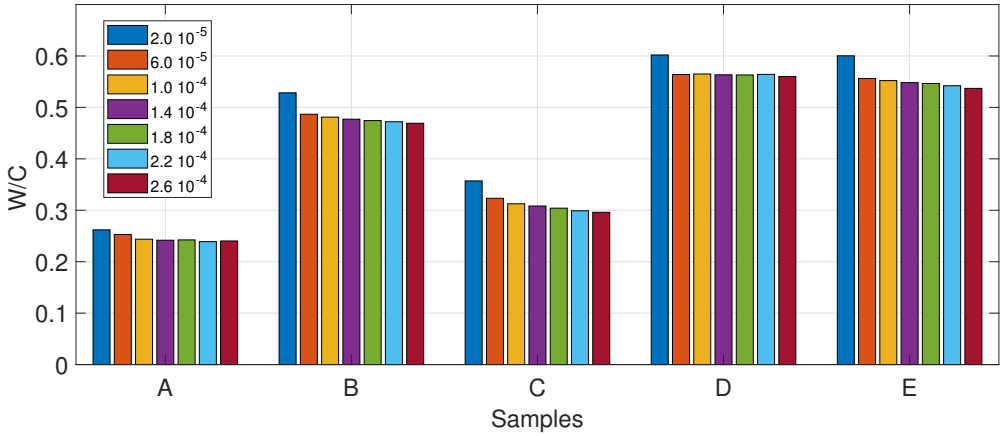

Figure 4.10: W/C estimation as a function of the minimum CH cluster size

termination improves, this shows that some of the areas that were assumed as CH probably were a different phase and were causing noise in the images. Also it shows that is better to focus more on the larger clusters rather than the small ones that are diffused into the matrix since those can be confused with unhydrated particles. Furthermore, by changing the threshold from $2.0 \cdot 10^{-5}$ (mm²) to $6.0 \cdot 10^{-5}$

(mm²) the W/C of almost all the samples decreased around 0.05, then the values started to stabilize. This also proofs that the cluster size has an influence in the estimation of the W/C, so its influence must be considered when using the technique. Finally, it was decided to use the results from the $2.6 \cdot 10^{-4}$ (mm²) since it had the highest coefficient of determination.

After changing the threshold and improving the correlation between the CH quantified and the W/C, still the W/C estimation of the APG samples was not good enough, therefore the next step was to understand why this happened. First, it was important to realize which type of CH was being quantified and which parameters affect its content and distribution. Taking in to account that CH crystals can be very small, the crystals that can be observed with the magnification that was used are known as "conspicuous Calcium Hydroxide". For a non carbonated CEM I cement, the parameters that affect this phase are the content, grading curve (size) and type of aggregate and the cement type.

In general terms, Portlandite tends to grow around the aggregates since in the interfacial transition zones (ITZ) there is a higher content of voids which allows the growth of the crystal. Poole and Sims [9], French [14] established that the type of aggregates influences the growth of CH clusters around them. The crystals prefer to grow around siliceous particles such as quartz instead of the carbonate rocks. Likewise, the amount of area available also influences the quantity of this phase, so a concrete with finer particles will have a larger quantities of CH clusters.

In comparison with the standards that only have quartz aggregates, the APG samples have calcareous and quartz particles, and as it can be seen in figure 4.11 the CH clusters are located close to the latter type of aggregates which will reduce its content as explained in the previous paragraph. Likewise, the maximum aggregate size of the APG samples was 10 mm while for the standards the value that was measured from the thin sections was 20 mm, meaning that on the one hand the type of aggregates of the APG samples should reduce the content of CH but on the other the aggregate size should increase it.

Poole and Sims [9] points out that the Calcium Hydroxide is only produced by the C_3S, C_2S and free lime in the cement, also when these components react, each of them produce a different amount of CH as it can be seen in equations 2.15 and 2.16. For example, C_3S produces up to 4 times more CH in comparison with C_2S, meaning that regardless of the degree of hydration or W/C, the CH content will be different for every type of cement.

Unfortunately for the APG samples the cement used was only specified as CEM I, although based on the comments given by them it can be said that it was normal strength cement while for the standards the cement used was CEM I 32.5 R. Overall, the difference in cement and aggregate between the two sets of samples has clearly an effect in the CH content, making the standards incompatible with the unknowns, nevertheless, it was seen that the CH content correlates properly with the W/C, so with right standards, this parameter could be estimated for an unknown sample.

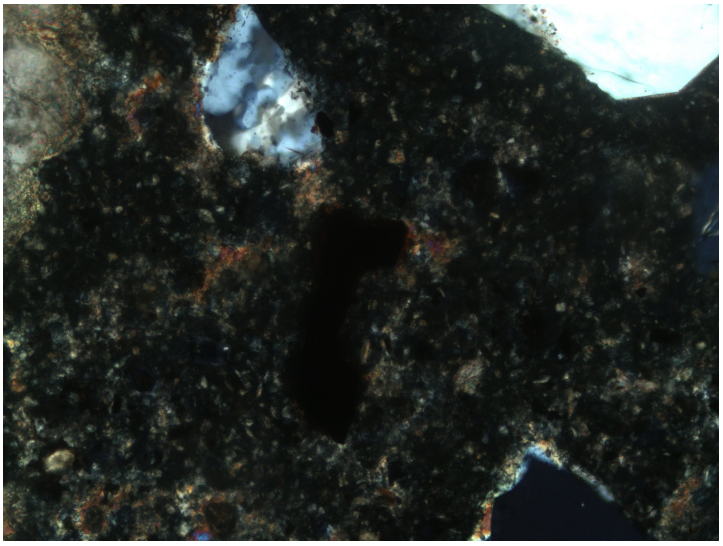

Figure 4.11: Sample D1 - CPL mode

Calcium hydroxide clusters geometry

The approach used for this technique has a big advantage over the UV light methodology, for the latter the result of every image is only a number while for this one is an image that among other parameters gives the CH content. With this in mind, it was decided to use the CPL images to analyse the geometrical features of the phases and see if these parameters changed depending on the W/C. The parameters that were analysed are the area and the circularity. Figure 4.12 shows the histogram of the area distribution of the standards and the APG samples.

Poole and Sims [9], French [14] established that for a high W/C the CH crystals tend to be coarse, well defined and grow at the ITZ, while for low W/C they tend to grow uniformly distributed in the matrix. This idea is seen in figure 3.16 where for W/C = 0.60 the CH crystal are around the aggregates and for W/C = 0.30 this phase is dispersed in the paste. Likewise, except for W/C = 0.30 and 0.35, figure 4.12 (a) confirm the previous statements by showing a trend in which the amount of clusters with an area of $2.6 \cdot 10^{-4}$ mm² tends to increase with a decrease of the W/C, meaning that high W/C have larger cluster while low W/C tend to have smaller ones. On the contrary, figure 4.12 (b) shows that for the APG samples the size distribution is heterogeneous since the CH is usually diffuse into the matrix and there are less clusters around the aggregates. For instance, sample A1, has the lowest amount of small clusters, while E2 that has a high W/C has a larger amount.

Figure B.4 (a) shows for the standards that the circularity distribution is very similar for all the samples regarding of their W/C. At first there is a peak for low circularity, that is related to the cluster in the ITZ which have a large area and then the behaviour is completely heterogeneous. On the other hand, for the APG samples, figure B.4 (b) doesn't show any zone of interest or differences between the samples, due to the fact that the CH is in general diffuse in the matrix causing that its circularity becomes more erratic.

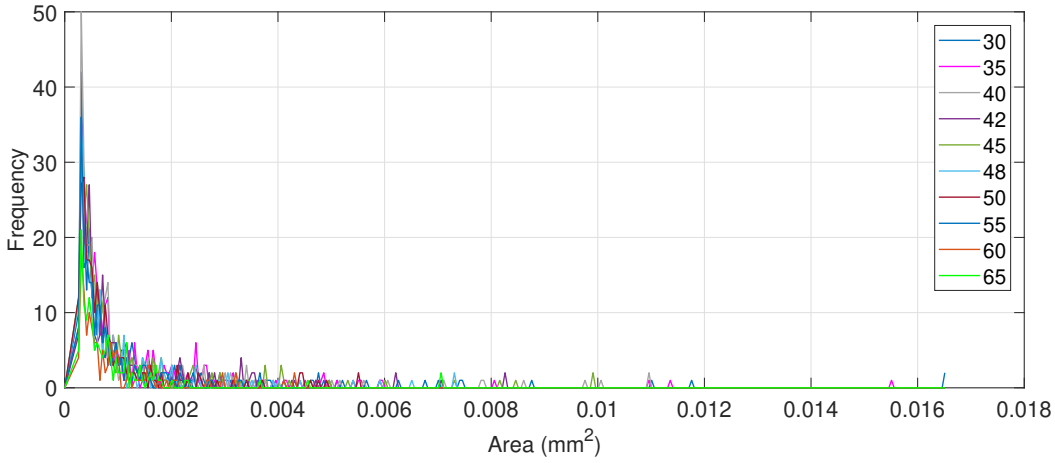

(a)

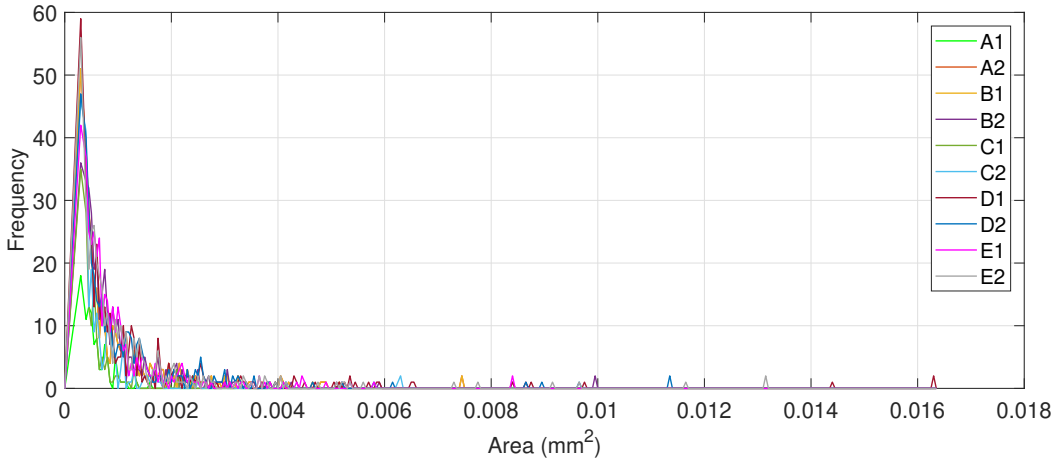

(b)

Figure 4.12: (a) Area histogram standards. (b) Area histogram APG samples.

For the areas, it was also measured the maximum, standard deviation and average values. It is very important to clarify that 0.30 and 0.35 samples had crystals considerably higher than the average. These crystals were due to the entrapped air probably product of a poor compaction of the concrete. Their values were taking into account for the CH quantification, nevertheless, for the statistical analysis they were removed because they were atypical, and more important, they don't represent the real size of the clusters. Figure 4.14 shows large CH crystal located in an entrapped air for a W/C = 0.30. For the standards, figure 4.15 shows the values of each parameter, and table 4.4 shows the coefficient of determination between them and the W/C and the CH content.

The parameters show a tendency in which all the values tend to increase with high W/C which is expected. As mentioned earlier, high W/C samples tend to have large CH clusters but they will also have small crystals in the matrix causing an increase in the mean and standard deviation while low W/C samples grow uniformly in the cement paste causing the opposite effect. For the APG samples, the same information is shown in figure 4.16 and table 4.5.

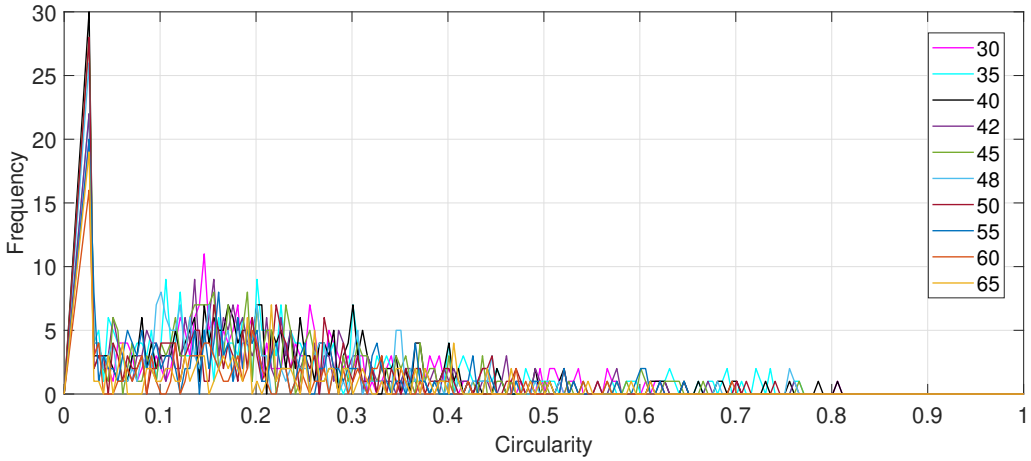

(a)

Figure 4.13: (a) Circularity histogram standards.

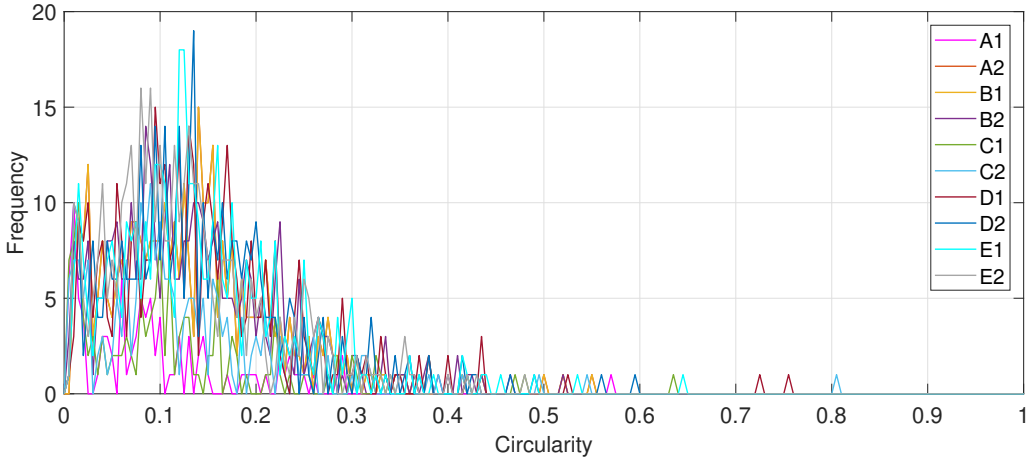

(b)

Figure 4.13: (b) Circularity histogram APG samples.

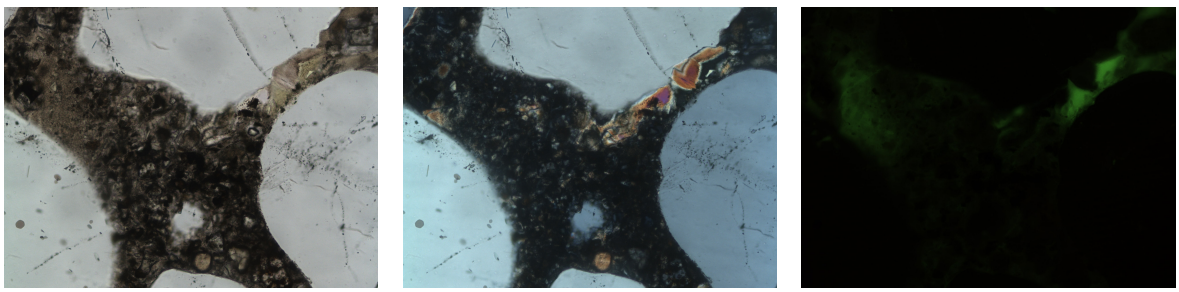

(a) (b) (c)

Figure 4.14: (a) PPL micrograph (b) CPL micrograph. (c) UV light micrograph. The micrographs show how the crystal grows in the entrapped void and it is considerably larger in comparison with other CH from the image.

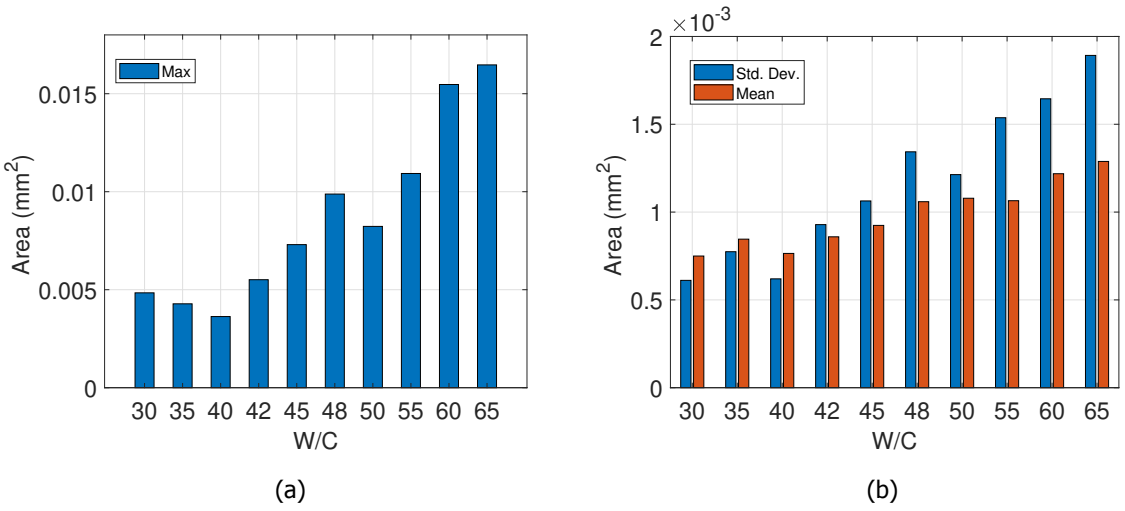

Figure 4.15: CH Max, mean and σ values - Standards

	W/C	CH Content (CPL)
Mean	0.91	0.92
σ	0.93	0.89
Max	0.89	0.87

Table 4.4: Coefficient of determination R^2 between max, mean and σ with W/C and CH content - Standards

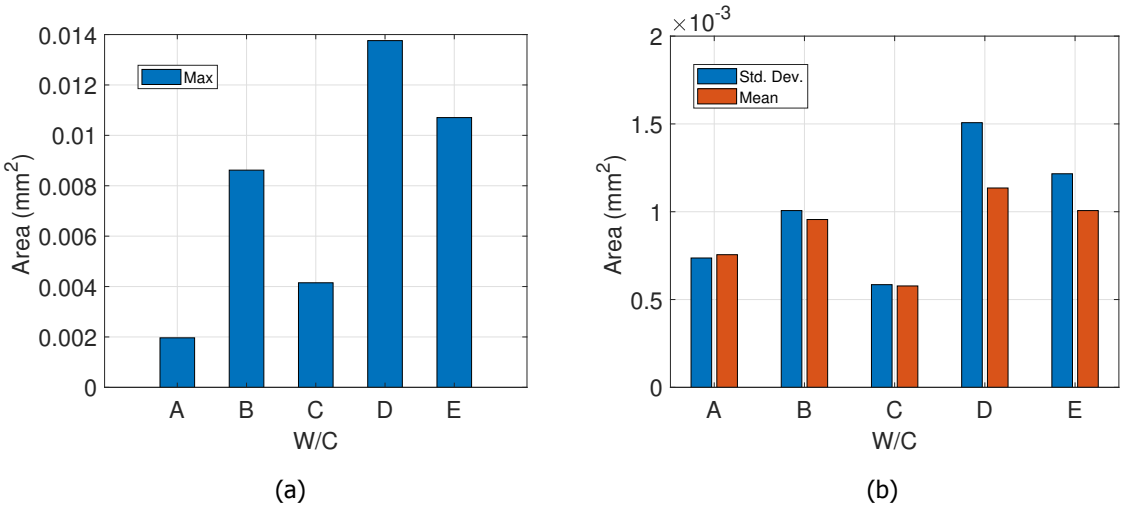

Figure 4.16: CH Max, mean and σ values - APG samples

Similarly to the standards, in the APG samples the CH content has a direct relation with the maximum, mean and standard deviation values. With this in mind, it was decided to do a linear regression for these values and the W/C and then estimate the W/C of the unknowns. The results are shown in figure 4.17.

	CH Content (CPL)
Mean	0.81
SD	0.84
Max	0.89

Table 4.5: Coefficient of determination R^2 between max, mean and σ with W/C and CH content - APG samples

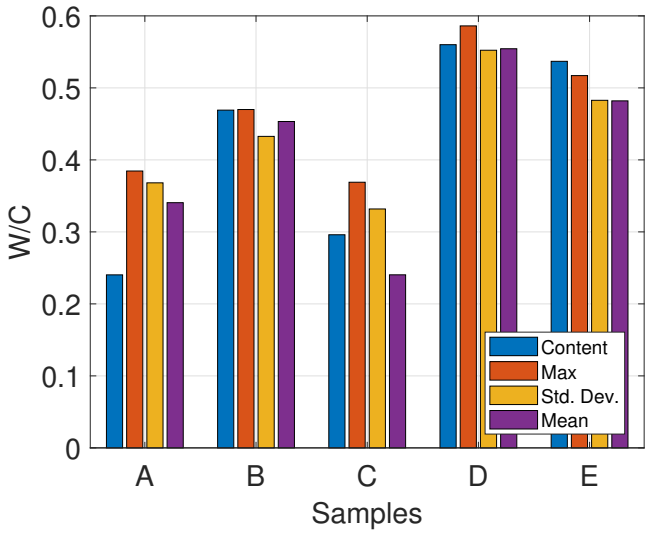

Figure 4.17: W/C estimation APG samples based on statistical parameter

The bars show that these 3 statistical parameters give results that are better than the ones obtained from the CH quantification approach in the sense that they are more logical. The value for samples A and C are still the ones with the low W/C but the value of the former is not as low as before, likewise there is now a larger difference between the values of the W/C of the other 3 samples which was also an issue before. The next step was to define which result was more reliable. It was decided that the maximum value approach gave the best results for different reasons. First, this solves the problem of the similarity between the CH and the unhydrated particles because the maximum size areas are the large clusters of Portlandite which look completely different from the other phases. Moreover, this approach assumes that only the conspicuous CH is being analyze, so the influence of the smaller crystals or any other small phase that might affect the results is neglected. Also, it shows that the influence of the cement type and the aggregate type that was affecting the CH quantification is now mitigated.

Finally, it was decided to plot the area of the CH clusters vs their circularity for the standards and the APG samples, all the figures can be seen in annex B.2.2. In figure 4.18 there is a plot of the area vs circularity for high, mid and low W/C of the standards and the APG samples.

It is important to realize that regarding of the CH content between the standards and the APG samples both figures have a similar trend, for the samples with low W/C the scatter gets closer to the Y axis and for the high W/C the scatter tends to extend in the X axis direction. Overall the maximum, mean and standard deviation values are independent of the cement type and the aggregates, since it

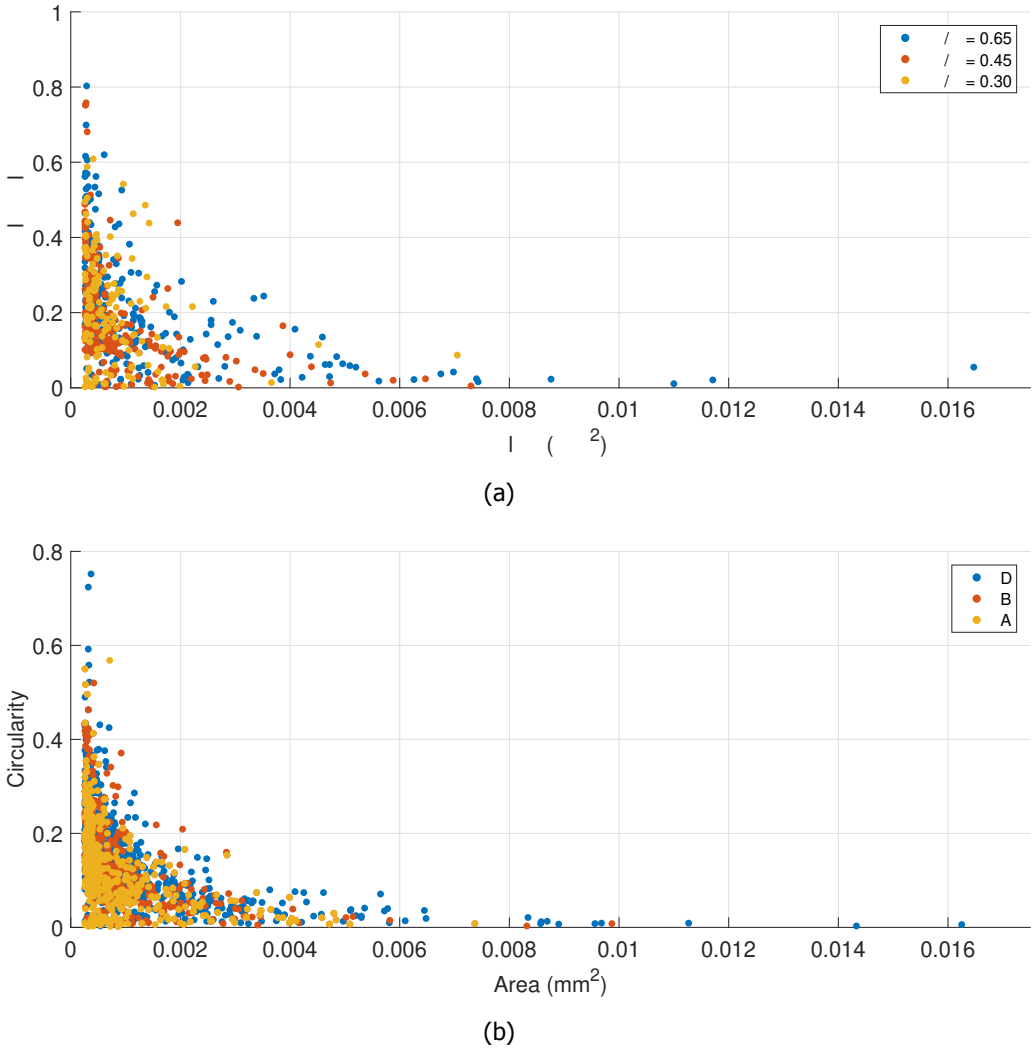

Figure 4.18: (Area vs Circularity. (a) Standards, 0.30, 0.45 and 0.65. (b) APG samples A, B and D

was seen that for both sets the trend between them and the W/C was similar. With this in mind, the information given by these figures can be used to assess the W/C estimation, for instance, if sample A has a lower mean value or standard deviation in comparison with sample B, it means that the latter has a higher W/C, so in case of doubt that information can be used to double check the results obtained from other approaches.

4.3. Scanning electron microscopy

4.3.1. W/C estimation APG samples

After analysing and thresholding the BSE micrographs, the percentage of pores, hydration products and unhydrated cement grains were plugged in equations 2.10 to 2.12. Unfortunately, the oxide composition and the density of the cement were unknown, so the values for the volumetric ratio of hydration products to the reacted cement δ_v and the density were assumed for the moment as 2 and 3.15 $\frac{M}{L^3}$ respectively since they are the values typically assumed when there is no further information.

It's also important to mention that since these values are used for all the calculations, a change in them will not have significant impact in the results. The W/C obtained with the different approaches can be seen in table 4.6.

Approach	A	B	C	D	E
1st	0.85	0.97	0.95	1.08	0.99
2nd	0.56	0.55	0.58	**0.65**	0.57
3rd	0.40	**0.46**	0.44	0.49	**0.44**
4th	**0.33**	0.39	**0.35**	0.39	0.38

Table 4.6: W/C estimation SEM + Powers and Brownyard

As it can be seen in table 4.6, there is a big scatter depending on the method, at first it can be said that non of the approaches is right since they all give values that are very similar between each other, nevertheless from the images themselves it is known that some of them have a W/C considerably different from others. For instance, the amount of unhydrated cement grains in sample A are higher than in sample D, meaning that sample A had a lower amount of water, nevertheless, the results are similar.

Based on these results, it can be said that the methodology proposed by Wong *et al.* [11] was partially reproduced. Nevertheless, since the information was already there, it was decided to choose the best approach for every sample and analyse the data. The values in bold in table 4.6 are the ones that are assumed to be correct for every samples. These values were obtained by seeing how good the thresholds were actually segmenting the capillary pores from the images, as expected, approach number one included as pores parts that were clearly hydration products. For example, for samples A and C, only the 4th approach didn't take into account the hydration products.

It is important to mention that even if the thresholds sometimes underestimated or overestimated the capillary pores or the unhydrated cement grains they were not changed since the idea was to see how good is the technique. An example of the histogram, cumulative histogram, the threshold for the unhydrated cement grains and capillary pores and example of the segmentation based on each of them can be seen in figures 4.19 to 4.23.

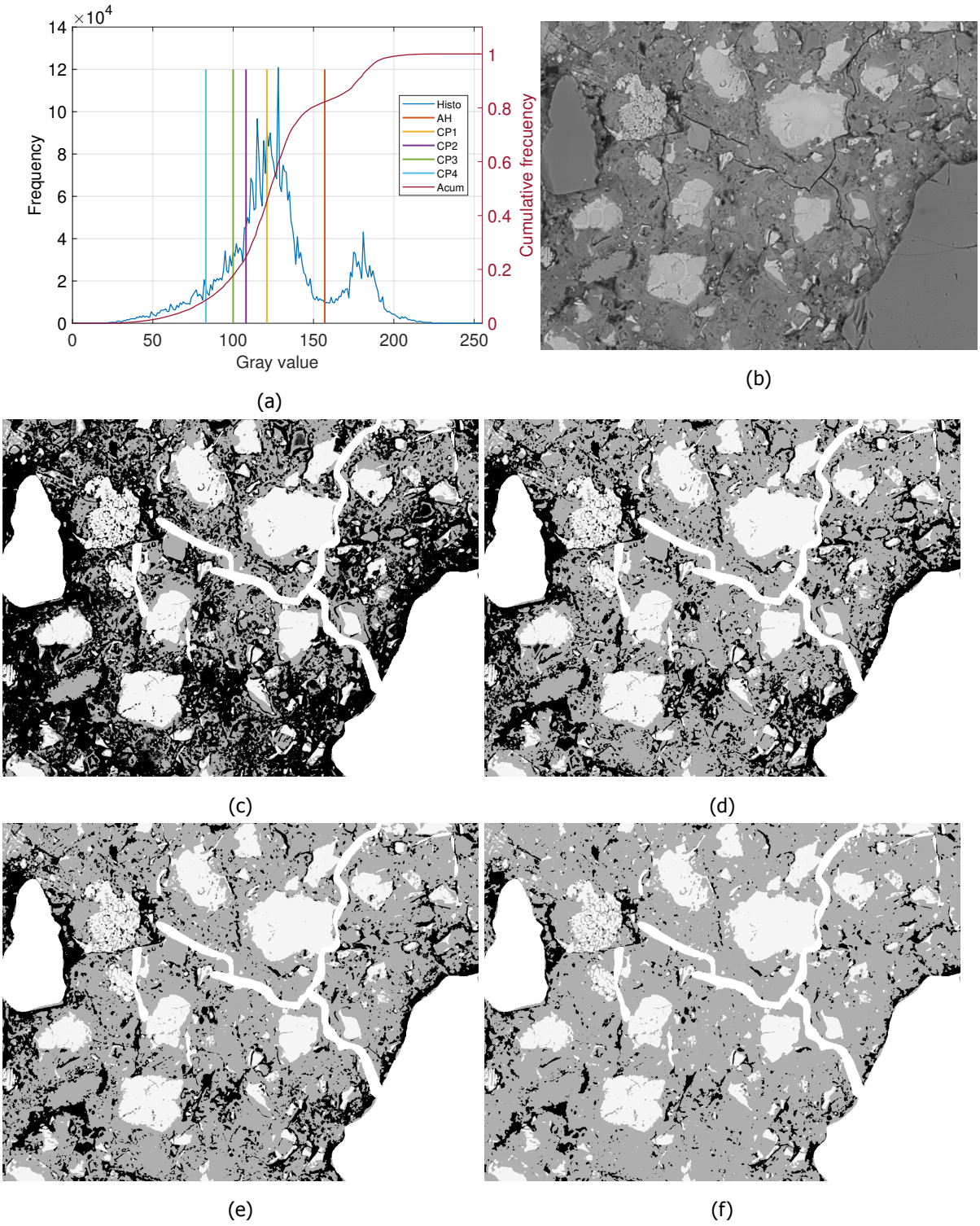

Figure 4.19: Micrograph A10. (a) Histogram, cumulative histogram, unhydrated cement grain and capillary pores thresholds. (b) Original BSE micrograph. (c) Segmentation CP1. (d) Segmentation CP2. (e) Segmentation CP3. (f) Segmentation CP4.

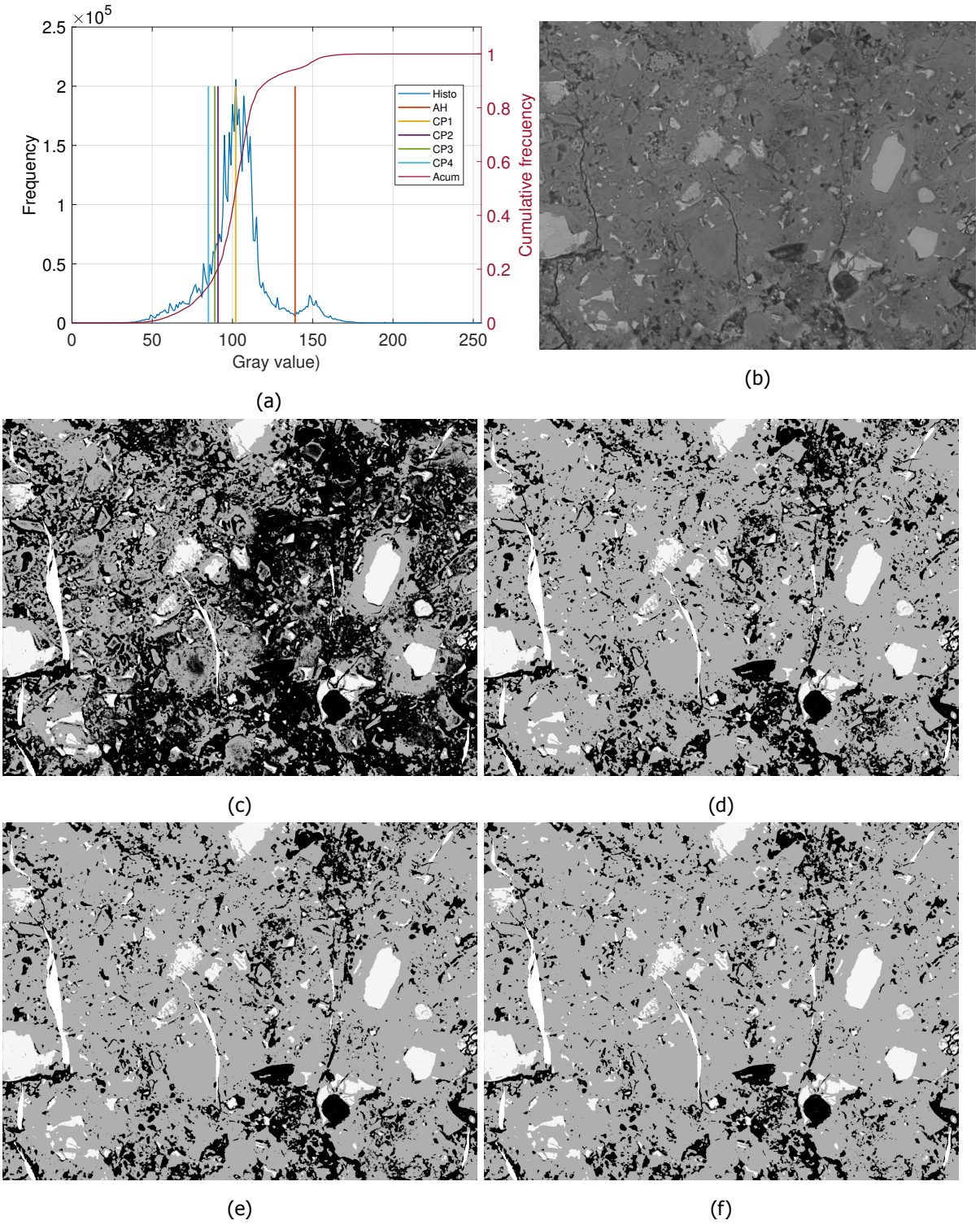

Figure 4.20: Micrograph B25. (a) Histogram, cumulative histogram, unhydrated cement grain and capillary pores thresholds. (b) Original BSE micrograph. (c) Segmentation CP1. (d) Segmentation CP2. (e) Segmentation CP3. (f) Segmentation CP4.

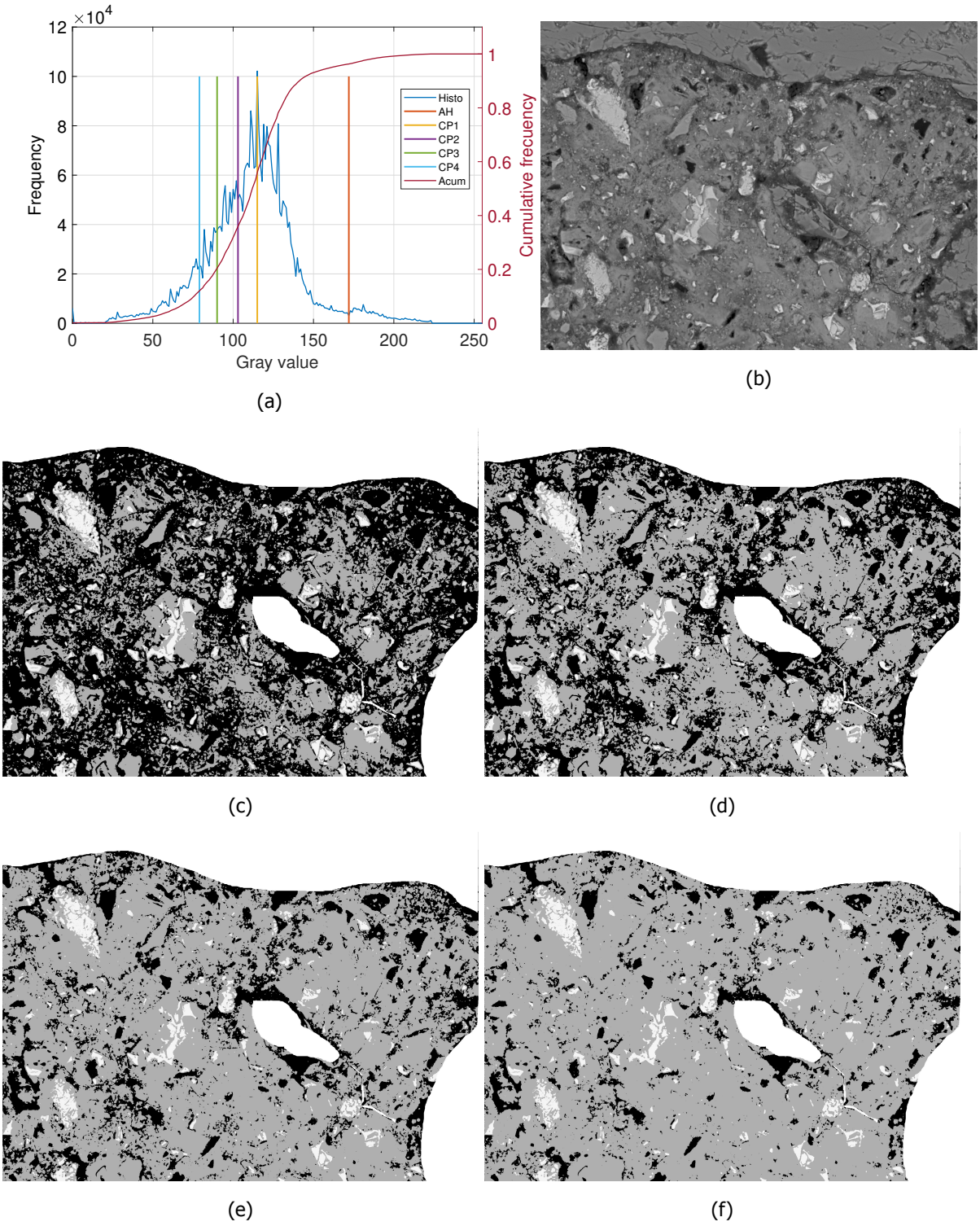

Figure 4.21: Micrograph C14. (a) Histogram, cumulative histogram, unhydrated cement grain and capillary pores thresholds. (b) Original BSE micrograph. (c) Segmentation CP1. (d) Segmentation CP2. (e) Segmentation CP3. (f) Segmentation CP4.

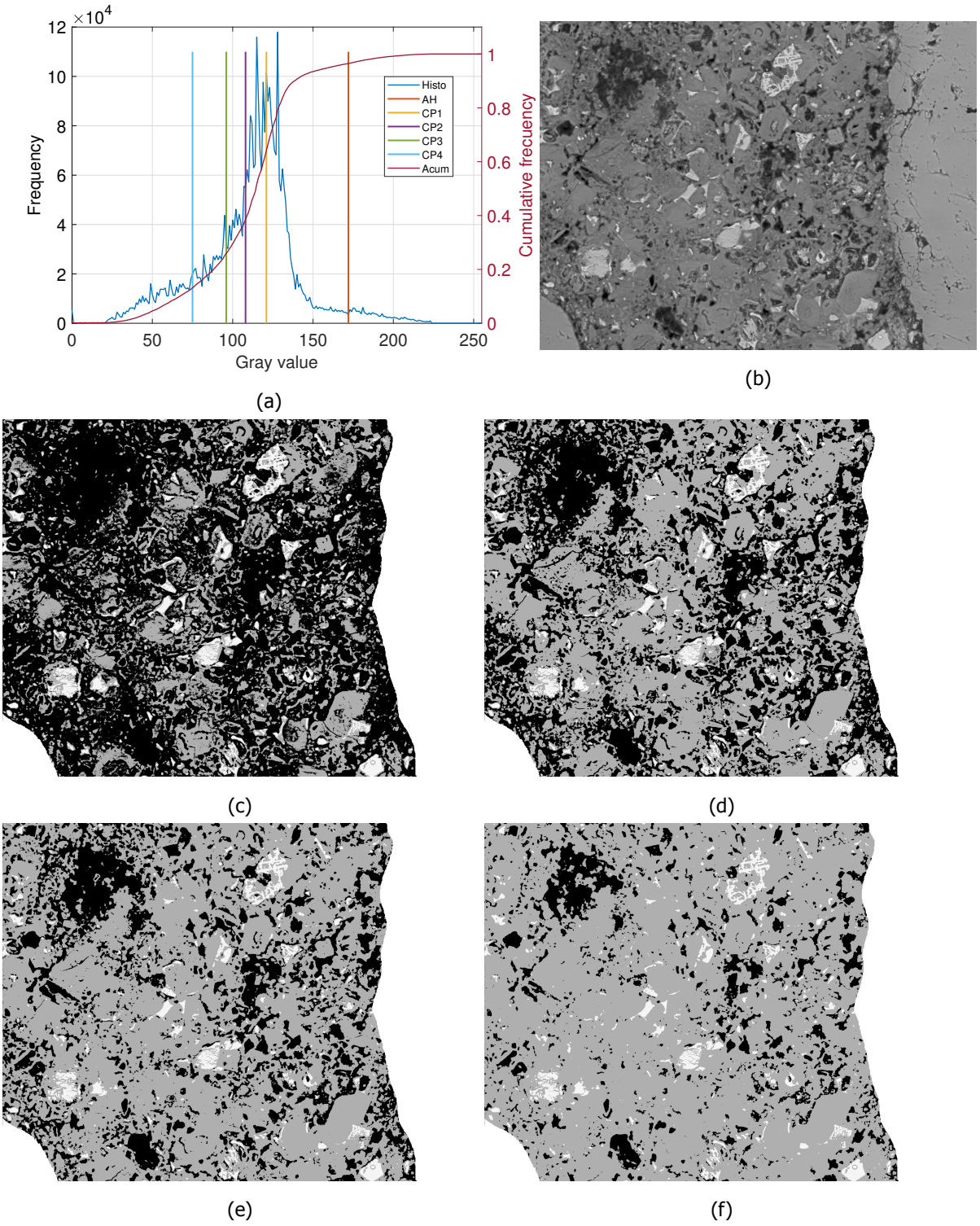

Figure 4.22: Micrograph D03. (a) Histogram, cumulative histogram, unhydrated cement grain and capillary pores thresholds. (b) Original BSE micrograph. (c) Segmentation CP1. (d) Segmentation CP2. (e) Segmentation CP3. (f) Segmentation CP4.

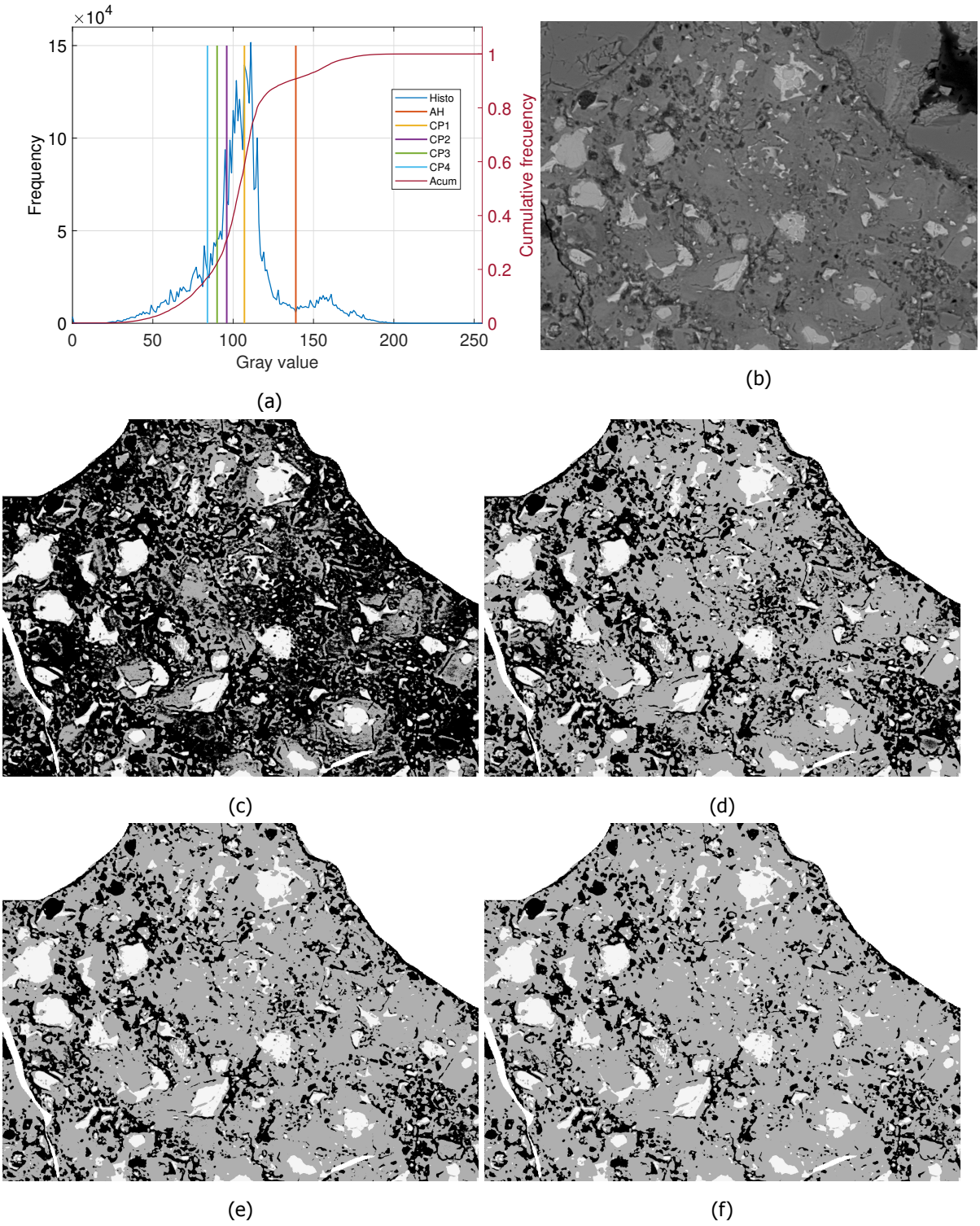

Figure 4.23: Micrograph E25. (a) Histogram, cumulative histogram, unhydrated cement grain and capillary pores thresholds. (b) Original BSE micrograph. (c) Segmentation CP1. (d) Segmentation CP2. (e) Segmentation CP3. (f) Segmentation CP4.

The degree of hydration of every sample was obtained using the formula 2.13. Table 4.7 shows the results obtained. As expected, the approaches that assume a higher volume of capillary pores have a lower degree of hydration, which is expected based on section 2.2. From the previous step it was defined which approach suit better each sample, therefore, in order to be consequent, the same methodology was used to define the degree of hydration of the samples, these values are also shown in bold.

Approach	A	B	C	D	E
1st	0.66	0.81	0.79	0.81	0.69
2nd	0.74	0.87	0.85	**0.87**	0.78
3rd	0.79	**0.89**	0.87	0.89	**0.81**
4th	**0.81**	0.90	**0.89**	0.90	0.83

Table 4.7: Degree of hydration SEM + Powers and Brownyard

4.3.2. Parameters correlation with W/C

It was decided to make indirect correlations between the W/C and the cement grains, capillary pores, degree of hydration and hydration products. Figure 4.24 shows the results obtained with the coefficient of determination R^2 for each case.

It can be seen that the correlation obtained with the cement grains and the degree of hydration is poor, specially in comparison with the other 2 parameters. There are two probable reasons for a poor correlation between the W/C and the cement grains, its size and distribution. On the one hand, assuming a single cement grain particle, when this one starts to hydrated, the hydration products will form around it and create a shell which will delay the further hydration since now the water has to pass through the shell by diffusion. If the grain is larger, the reaction process will be slower in comparison with small grains that sum up for the same area since the latter have more area exposed and they can react faster.

For the distribution of the grains, assuming two grains, once they start to react, their outer products will start to form until the moment in which they will overlap, at that moment, the areas of the grains that are close to each other will become less accessible for the water in comparison with another two grains that have a larger distance between them. The overlap of the hydration products will also delay the hydration process. Based on this analysis, the author agrees with Sibbick *et al.* [18] who says that "*the spacing and number of residual cement grains in the hydrated paste can be significantly affected by delays and acceleration in the hydration rate and the size of the original cement particles.*" This appreciation was done for the UV light method, but it can also be extended to SEM methodologies.

Even though the degree of hydration has a low correlation, the trend that is shown is logic, samples with higher content of water will have a higher degree of hydration since more hydration products can be produced in comparison with samples with the same amount of cement but lower water con-

tent. Moreover, the equation for the degree of hydration is a function of the cement grains and the hydration products, therefore if the former has a lower correlation, it is expected the the DOH will have a similar behaviour. Likewise, as mentioned in section 2.5.2, this value usually have other purposes such as monitor the developed of the mechanical properties of concrete rather than the W/C.

For the capillary pores, the results obtained are in line with the ones obtained by Sahu *et al.* [27] in which the author correlated the porosity of BSE images and the W/C, although it's important to mention that each author had its own methodology. This result also shows that indeed the capillary pores are strongly related to the W/C ratio even if it is measured through UV light or by SEM which can be supported by saying that in all the cases the coefficient of determination R^2 has been higher than 0.90. Finally, the hydration products have a good correlation since this phase complements the capillary voids, for a constant volume, samples with high W/C will have high capillary pores and low hydration products as it's shown in the the graphs, even when the degree of hydration of the samples is also high.

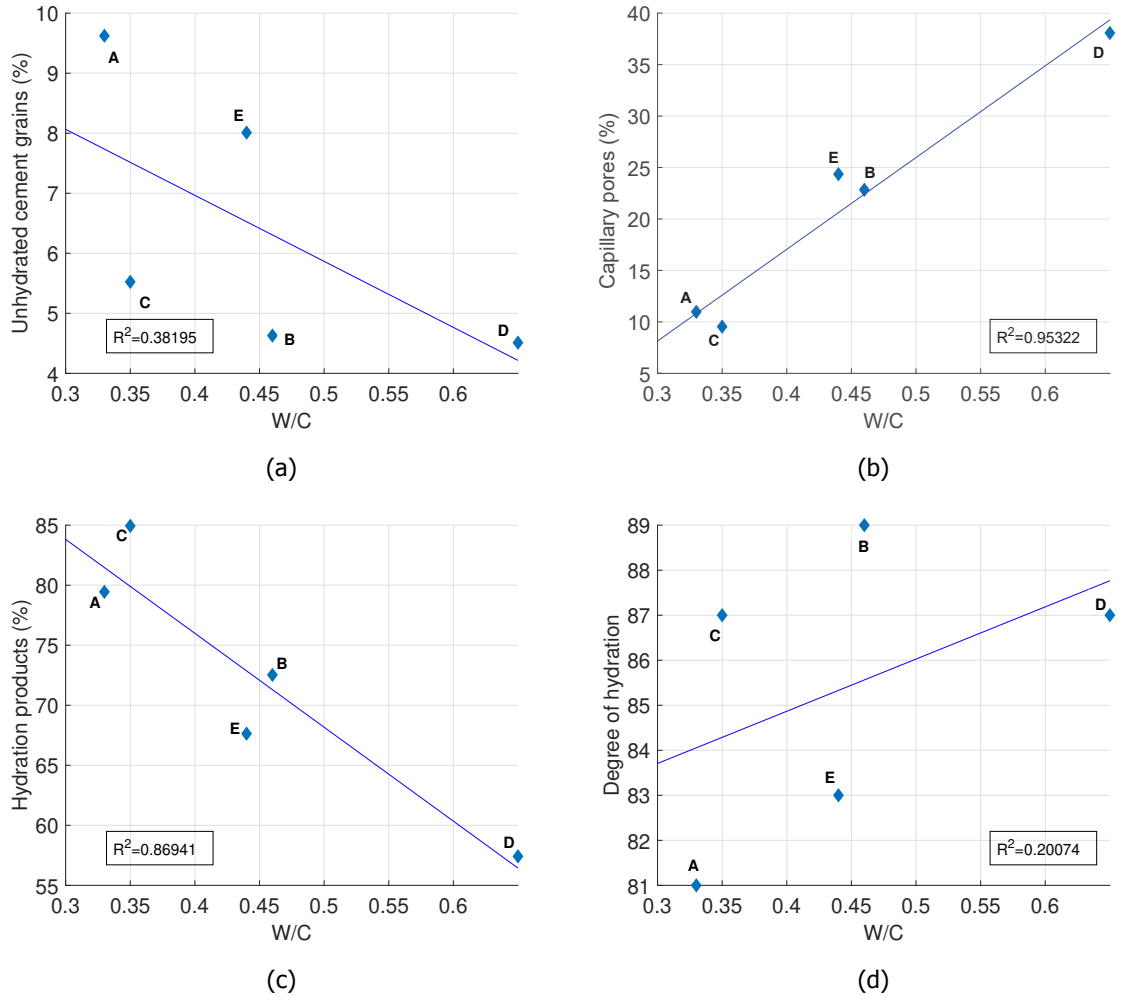

Figure 4.24: Correlations between W/C and Unhydrated cement grains, Capillary pores, Hydration products and Degree of hydration

4.4. TGA Analysis

The results obtained in figure 4.25 show the importance of dividing the CH weight loss by the total amount of water loss. For instance, in figure 4.25 (a), sample C has a high content of CH, nevertheless by dividing its value by the water loss, its value is reduced considerably in comparison with the other samples. Since this methodology is an indirect approach and there are no standards to compare its

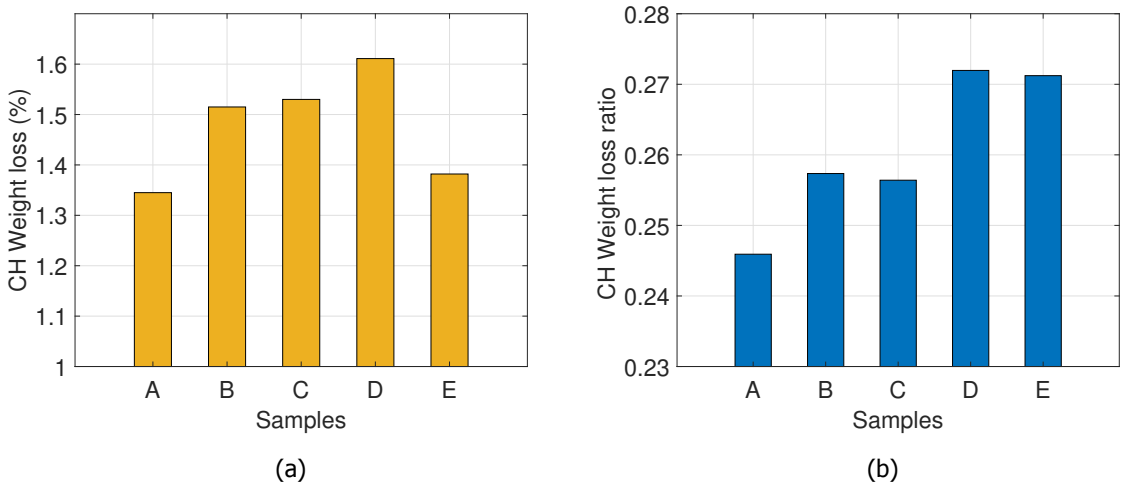

Figure 4.25: (a) CH weight loss (b) CH weight loss ratio

results, the W/C of the APG samples cannot be obtained using this technique. Nevertheless, the results show that some samples have a higher content of CH and when these values are compared with the results from the other techniques a trend is shown, the samples with the higher W/C are the ones with the higher CH content. Likewise, the results obtained can be used to double check the ones from the other approaches, especially since the TGA is the technique that uses the highest amount of mass, being the most representative technique.

5

Comparison between the techniques and APG real results

5.1. TU Delft Standards

The comparison for the results obtained by the TU Delft standards is between the porosity and the Calcium Hydroxide. At first, it can be thought that the parameters are not comparable because they are measuring completely different things, nevertheless, as it was seen in figure 2.1, the W/C and the degree of hydration influence the porosity and the hydration products. For a constant degree of hydration, the higher the W/C, the higher the volume of voids and hydration products and the lower the amount of unhydrated particles. Table 5.1, shows the coefficient of determination R^2 between the W/C, the average pixel value, and the CH cluster size through CPL. The results used for the UV light are the ones obtained from the "RF2" which was considered as the most reliable from this technique.

	W/C	**CH cluster size (CPL)**	**AVG Pixel Value (UV Light)**
W/C	1		
CH Cluster size (CPL)	0.88	1	
AVG Pixel Value (UV Light)	0.95	0.84	1

Table 5.1: Standards results comparison

As mentioned before, the R^2 between the W/C and the techniques have a good value proving that a good correlation exists and that the porosity and the CH content can be used to estimate this value. Moreover, the correlation between the CPL and the UV light methodology is very interesting since it

supports the idea from figure 2.1 mentioned in the previous paragraph even if each technique has its own and independent methodology.

5.1.1. UV light + CPL methodologies

In the previous chapter, the correlation was done individually for the UV light and CPL methodologies, although since these results were good it was decided to do a correlation including both parameter and the W/C to see if there was an increase in the coefficient of determination. Figure5.1 shows the result obtained:

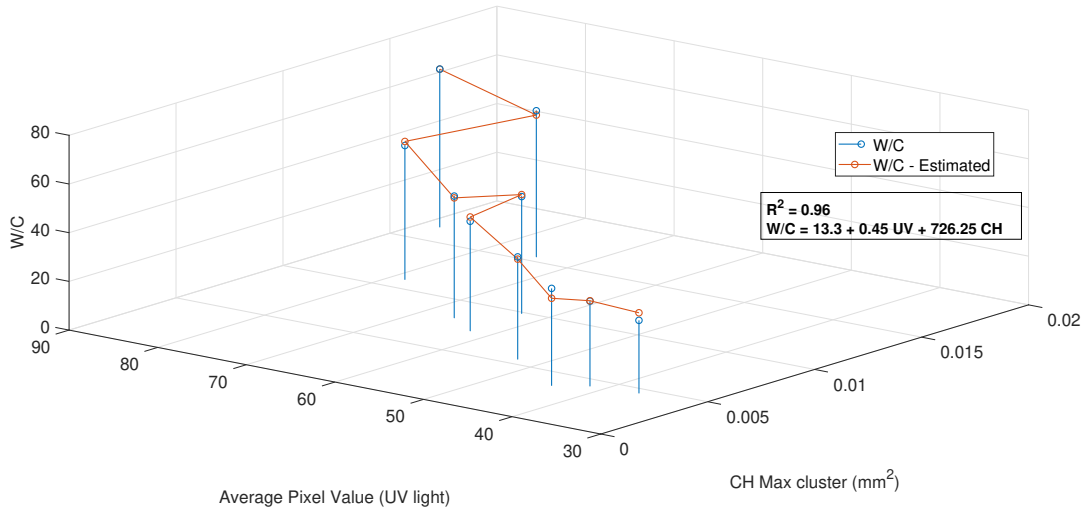

Figure 5.1: CH content (CPL), Average pixel value (UV light) vs W/C

The result obtained improves the R^2 , showing that the use of both techniques can give a more accurate value for the W/C estimation. Likewise, since both techniques used the same thin sections and the equipment is basically the same, only that for the CPL the 1/4 λ filters are required, there is no reason of why the estimation of W/C shouldn't be done through both methodologies, although further research must be done, especially for the CPL methodology. The W/C of the APG samples was estimate using this methodology, the results can be seen in table 5.2. Furthermore, it was decided to create a contour plot to see the influence of these parameters with the W/C value which is shown in figure 5.2.

Sample	**A**	**B**	**C**	**D**	**E**
W/C(UV+CPL)	0.34	0.46	0.36	0.59	0.49

Table 5.2: W/C estimation APG samples using UV+CPL approach

As expected, a higher content of CH and a higher average pixel value are the ones that give the higher W/C. It can be seen that for a constant average pixel value the CH content variation has a low influence in the W/C ratio in comparison with the opposite case. This shows that W/C measurements are more sensitive to the quantification of the UV light rather that the CH cluster size. Also, the figure can be used as a chart to estimate the W/C of the unknown samples which can be very practical.

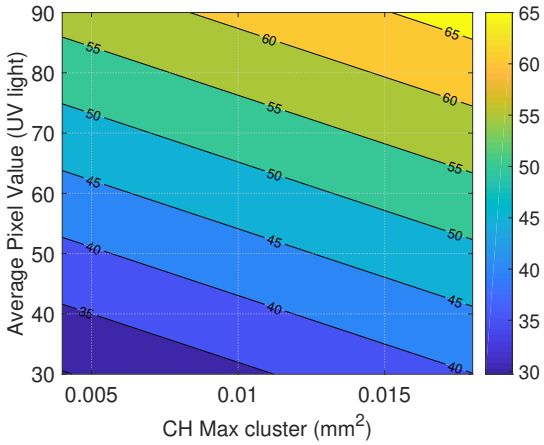

Figure 5.2: Contour plot, W/C as a function of the Average pixel value and the CH max cluster size

5.2. APG Samples

Simarly as the standards, the results from the APG samples were compared. Since the W/C couldn't be estimated for the TGA, it was deciced to do a comparison between the parameters that were measured. For the case of the SEM + Powers and Brownyard, it was decided to use the porosity because this value had the highest R^2 with the W/C that was estimated. Table 5.3 shows the coefficient of determination between the techniques and figure 5.3 shows the normalize values of the results for each sample obtained by the different techniques. The actual values can be seen in C.

	CH cluster size (CPL)	**CH Ratio (TGA)**	**AVG Pixel Value (UV Light)**	**Porosity (SEM)**
CH cluster size (CPL)	1			
CH Ratio (TGA)	0.70	1		
AVG Pixel Value (UV Light)	0.30	0.81	1	
Porosity (SEM)	0.16	0.67	0.97	1

Table 5.3: APG results comparison

The CH content trough CPL has a correlation of 0.70 wit the TGA, one of the differences between them is that in the former only the maximum size of Calcium hydroxide clusters are quantified while in the TGA all the CH that was available was measured, although for the latter the mass loss was divided by the total amount of chemically bound water that can affect the results. Moreover, the UV light has a good correlation with the TGA, but a very low one with the CH clusters which might be due to the fact that the CH distribution is affected by parameters that don't influence the average pixel value quantification.

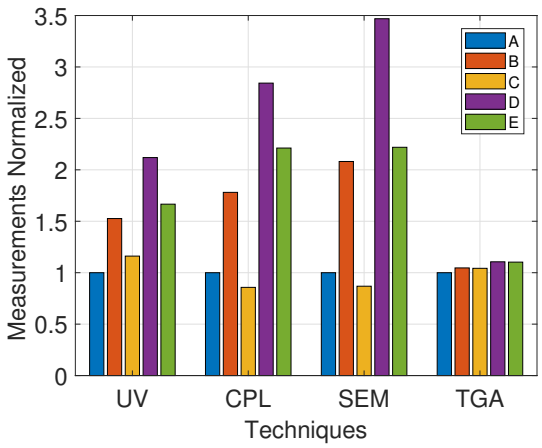

Figure 5.3: APG results normalize

The correlation between the TGA and the SEM + Powers and Brownyard can be influenced by difference in the mass analysed, the former took into account up to 1000 times more mass as it will be explained in the following section. Nevertheless, the highest R^2 is between the SEM and the UV light methodology, this result is similar as the one obtained by Sahu *et al.* [27] who quantified the porosity with each technique using similar approaches.

Finally figure 5.3 shows that in general, the order of the samples is always the same independently of the technique, the samples with the highest values is D, then E, B, C and finally A. Although, the last two change their order for the CPL and SEM approaches with a minor difference. This shows that regarding of the technique, all the results are pointing in the same direction and also show that the W/C estimation can be done in several ways, also it gives the confidence to use the techniques to double check the results among each other.

5.3. APG samples real results

The real APG W/C ratios were given in September 2018, therefore until this moment, the results obtained and their analysis was done without initially knowing the actual W/C of the APG samples. This was very important since all the work that has been done didn't have any bias and the author had to research about the reasons for the results that were obtained without having a guideline. Table 5.4 shows the real restuls from the APG samples and figure 5.4 compare them with the ones obtained by the UV light, CPL, UV+CPL and SEM techniques with the real values.

After analysing the final results, one of the things that was more surprising was that samples B had a

Sample	**A**	**B**	**C**	**D**	**E**
W/C	0.35	0.50	0.40	0.55	0.45

Table 5.4: W/C real values APG samples

higher W/C than sample E. As it can be seen in the document, the values of the parameters that are correlated with the W/C were always higher for sample E in comparison with sample B, meanwhile, for the

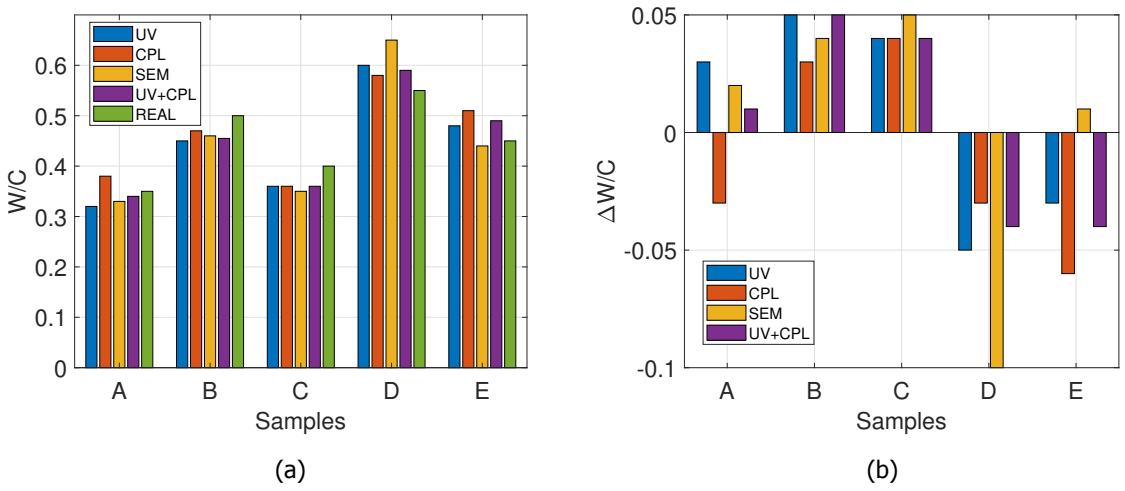

Figure 5.4: CH content TGA

other 3 samples the order was correct, sample A has the lower W/C, then C and D had the highest value.

It can be seen that the results obtained by the UV light and CPL techniques are in general close to the real values. Moreover, the use of the UV+CPL techinque is very useful since it conpensate for a high or low value for either of the techiqnues. For instance, for sample A, the UV light value is lower than the real, the CPL is higher and the UV+CPL is in the middle of both of them and its value gets closer to the real one, so it can be said that the use of both approaches gives better results. Finally, for high W/C, the SEM methodology overestimates this value as it can be seen in sample D due to the problem with the definition of a proper boundary to segment the capillary pores from the rest of the images.

5.4. Which technique gives the best results?

Once the results from the APG samples were obtained, the author learned and realized about the strengths and weakness of the techniques, now the next step was to evaluate those aspects to know which technique gives the best results. It is important to clarify that the fact that the TGA techniques couldn't be used to estimate the W/C doesn't mean that the techniques is wrong but that the author didn't have a proper set of standards to estimate the W/C. Also, for the UV+CPL approach, each technique will be discuss independently and then based on it a discussion will be done for the use of the technique.

Three guidelines were considered to evaluate the techniques, the representativeness, the reproducibility and the reliability. For each of them a subjective score from 1 to 5, being 5 the best grade, will be given and at the end the technique with the highest average score will be considered as the best. Also, it was decided to give to each guideline a different weight since they have a different level of importance. The representativeness will have a value of 30%, the reproduciblity of 30% and the reliability of 40%.

For the representativeness, the methodology of every technique takes into account that the amount of samples should be enough so the cumulative average value of the results becomes constant, although it is also important to consider the mass that is being analysed in comparison with the total mass of concrete. The reproducibility, takes into account the importance of reproducing the techniques in a systematic way, achieving values that are logical and in theory the same or very close the real ones. For example, even without knowing the real values of the APG samples, one can know that the values obtained for the SEM technique were wrong, therefore its reproducibility is low. Finally, the reliability is the most important aspect since is the one that gives more confidence towards deciding between the same result from different techniques.

5.4.1. Representativeness

For the scope of this research, the representativeness is only for the samples that are being analysed, meaning that there will not be a discussion about this aspect regarding ”big” structural elements such as beams and columns, nevertheless, this aspect should be discuss in a new project.

An implicit assumption was done at the moment of using the standards to estimate the W/C using the UV light and CPL modes, each of the ten thin sections represented the mass of concrete that is indicated in annex A.1.1 which is in average 48.32 kg, therefore that assumption will be taken into account to evaluate the representativeness of the techniques.

The first step was to quantify the mass of concrete that had been analysed from the standards and compare it with their own mass. To compute this mass, it was assumed that the thickness of the thin sections was 32 µm and the density of the concrete was 2500 $^{kg}/_{m^3}$. Since the area of the micrographs acquired is known, this value was multiplied by the thickness to obtain the volume and then by the density to get the mass. Table 5.5 shows for the standards a ratio between the total mass and the one that was analysed for the UV light and CPL modes. Likewise, table 5.6 shows a similar information for the APG samples and figure 5.5 shows the mass in milligrams that was analysed for every technique.

Technique	Mass (kg)	% Analysed
UV light	$2.0 \cdot 10^{-6}$	$4.13 \cdot 10^{-6}$
CPL	$5.75 \cdot 10^{7}$	$1.19 \cdot 10^{-6}$

Table 5.5: % Mass Analysed - Standards

Technique	Mass (kg)	% Analysed
UV light	$2.0 \cdot 10^{-6}$	$8.15 \cdot 10^{-4}$
CPL	$5.75 \cdot 10^{7}$	$2.35 \cdot 10^{-4}$
SEM	$1.02 \cdot 10^{-7}$	$4.20 \cdot 10^{-5}$
TGA	$1.04 \cdot 10^{-4}$	$4.24 \cdot 10^{-2}$

Table 5.6: % Mass Analysed - APG Samples

The percentage of mass that represents the standards is considerably lower than the one from the

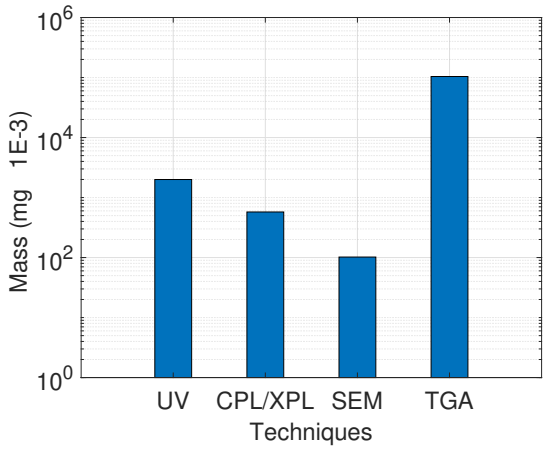

Figure 5.5: Mass Analysed - APG Samples, log scale

APG, for instance the ratio between the percentage of mass analysed by CPL for the standards and the SEM for the unknown is 35 times and in comparison with the TGA is 35678 times. This means that for the total mass of the APG samples the techniques were sufficiently representative. Likewise, as it was seen in the previous section, in general terms the results from the techniques have a good correlation between each other regardless of the mass difference. Nevertheless, it is important to point out that as it was shown in figure 5.5 there is an important difference in mass for each technique, based on it, TGA has the highest score, followed by UV light, CPL and finally SEM. Table 5.7 shows the score for every methodology based on the representativeness.

Technique	Score
UV light	4.5
CPL	4.5
SEM	4.0
TGA	5.0

Table 5.7: Score Representativeness - APG techniques

5.4.2. Reproducibility

In this document the reproducibility is defined as how easily can be a technique reproduced in a systematic way. For instance, the UV light method is usually done by visual comparison which is not a reproducible methodology since it depends on the criteria and the experience of the person in charge. The reproducibility is divided into 3 stages, the samples preparation, the image acquisition and the ignition of the samples for the microscopy and TGA techniques respectively and the data analysis.

In general terms, the samples preparation for all the techniques can be reproduced since all of them follow a standard procedure. Although, for the TGA, all the non-chemically bound water must be evaporated. This process can take up to 3 weeks in comparison with the other techniques in which the sample preparation of a thin or polish section can be done in 2 or 3 days.

For the image acquisition, there are different aspects to consider. For the UV light there is not a clear protocol or approach to follow more than ”taking the best picture”, this affects the reproducibility of the method since every person can have their own idea of what a ”good picture” looks like. For the CPL method, there is also a similar problem, in which the person has to take a ”good picture” based on their own criteria but also there is a guideline in which the person has to take picture thinking on how easily can be the image segmented in the following step. This boundary condition improves the reproducibility of the technique. For the SEM methodology, Wong and Buenfeld [3] established some guidelines such extending the histogram in the dynamic range but also avoid the first and last pixel values of the gray scale which also helps in the reproducibility of the methodology. For the TGA, the samples ”only” have to be place in the equipment and be ignited.

In the last step, the UV light method has a straight forward methodology in which based on the histograms an upper and lower boundary are defined and then the average pixel value of every sample is obtained and the best correlation is computed. It’s worth mentioning that the methodology was used for different set of images with different settings and for all the cases it worked fine. For the CPL methodology the approach is similar but it requires more effort since a lot of computational power is required to train the classifiers, also they need to be checked for every set of images and in some cases trained again.

For the SEM methodology, the replication was done partially because achieving the threshold values for the right segmentation was challenging, nevertheless, with the combination of different approaches, good results were obtained and they could be analysed. Furthermore, it was necessary to know the chemical composition of the cement that is not always available as in this case.

Finally for the TGA, once the boundaries for the CH content, calcareous aggregates (if present) and the chemically bound water were defined the results could be obtained faster than the other techniques, although defining the boundaries can be difficult sometimes especially for the aggregates. Table 5.8 gives a score for every step based on the criteria mentioned before.

Technique	Sample preparation	Data acquisition	Data analysis	Total score
UV LIGHT	5.0	4.0	5.0	4.67
CPL	5.0	4.5	4.5	4.67
SEM	5.0	4.5	3.0	3.83
TGA	4.0	5.0	5.0	4.67

Table 5.8: Score Reproducibility - APG techniques

5.4.3. Reliability

The reliability is defined as how trustful are the results in the sense of how easily are they affected by external parameters and if this can be controlled regardless of the fact that the results are right or wrong. The principle of the UV light method is to measure the porosity of the concrete by quantifying

the light intensity from the epoxy, therefore any parameters that affects this measurement will affect the W/C ratio. As it was mentioned in the document, for every step of the procedure different parameters affect the average pixel value, for the sample preparation the thickness and the epodye content and then for the micrographs acquisition the microscope and camera settings. This shows that the reliability of the technique is not good since the light intensity is affected by many aspects that are in principle controlled but that a change in them cannot be easily perceived by the naked eye.

For the CPL method the microscope and camera settings can also influence the results. Likewise, as it was shown in figure 2.6 the CH quantification is affected by the thickness of the thin section. In principle thanks to the classifiers the effect of these variables and of a wrong segmentation can be fixed by improving the segmentation training. Nevertheless, checking the images can be difficult especially for the APG samples in which the CH clusters are in general diffused in the paste instead of being around the aggregates making them sometimes difficult to define their boundary. This issue has a higher impact in low W/C samples in which a change in the boundary of the clusters can have a major impact in their size.

The results of the SEM + Powers and Brownyard, are only affected by the microscope, nevertheless, the user can also check if the segmentation is correct and if not, new threshold limits can be chosen to improve the methodology. Also the technique allows further research such as quantify the porosity, unhydrated grains, hydration products and degree oh hydration which are also related with the W/C.

In general terms, the TGA technique is used only for cement paste, since the aggregates can affect its results especially if they are calcareous. The APG samples had calcareous aggregates therefore a threshold was define so the mass loss from the CO_2 was not considered. This idea work fine but still in this range there was also a lost of chemically bound water that couldn't be quantify and that affects the results. Furthermore, if the concrete was carbonated, the carbonation couldn't be detected easily since the mass loss from calcium carbonate that is created would overlap with the one from the aggregates. It can be said that the problem with this technique is that the user cannot choose the parts to analyse, therefore undesired zones such as carbonated areas or the aggregates are also analysed and they can affect the final results. Finally table 5.9 gives a score based on the criteria mentioned before.

Technique	Score
UV light	4.0
CPL	4.5
SEM	5.0
TGA	4.0

Table 5.9: Score Reliability - APG techniques

5.4.4. Final Results

Table 5.10 summarizes the scores for the aspects and gives the average for each of them:

Technique	Representativeness	Reproducibility	Reliability	Average score
UV LIGHT	4.5	4.67	4	4.35
CPL	4.5	4.67	4.5	4.55
SEM	4	4.17	5	4.45
TGA	5	4.67	4	4.50
CPL+UV	4.5	4.67	5	4.75

Table 5.10: Final Score - APG techniques

It can be seen that in general terms all the techniques perform good, nevertheless the CPL technique has the highest score as an independent technique. It offers a new approach to estimate the W/C, also by deciding to analyze only the largest clusters of the samples, the quantification of the CH that is affected by its similarity with the unhydrated phases is mitigated. Another advantage is that it analysis a good amount of mass and it can be reproduced as easily as the UV light, although it requires more computational power. Thanks to the classifiers, the user can check in every step if the CH clusters are being segmented properly, and if not, a new classifier can be used allowing to compensated for the external parameters that could affect the images.

On the other hand, the UV light technique is also easy to reproduce but still it's reliability is compromised due to the large amount of variables that can affect the light measurements. Even though, it gave good results for the W/C estimation of the APG samples. The reason for this is that all the parameters that could have affected the measurements were controlled during the process, the amount of epodye, the thickness of the sections and the microscope and camera settings were always the same for the standards and the unknowns. This proofs that the technique is useful and can be reliable if all the precautions are taken.

For the CPL+UV methodology, the values obtained for the representativeness and the reproducibility are the average of both of the techniques but for the reliability it has a 5.0. The reason for this is that in order to obtain a results, the technique requires two different inputs, therefore its output is in a certain way double check automatically. Likewise, for this same reason the standards have the highest coefficient of determination R^2 with a value of 0.96. Similarly, as mention earlier, in most of the cases when a result from UV light or CPL was higher or lower in comparison with the real values, either of the techniques compensate for the other, causing that the final result of the UV+CPL was closer to the real APG values.

The TGA also obtained a high score which is of interest because it opens the opportunity to estimate the W/C using an approach different from the microscopy ones. Unfortunately since there were no standards, the technique couldn't be tested properly, therefore it will be very interesting to make standards with only cement and then concrete and estimate the W/C of the unknowns. In comparison

with the CPL, this method has the advantage that it analyses all the CH crystals in the sample regarding of their size which was an issue for the former especially for low W/C samples.

The SEM + Power and Brownyard have the higher reliability because the way the different parameters are measured is trustful and can be checked and if necessary correct. The problem is that it analyses a small amount of mass and its reproduction is challenging for different reasons. First, the technique has issues in the segmentation of the images because it is very difficult to find a methodology that threshold all the images of the samples and obtained a satisfactory results. Likewise, the user must be able to recognize all the phases which can be challenging for low W/C. If these issues are solved and the technique is reproduce in an easier way it can be another very good alternative. In the mean time, in comparison with the real values, for high W/C the technique overestimated the value because of its segmentation problems.

6

Conclusions and Recomendations

6.1. Conclusions

Based on the sample preparation, data analysis, the results obtained and the comparison of the different techniques the following conclusions were obtained:

1. The sample preparation is fundamental for the W/C estimation because the techniques proposed in this document use the data from the samples as an input value, therefore if they are not done properly, the results obtained will be wrong. To avoid this, the aspects that can affect the measurements of the W/C estimation must be controlled in every step of the methodologies.
2. The results from the standards and the APG samples show that there is a relation between the porosity, the calcium hydroxide features and the W/C. Likewise, this shows that the W/C can be measured with different techniques apart from UV light which has been used for a long period of time without a major improvement in its procedure. The results from this document open the door to the use and study of new approaches such as CPL and TGA, and to a quantitative approach of the UV light methodology.
3. The use of the three guidelines, the representativeness, the reproducibility and the reliability showed that the best technique on its own is the circular polarization microscopy (CPL), although the UV+CPL technique is better. It also showed that each technique has its own pros and cons, and based on it, special attention and improvements can be done to those aspects in order to make them more reliable.
4. The methodology proposed for the UV light microscopy is based on the use of standards and it gives an alternative for the visual comparison approach by providing a methodology that can be quantified and replicated. Likewise, the use of reflected light and of modern photography tools such as white-balance process and the flat field correction allows more accurate values for this technique. Nevertheless, it is important to be aware of the parameters such as the fluopigment (epodye) content and sample thickness that can affect the measurements.

5. The CPL and XPL methodology has less constraints than the UV light and thanks to the plugin Weka Trainable Segmentation some of the parameter that affect the measurements can be compensated. Moreover, since the CPL technique reveals around twice the area of the XPL, the former gave more reliable results. Nevertheless, if the 1/4 λ filters for the CPL are not present, the XPL can also give a good insight about the W/C.

6. The magnification used for the CPL and XPL allowed to cover sufficient area in comparison with the SEM micrographs. Also, since it is a microscopy technique, the person can choose which zones to analyse. This is not possible with the TGA in which all the samples are analysed, including parts that can affect the results. Moreover, the use of the UV+CPL provides better results for the W/C estimation, so it is advisable to do further research especially towards this direction.

7. The used of the plugin Weka Trainable Segmentation is not only useful for the CH quantification but also for further features such as its geometrical properties, that for this case was very important for the W/C estimation. It can also be used for other aspects such as the reactivity of the mineral admixtures, indication of freeze and thaw damage and leaching in concrete.

8. The SEM + Powers and Brownyards methodology has a solid background, although its reproducibility is quite challenging due to the process of obtaining the right thresholds for the segmentation, specially for the capillary pores. Also, due the magnification used, the area that it covers is smaller in comparison with the other techniques. Nevertheless, it is the only technique that doesn't require standards which is a big advantage but it requires the chemical composition and density of the cement.

9. The TGA methodology opens the possibility for the estimation of W/C using an approach that doesn't rely on microscopy. It has the big advantage of quantifying a big mass of concrete in comparison with the other techniques. However, the results can be affected by the aggregates especially if they are calcareous. The TGA can be used as a very good tool to double check the results from the other techniques.

6.2. Recomendations

1. Since a subjective score was given to the techniques in this document with the idea of defining which one had the best results, it would be of interested to turn this into a survey and ask people from the field to judge the proposed methodologies and analyse their answers.

2. This work is one of the first attempts to estimate the W/C through the use of CH, therefore further research is required. In this document, it was concluded that the CH cluster size is a function of the W/C so it will be of high interest to keep investigating in this direction. An ideal conclusion would be that based on the Portlandite cluster size, the W/C of a concrete sample can be estimated, meaning that the use of standards will not be required anymore.

3. Similarly, it will be of interest to define a set of W/C samples, acquire several UV light micrographs and normalize their values. With this it can be analyse if eventually the average pixel value of a concrete sample is independent and doesn't require standards. Once the UV light and the CPL

approaches are independent, a new equation can be done to correlate both values with the W/C, so both techniques can be used without the need of standards.

4. The TGA technique should be executed first with cement paste samples and then with concrete, both with varying W/C ratio. This will allow a better understanding of the influence of the aggregates in the CH quantification and its correlation with the W/C.

5. The representativeness of the techniques is still an issue that must be discussed. The author proposes for a future research to cast beams and columns with different W/C, take samples from different parts of the elements and use the techniques that are proposed in this document to see how many of them are required to achieve a convergence in the results. It might be expected to require a larger number of samples for the columns due to a higher chance of segregation in comparison with the beams.

A

Apependix A

A.1. Samples

A.1.1. TU Delft standards

W/C	30	35	40	42	45	48	50	55	60	65
Gravel (kg)	19.43	19.35	18.84	17.8	17.582	17.41	17.52	17.03	16.29	16.28
Sand (kg)	16.55	17.86	18.84	19.28	19.042	19.63	19.76	20.81	21.59	21.56
Cement (kg)	10	8.58	7.76	7.86	7.789	7.3	7	6.36	6	5.7
Water (kg)	3.23	3.25	3.37	3.57	3.774	3.78	3.78	3.79	3.89	3.99
Total mass (kg)	49.21	49.04	48.81	48.51	48.19	48.12	48.06	47.99	47.78	47.53
Density (kg/m3)	2465	2400	2442	2427	2410	2407	2404	2400	2389	2378

Table A.1: TU Delft Standards mix design

A.2. Scanning Electron Microscopy, Scripts BSE images

A.2.1. Unhydrated cement grains

```
df=df[0:252,]
rta=matrix(nrow = 5,ncol = 31,byrow = FALSE)
rta[,1]=c('','Primer máximo','Valle 1', 'Valle 2','Segundo Máximo')
rta[1,]=colnames(df)
for(i in 2:31){
   col=i
  cum_max=cummax( df[2:nrow(df),col])
  st_max=as.numeric(labels(sort(-table(cum_max))[1]))
  st_max_index=df[which(df[,col]==st_max),1]
    act=as.data.frame(df[which(df\$Value>st_max_index),col])
  colnames(act)=c('hist')
    cum_min=cummin(act\$hist)
  val_min=as.numeric(labels(sort(-table(cum_min[which(cum_min>0)]))[1]))
  val_min_index=df[which(df[,col]==val_min),1]
   nd_max=max(df[which(df\$Value>val_min_index),col])
  nd_max_index=df[which(df[,col]==nd_max),1]
  if(nd_max==st_max){
    val_min2=0
    val_min_index2=0
  }else{
      val_min2=min(df[which(df\$Value>st_max_index&df\$Value<nd_max_index),col])
    val_min_index2=df[which(df[,col]==val_min2),1]
       }
  rta[2:5,i]=c(st_max_index[1],val_min_index[1],val_min_index2[1],nd_max_index[1])
}
```

A.2.2. Porosity, Approach No. 1, No.2 and No. 4

```
df=df[1:254,]

rta=c()
rta2=c()

for (i in 2:31){
  acum=cumsum(df[,i][0:254])
  acum=rollmean(acum, 3)
  derivada=diff(acum)
  derivada2=diff(derivada)
  plot(derivada,type='l')
  plot(derivada2,type='l')
  which.max(derivada)
  prop=derivada/acum[1:251]
    plot(acum,type='l')
   title(main = colnames(df)[i])
   abline(v = which.max(derivada), col = "gray60") #El punto
   text(which.max(derivada), 200000, labels =  which.max(derivada))

  m1=derivada[which.max(derivada)]
  x1=which.max(derivada)
  y1=acum[which.max(derivada)]
  b1=y1-m1*x1

  m2=derivada[which.max(prop)]
  x2=which.max(prop)
  y2=acum[which.max(prop)]
  b2=y2-m2*x2

  pto=(b2-b1)/(m1-m2)
  rta[i-1]= pto
  rta2[i-1]=x1
}
names(rta)=colnames(df)[2:ncol(df)]
names(rta2)=colnames(df)[2:ncol(df)]
```

A.2.3. Porosity, Approach No. 3

```
df=df[1:250,]
rta=c()
AA=2

for(i in 2:31){
    acum=cumsum(df[,i][0:254])
    acum=rollmean(acum, 3)
   derivada=diff(acum)
      acum=as.data.frame(acum)
  acum$index=seq(1:nrow(acum))
  derivada=diff(acum$acum)
  derivada[252]=1
  cum$prop=derivada/acum$acum
    reg=lm(acum$acum[1:which.max(acum$prop)] ~ acum$index[1:which.max(acum$prop)])
  coef=reg$coefficients

  x1=0
  y1=0

   acum$m=(acum$acum-y1)/(acum$index-x1)
    plot(x=acum$index,y=acum$derivada,type='l')
  plot(x=acum$index,y=acum$m,type='l')
  which.max(acum$m)
    reg2=lm(acum$acum[which.max(diff(derivada)):which.max(acum$m)] ~
acum$index[which.max(diff(derivada)):which.max(acum$m)])
  coef2=reg2$coefficients
    rta[i-1]=round((coef[1]-coef2[1])/(coef2[2]-coef[2]),0)


  if (i ==AA){
    write.csv(file='Ejemplo_Met1.csv',x = acum)
  }
}

names(rta)=colnames(df)[2:ncol(df)]
```

B

Appendix B

B.1. UV light

B.1.1. W/C estimation APG samples

Sample	RF1	RNF1	TF1	TNF1	RF2	RNF2	TF2	TNF2	Visual	RF3
A	0.32	0.32	0.30	0.30	0.31	0.31	0.30	0.30	0.30	0.27
B	0.49	0.49	0.48	0.48	0.45	0.45	0.45	0.45	0.43	0.43
C	0.36	0.37	0.35	0.35	0.35	0.35	0.34	0.34	0.35	0.29
D	0.58	0.58	0.56	0.56	0.57	0.57	0.60	0.60	0.52	0.54
E	0.46	0.46	0.45	0.45	0.48	0.48	0.48	0.48	0.46	0.39

Table B.1: W/C estimation UV light mode

Sample	RF1	RNF1	TF1	TNF1	RF2	RNF2	TF2	TNF2	Visual	RF3
A	0.32	0.32	0.31	0.31	0.32	0.32	0.30	0.30	0.30	0.29
B	0.49	0.49	0.48	0.49	0.45	0.45	0.45	0.45	0.43	0.46
C	0.36	0.36	0.35	0.35	0.36	0.36	0.34	0.34	0.35	0.31
D	0.58	0.58	0.57	0.57	0.60	0.60	0.60	0.60	0.52	0.59
E	0.46	0.46	0.45	0.45	0.48	0.48	0.48	0.48	0.46	0.41

Table B.2: W/C estimation UV light mode - fix boundaries

B.1.2. Epoxy thin section results

	Thickness (mm)			
Epodye content (%)	**28**	**40**	**50**	**60**
0.5	45.05	47.16	56.56	65.22
1	62.67	64.94	75.77	80.48
2	73.41	74.39	78.37	83.06
3	75.61	75.76	78.99	82.80

Table B.3: Effect of the thicnkess and epodye concentration on the average pixel value

B.2. Circular Polarization Microscopy

B.2.1. W/C estimation APG samples

	W/C (CPL)	W/C (XPL)	W/C (CPL-Mean)	W/C (CPL-Std dev)	W/C (CPL-Max)
A	0.25	0.27	0.38	0.37	0.34
B	0.66	0.66	0.47	0.43	0.45
C	0.35	0.35	0.37	0.33	0.24
D	0.74	0.79	0.59	0.55	0.55
E	0.73	0.78	0.52	0.48	0.48

Table B.4: W/C estimation CPL and XPL modes

B.2.2. Figures Areas vs Circularity

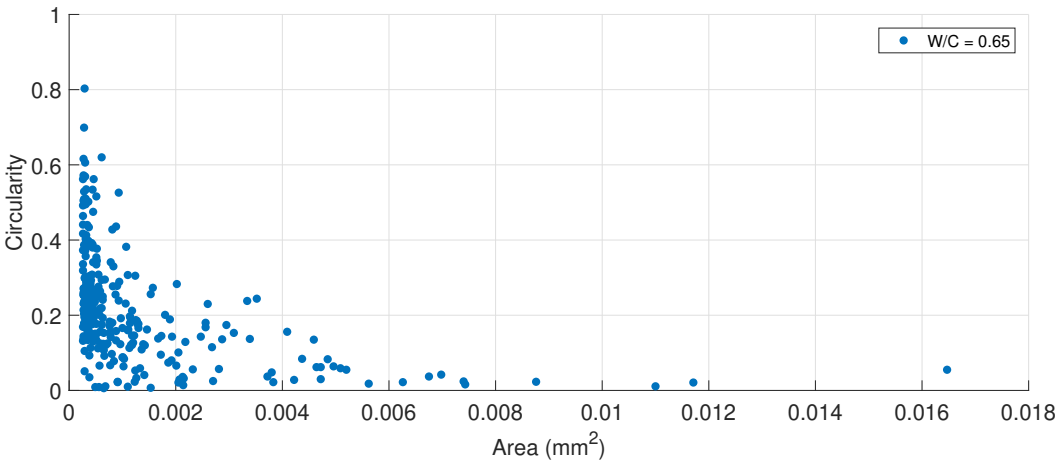

(a)

Figure B.1: Area vs Circularity. (a) W/C = 0.65

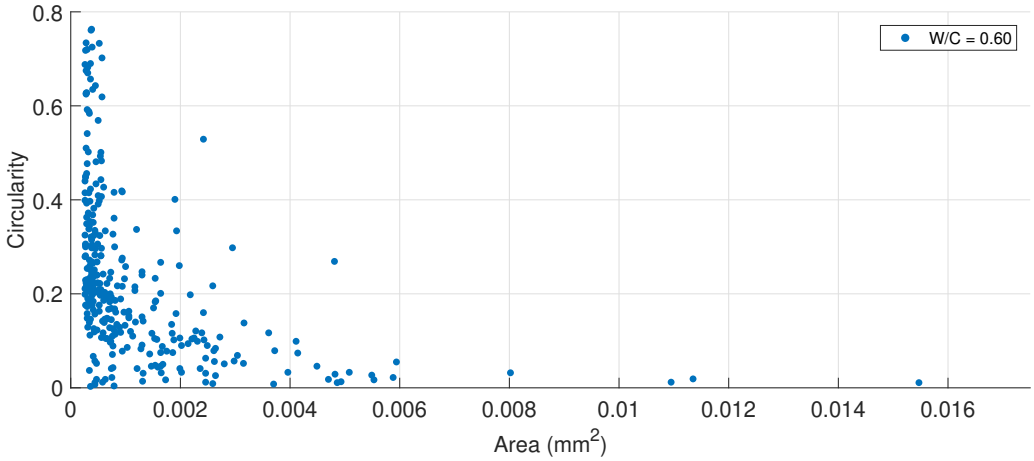

(a)

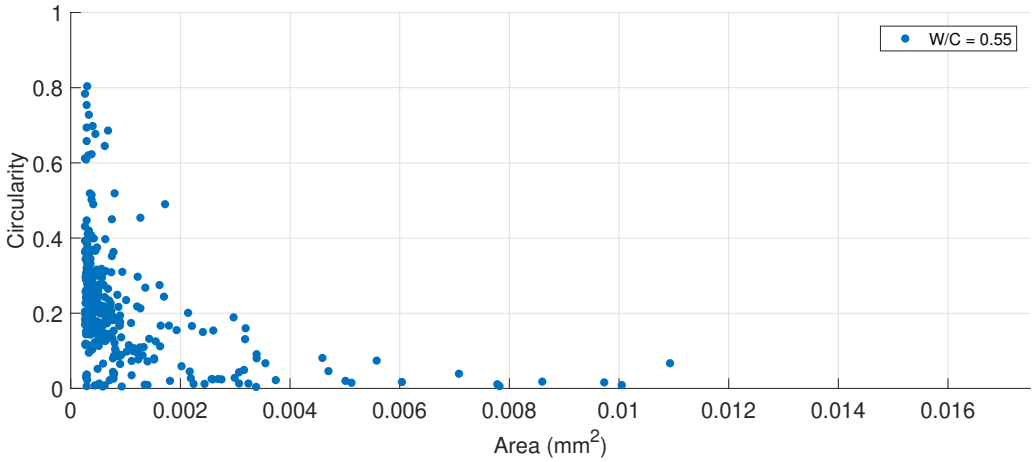

(b)

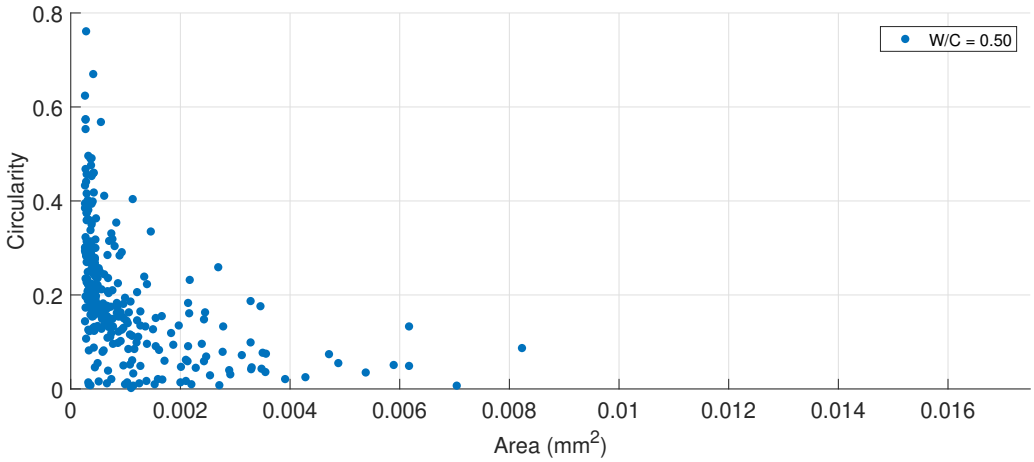

(c)

Figure B.2: Area vs Circularity. (a) W/C = 0.60. (b) W/C = 0.55. (c) W/C = 0.50

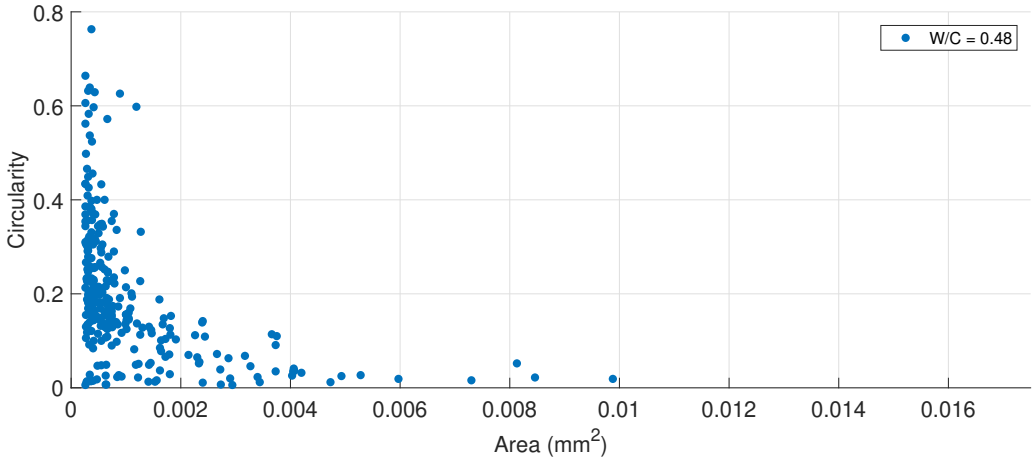

(a)

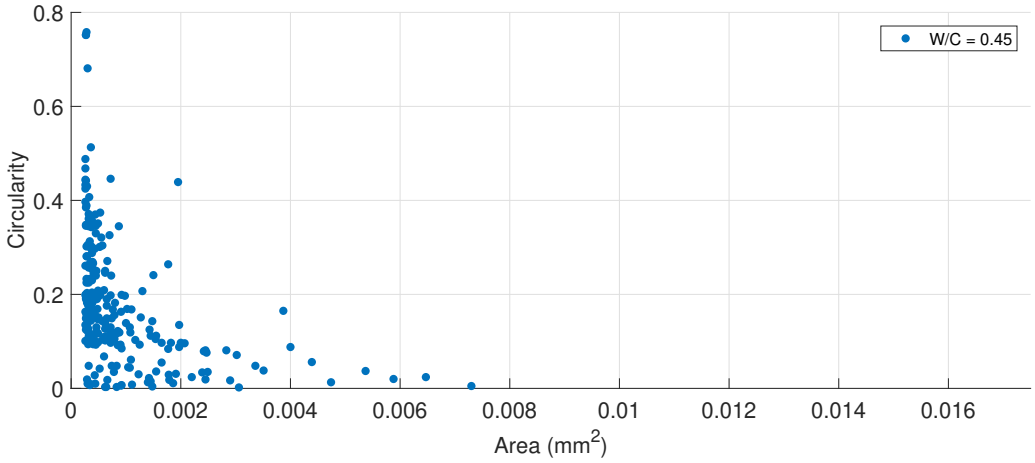

(b)

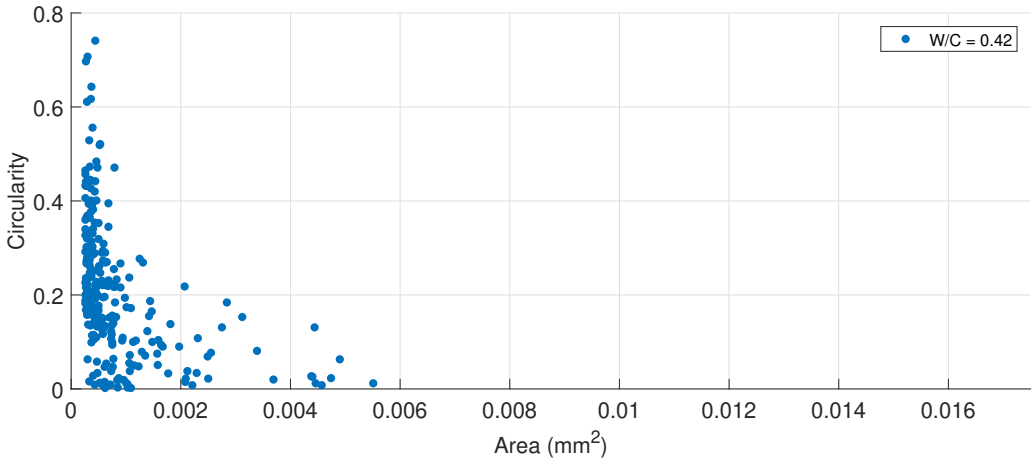

(c)

Figure B.3: Area vs Circularity. (a) W/C = 0.48. (b) W/C = 0.45. (c) W/C = 0.42

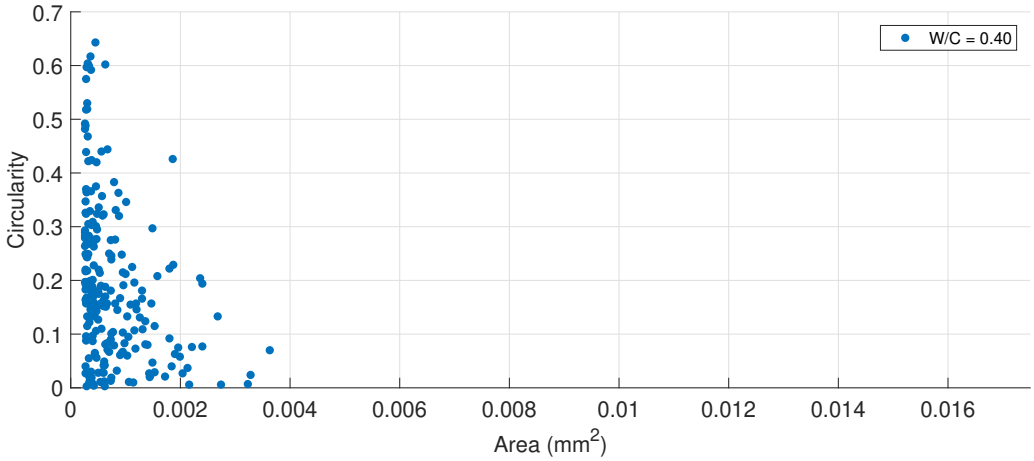

(a)

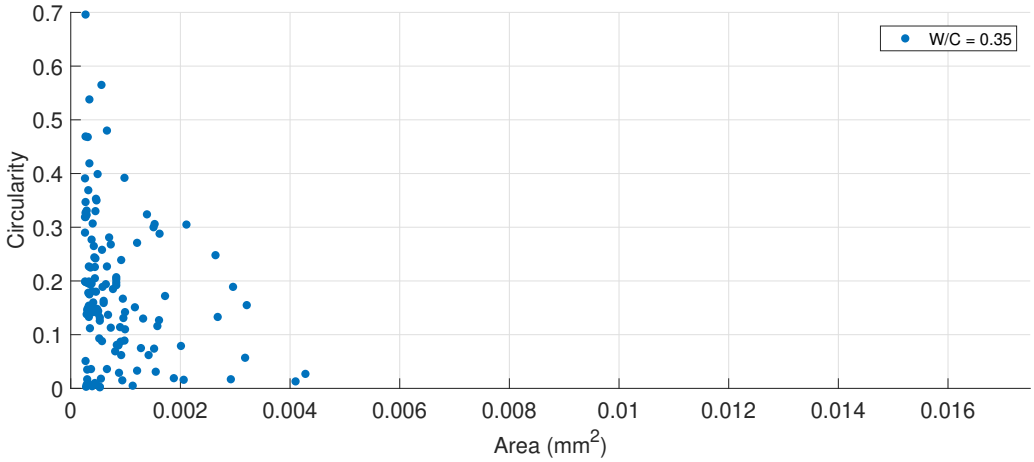

(b)

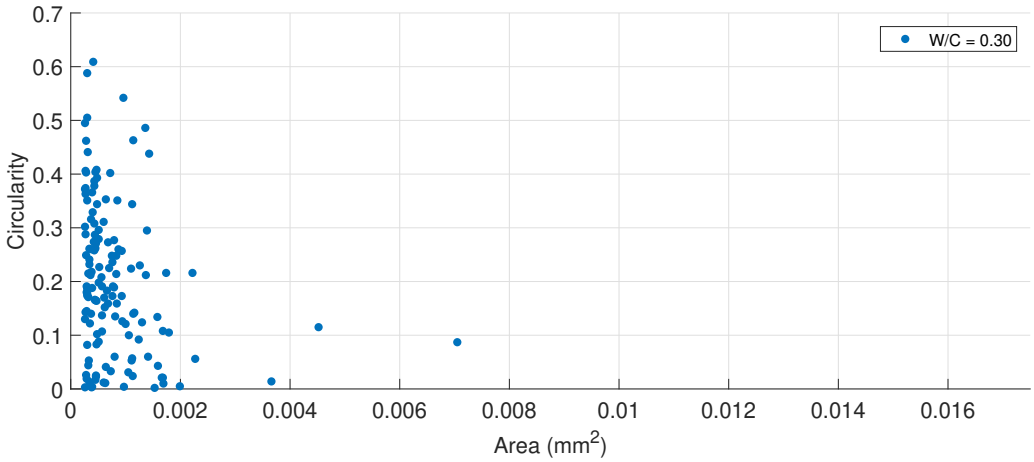

Figure B.4: Area vs Circularity. (a) W/C = 0.40. (b) W/C = 0.35. (c) W/C = 0.30

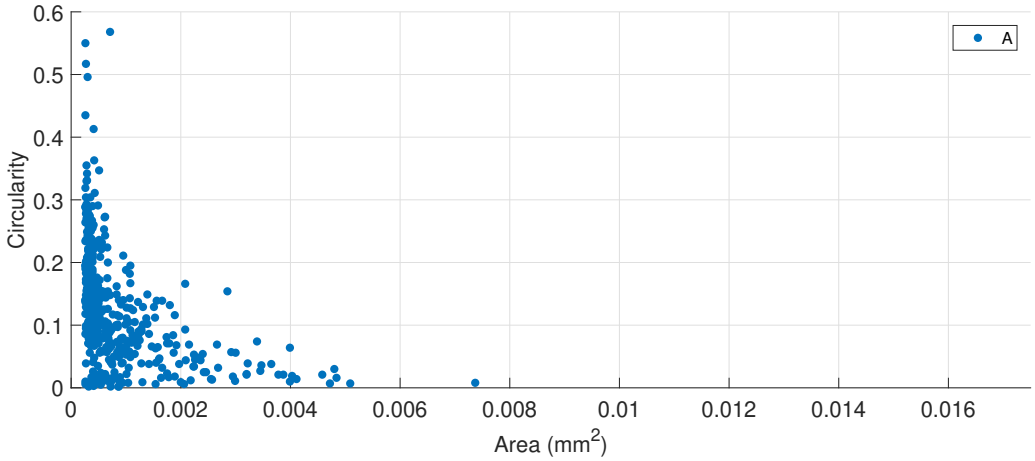

(c)

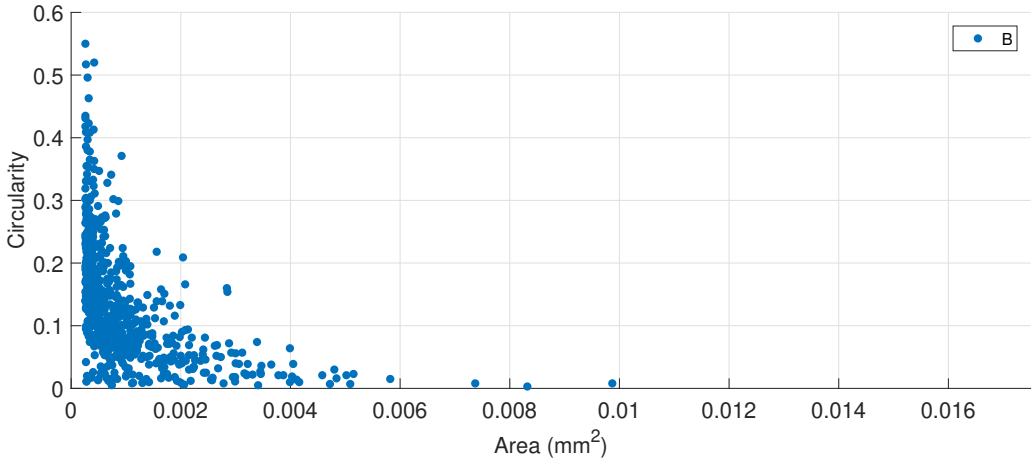

(d)

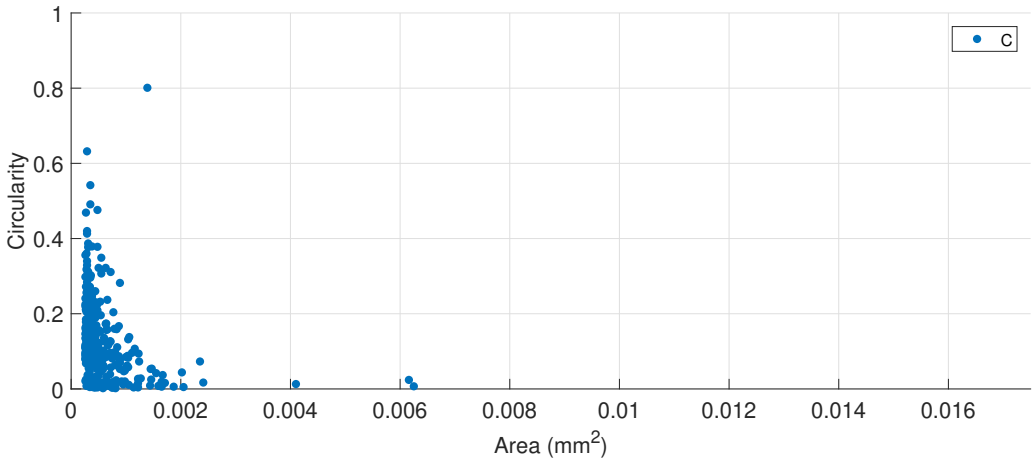

(e)

Figure B.4: Area vs Circularity. (a) APG Sample A. (b) APG Sample B. (c) APG Sample C

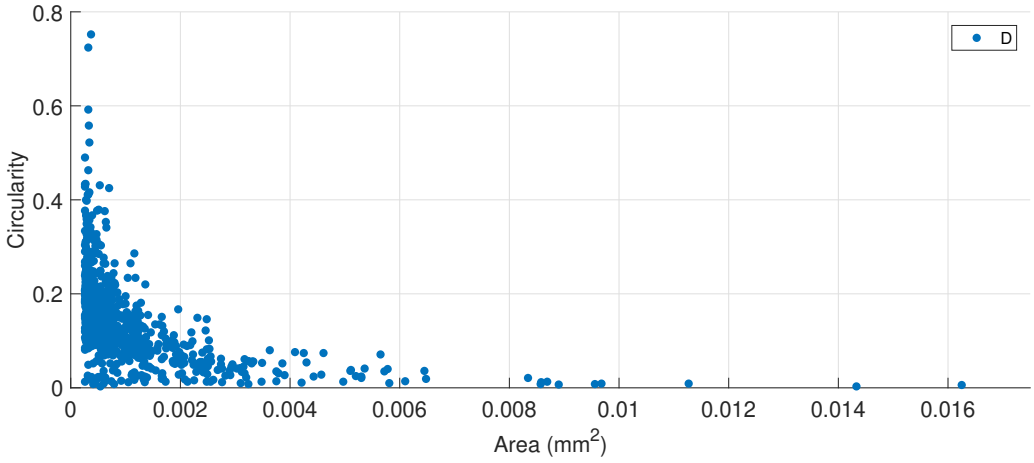

(f)

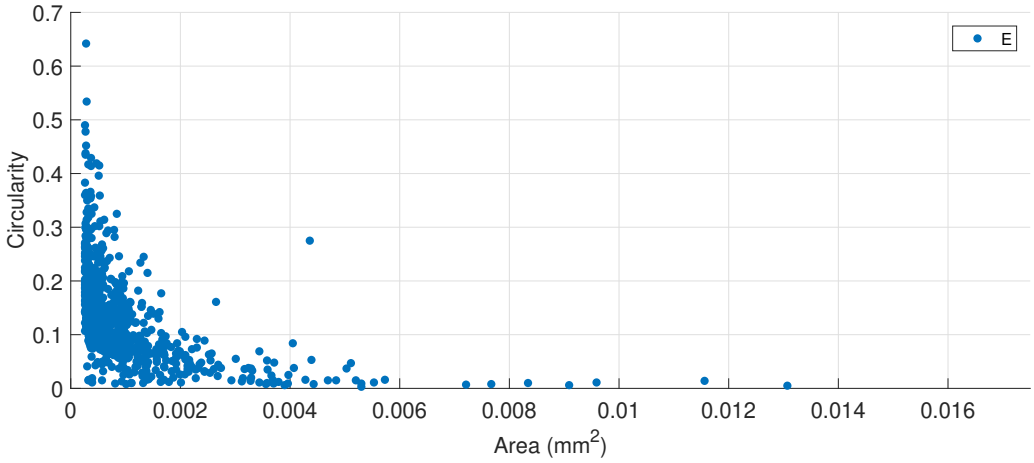

(g)

Figure B.4: Area vs Circularity. (a) APG Sample D. (b) APG Sample E.

B.3. TGA

B.3.1. TGA-DTG figures

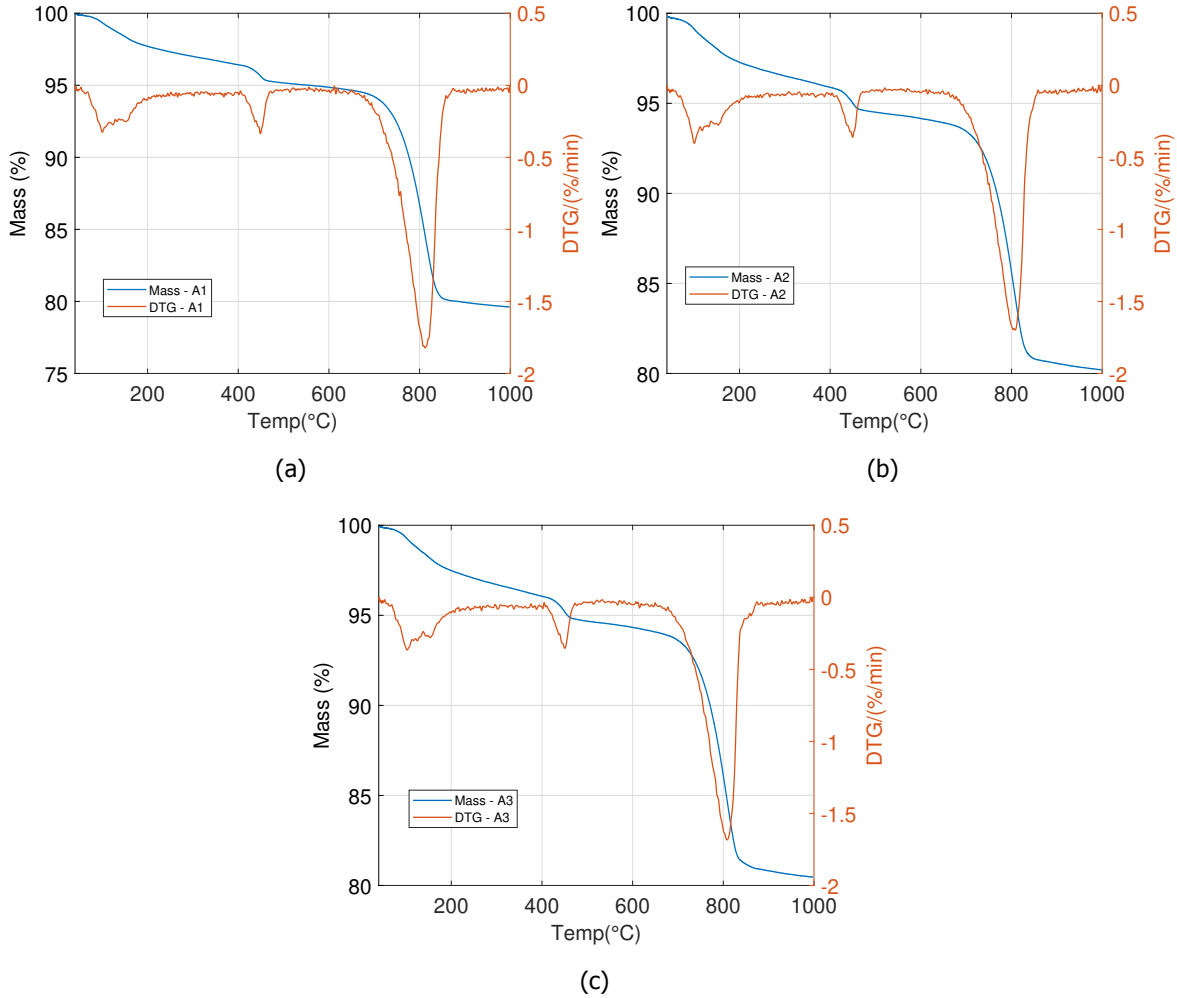

Figure B.5: APG Sample A, TGA-DSC results

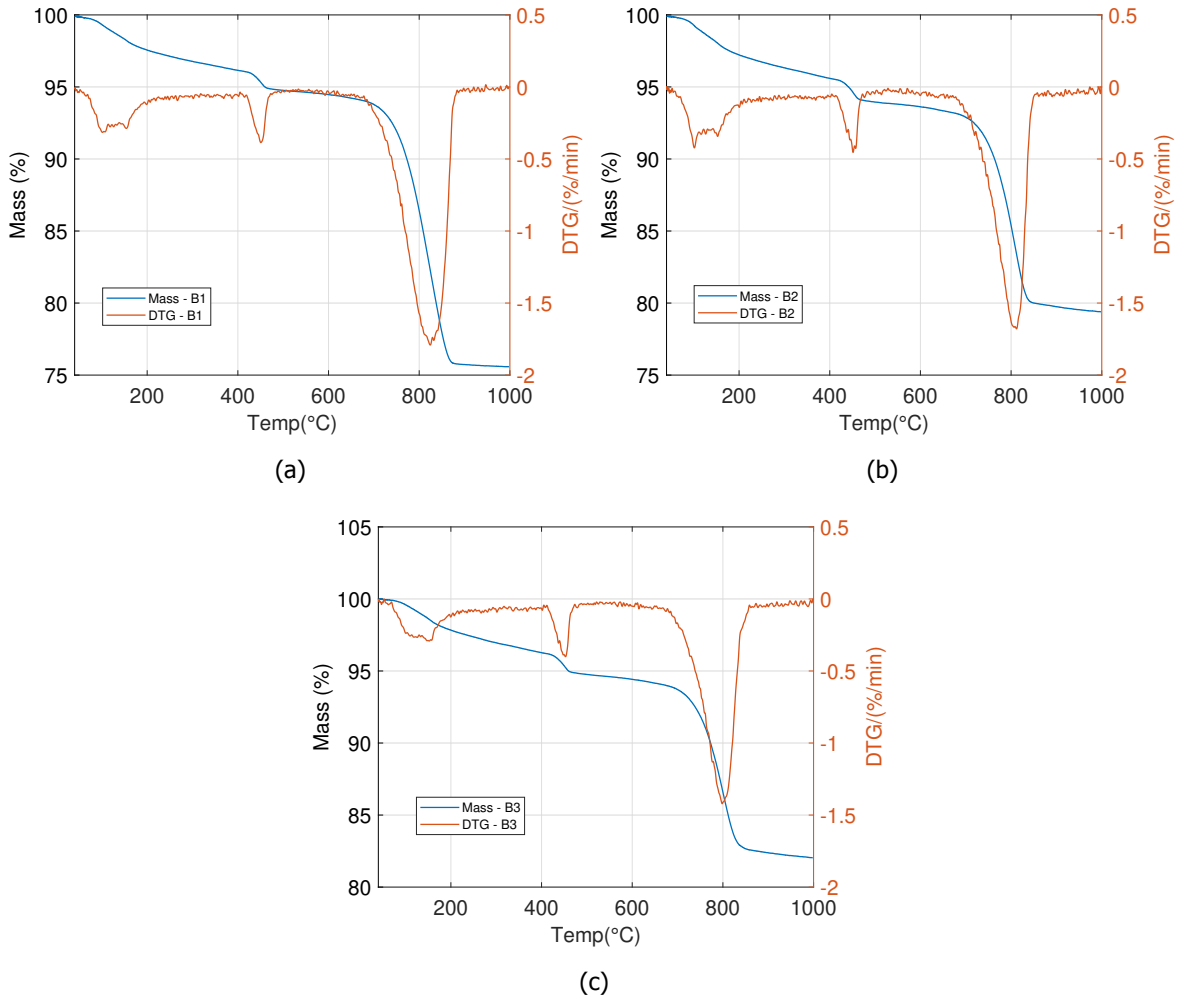

Figure B.6: APG Sample B, TGA-DSC results

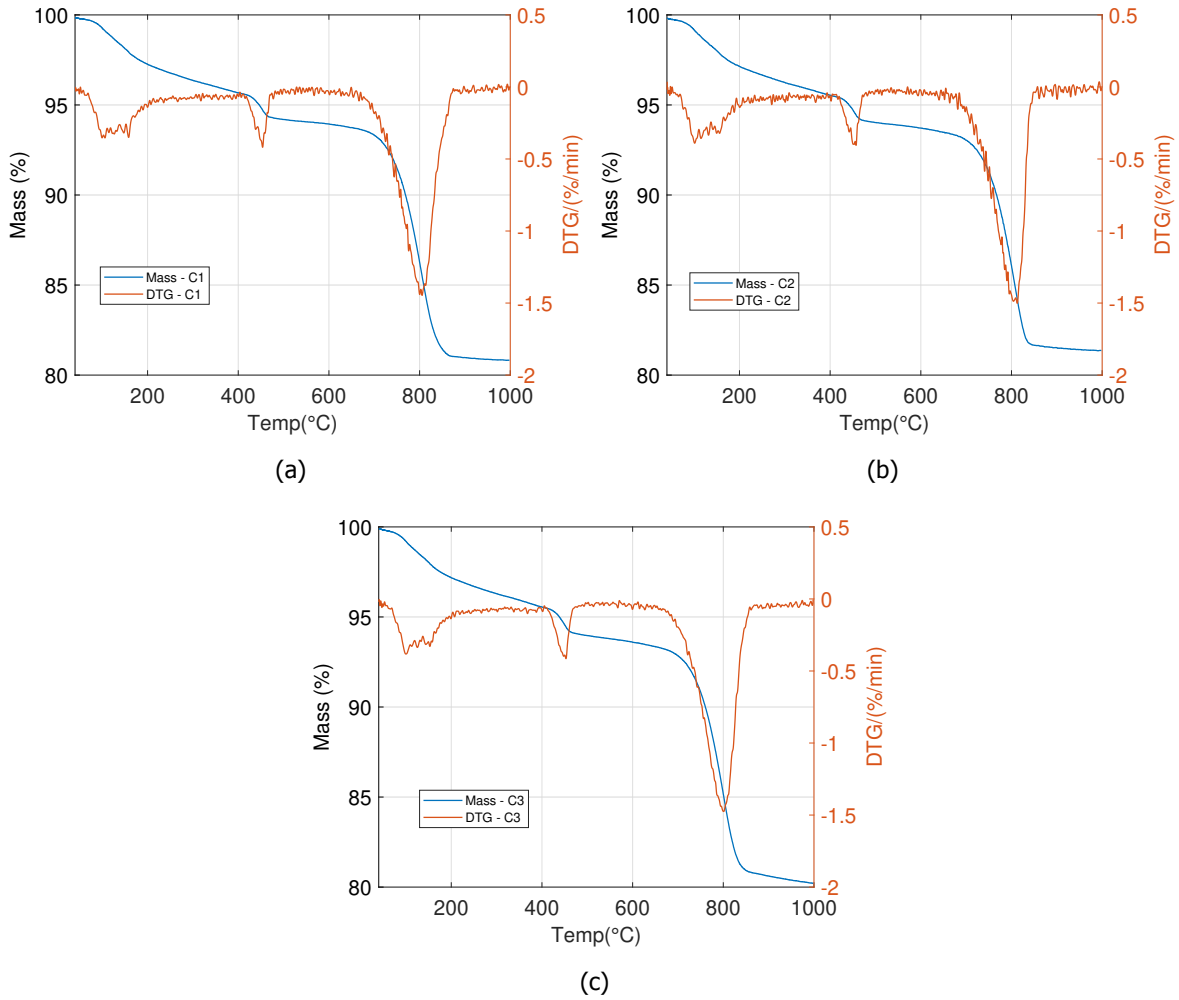

Figure B.7: APG Sample C, TGA-DSC results

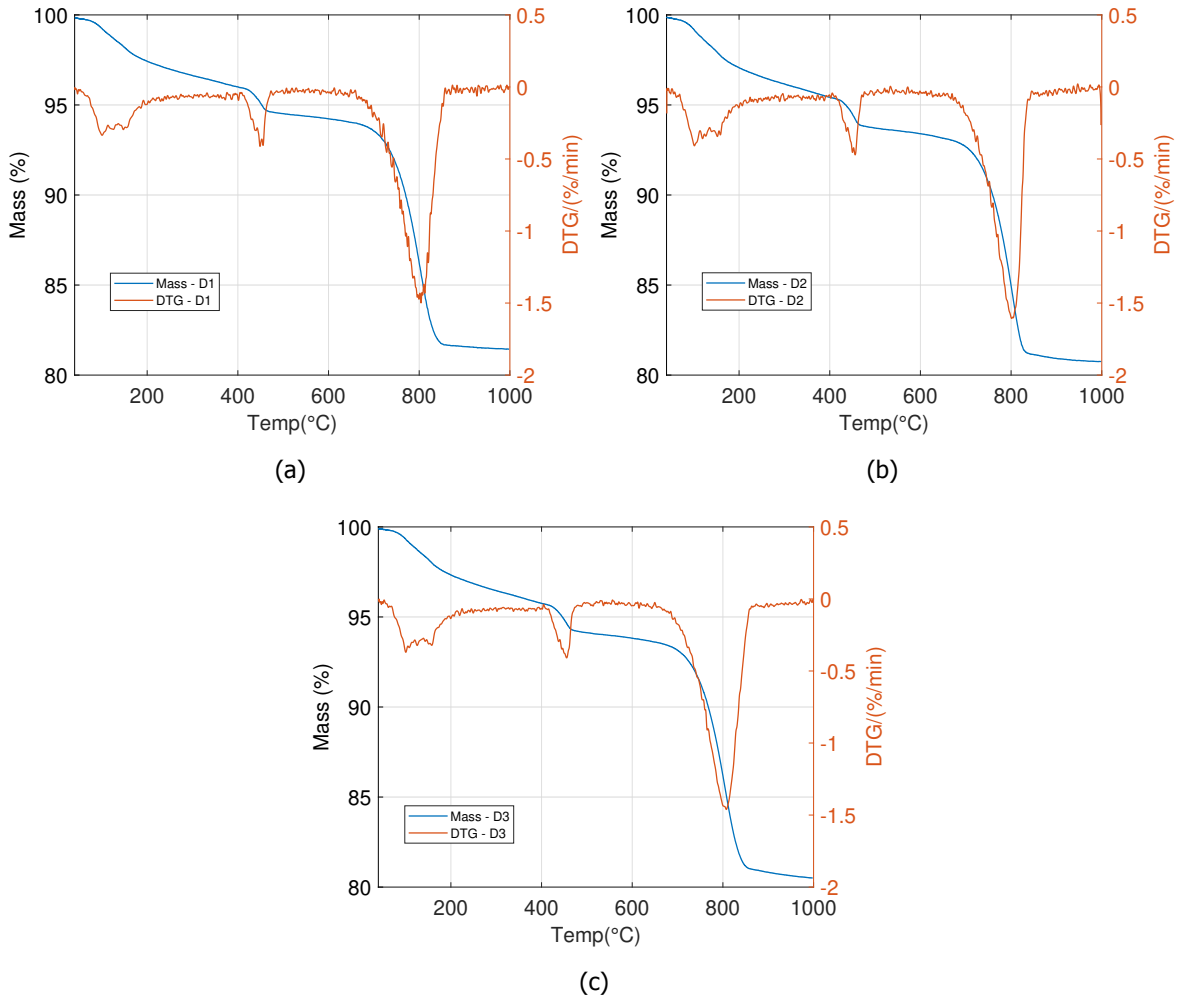

Figure B.8: APG Sample D, TGA-DSC results

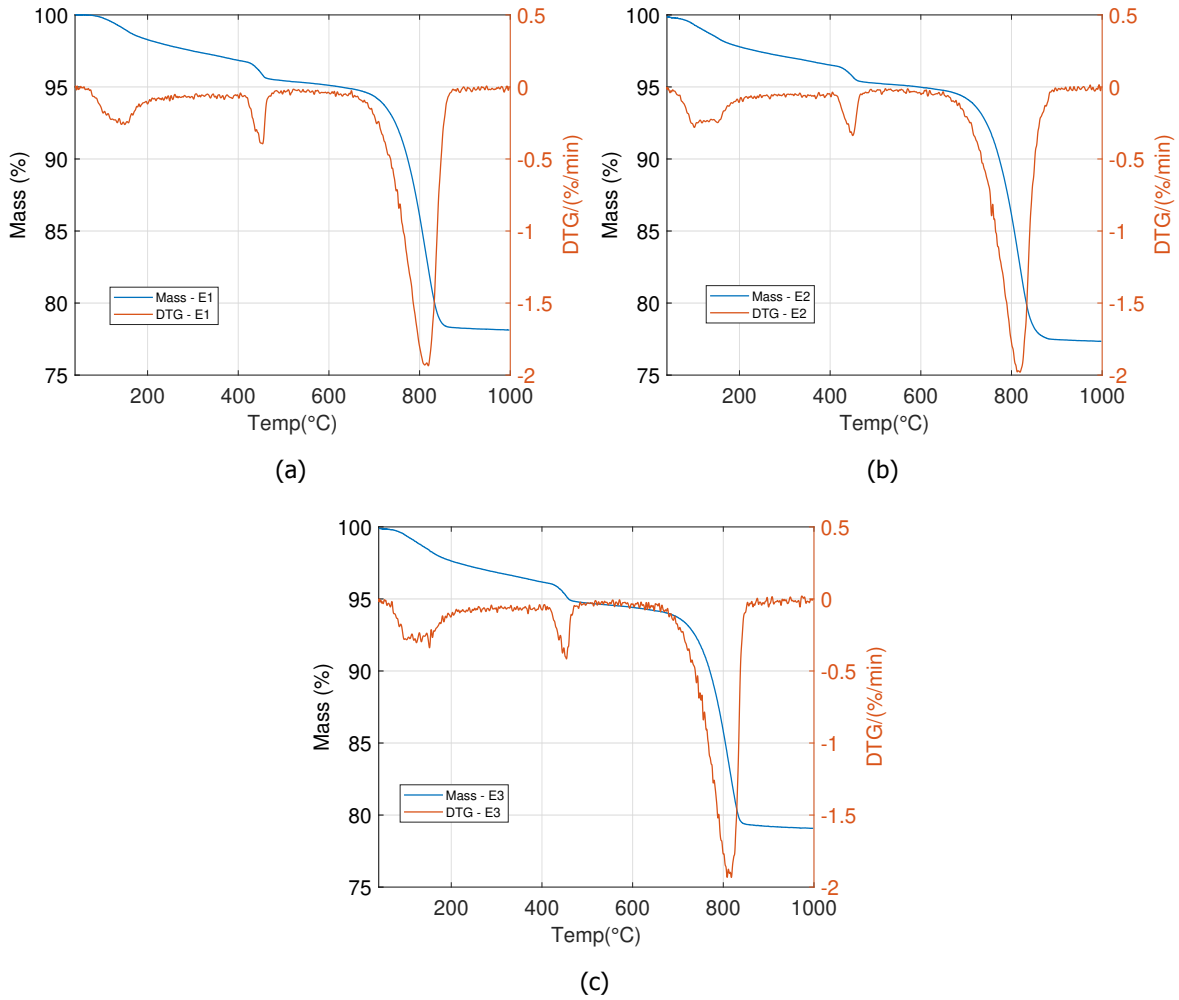

Figure B.9: APG Sample E, TGA-DSC results

C

Appendix C

C.1. APG Samples results summary

	CH Cluster size (CPL)	CH Ratio (TGA)	AVG Pixel Value (UV Light)	Porosity (SEM)
A	0.005	0.246	37.640	0.110
B	0.009	0.256	43.714	0.095
C	0.004	0.257	57.456	0.228
D	0.014	0.271	62.719	0.244
E	0.011	0.272	79.765	0.381

Bibliography

[1] E. STN, *206-1 concrete,* Part I, Specification, performance, production and conformity (2004).

[2] A. M. Neville, *Properties of concrete*, Vol. 4 (Longman London, 1995).

[3] H. Wong and N. Buenfeld, *Determining the water–cement ratio, cement content, water content and degree of hydration of hardened cement paste: Method development and validation on paste samples,* Cement and Concrete Research **39**, 957 (2009).

[4] N. Nordtest, *Build 361-1999,* Concrete, hardened: water-cement ratio .

[5] B. Standard, *Testing concrete,* Recommendations for the (1988).

[6] U. Jakobsen, P. Laugesen, and N. Thaulow, *Determination of water-cement ratio in hardened concrete by optical fluorescence microscopy,* Special Publication **191**, 27 (1999).

[7] U. Jakobsen and D. Brown, *Reproducibility of w/c ratio determination from fluorescent impregnated thin sections,* Cement and Concrete Research **36**, 1567 (2006).

[8] A. M. Neville, *Concrete: Neville's insights and issues* (Thomas Telford, 2006).

[9] A. B. Poole and I. Sims, *Concrete petrography: a handbook of investigative techniques* (CRC Press, 2016).

[10] H. Wong, M. Head, and N. Buenfeld, *Pore segmentation of cement-based materials from backscattered electron images,* Cement and Concrete Research **36**, 1083 (2006).

[11] H. S. Wong, K. Matter, and N. R. Buenfeld, *Estimating the original cement content and water–cement ratio of portland cement concrete and mortar using backscattered electron microscopy,* Magazine of Concrete Research **65**, 693 (2013).

[12] T. C. Powers, *The Nonevaporable Water Content of Hardened Portland-Cement Paste–Its Significance for Concrete Research and Its Method of Determination*, Tech. Rep. (1949).

[13] A. M. Neville and J. J. Brooks, *Concrete technology* (1987).

[14] W. French, *Concrete petrography: a review,* Quarterly Journal of Engineering Geology and Hydrogeology **24**, 17 (1991).

[15] O. Çopuroğlu, *Revealing the dark side of portlandite clusters in cement paste by circular polarization microscopy,* Materials **9**, 176 (2016).

[16] B. Erlin and R. Campbell, *Paste microhardness-promising technique for estimating water-cement ratio,* Special Publication **191**, 43 (1999).

[17] U. H. Jakobsen, V. Johansen, and N. Thaulow, *Estimating the capillary porosity of cement paste by fluorescence microscopy and image analysis,* in *Materials Research Society Symposium Proceedings*, Vol. 370 (Materials Research Society, 1995) pp. 227–227.

[18] T. Sibbick, D. Brown, B. Dragovic, C. Knight, and S. Garrity, *Determination of water to cementitious (w-cm) binder ratios by the use of the fluorescent microscopy technique in hardened concrete samples: Part i,* Conference On Cement Microscopy, Quebec city, Quebec, Canada **29** (2007).

[19] G. Einarsson and O. Copuroglu, *Estimating w/c ratio of opc and slag concrete, mortar and paste using image processing and analysis,* in *32nd International Conference on Cement Microscopy2010, ICMA: New Orleans, Lousiana* (2010) pp. 251–263.

[20] G. Einarssona and O. Copuroglub, *The effect of specimen age on the accuracy of w/c ratio estimation for opc and bfsc concrete,* BOOK OF EXTENDED , 29.

[21] T. Sibbick, S. Garrity, and C. LaFleur, *Determination of water to cementitious (w-cm) binder ratios by the use of the fluorescent microscopy technique in hardened concrete samples: Part iii,* Conference On Cement Microscopy, Rosemont, Illinois, USA **35** (2013).

[22] D. St. John, *The use of fluorescent dyes and stains in the petrographic examination of concrete* (Lower Hutt, N.Z. : Industrial Research Limited, 1994).

[23] M. de Rooij, S. Valckea, and W. Suitelaa, *An update on using image analysis to determine w/c ratio of concrete,* Euroseminar on Microscopy Applied to Building Materials, Liubljana, Slovenia **13** (2011).

[24] T. Sibbick and C. LaFleur, *Determination of water to cementitious (w-cm) binder ratios by the use of the fluorescent microscopy technique in hardened concrete samples: Part ii,* Conference On Cement Microscopy, Halle (Saale), Saxony-Anhalt, Germany **34** (2012).

[25] J. Elsen, N. Lens, T. Aarre, D. Quenard, and V. Smolej, *Determination of the wc ratio of hardened cement paste and concrete samples on thin sections using automated image analysis techniques,* Cement and Concrete Research **25**, 827 (1995).

[26] B. Mayfield, *The quantitative evaluation of the water/cement ratio using fluorescence microscopy,* Magazine of Concrete Research **42**, 45 (1990).

[27] S. Sahu, S. Badger, N. Thaulow, and R. Lee, *Determination of water–cement ratio of hardened concrete by scanning electron microscopy,* Cement and Concrete Composites **26**, 987 (2004).

[28] J. Liu and M. Khan, *Comparison of known and determined water-cement ratios using petrography,* Special Publication **191**, 11 (1999).

[29] R. Zoughi, S. D. Gray, and P. S. Nowak, *Microwave nondestructive estimation of cement paste compressive strength,* Materials Journal **92**, 64 (1995).

[30] T. Philippidis and D. Aggelis, *An acousto-ultrasonic approach for the determination of water-to-cement ratio in concrete,* Cement and Concrete Research **33**, 525 (2003).

[31] K. MacDonald and D. Northwood, *Rapid estimation of water-cementitious ratio and chloride ion diffusivity in hardened and plastic concrete by resistivity measurement,* Special Publication **191**, 57 (1999).

[32] A. Standard *et al.*, *Standard test method for electrical indication of concrete's ability to resist chloride ion penetration,* West Conshohocken, PA: ASTM International (2012).

[33] L. Bertolini, B. Elsener, P. Pedeferri, E. Redaelli, and R. B. Polder, *Corrosion of steel in concrete: prevention, diagnosis, repair* (John Wiley & Sons, 2013).

[34] G. Larsen, *Microscopic point measuring: A quantitative petrographic method of determining the ca (oh) 2 content of the cement paste of concrete,* Magazine of Concrete Research **13**, 71 (1961).

[35] K. Scrivener, R. Snellings, and B. Lothenbach, *A practical guide to microstructural analysis of cementitious materials* (Crc Press, 2016).

[36] G. Fagerlund, *Chemically bound water as measure of degree of hydration,* Method and potential errors. Report TVBM-3150, Lund University (2009).

[37] A. Standard *et al.*, *Standard test method for microindentation hardness of materials,* (2002).

[38] E. ASTM, *Standard test methods for rockwell hardness of metallic materials,* (2008).

[39] M. Yio, J. Phelan, H. Wong, and N. Buenfeld, *Determining the slag fraction, water/binder ratio and degree of hydration in hardened cement pastes,* Cement and Concrete Research **56**, 171 (2014).